The Role of Exonuclease-1 and its Interaction Partners in Genome Stability

Dissertation
zur
Erlangung der naturwissenschaftlichen Doktorwürde
(Dr. sc. nat.)

vorgelegt der

Mathematisch-naturwissenschaftlichen Fakultät

der

Universität Zürich

von

Wassim Eid

aus
Ägypten

Promotionskomitee

Prof. Dr. Alessandro Sartori
PD Dr. Stefano Ferrari (Leitung der Dissertation)
Prof. Dr. Claus Azzalin
Prof. Dr. Martin Scheffner

Zürich, 2012

-to Malika-

I was lucky to meet you before you left us forever

You will always be missed

Summary

Cells are constantly under the assault of endogenous and exogenous forms of damage that threaten genome integrity. Maintaining a complete, undamaged genome is a continual challenge and it is of vital importance to the cell and its progeny. To accomplish this, eukaryotes have evolved a complex signal transduction pathway that senses DNA lesions and triggers DNA repair. This complex signaling network is collectively known as the DNA damage response (DDR). Double strand breaks (DSBs) are the most cytotoxic DNA lesions. Unrepaired DSBs, or their misrepair, can cause gross chromosomal aberrations that may trigger carcinogenesis through activation of oncogenes or inactivation of tumour suppressor genes. Cells employ two main mechanisms to repair DSBs: non-homologous end-joining (NHEJ) and homologous recombination (HR). NHEJ takes place throughout the cell cycle, whereas HR is restricted to the S/G2 phases. Both in yeast and human cells HR is initiated by 5'-3' resection of DNA ends. This occurs in two-steps, with initial DNA "end-trimming" by the MRN complex and CtIP in human cells, followed by more extensive resection executed by EXO1 or BLM and DNA2.

In the first part of this study we investigated the molecular mechanism of the early step of DNA resection. We show that EXO1 is recruited to laser-induced DSBs in a CtIP and MRN dependent manner. We also show that EXO1 physically interacts with CtIP both *in vivo* and *in vitro* and, interestingly, this interaction restrains the exonucleolytic activity of EXO1 *in vitro*. We suggest that restraining EXO1 activity *in vivo* could prevent the formation of excessively long recombination intermediates that may hamper the faithful execution of HR. Accordingly, we provide evidence that CtIP and EXO1 act together to oppose NHEJ and promote the error-free repair of DSBs through HR, hence maintaining genome stability.

In the second part of this study we set out to identify proteins interacting with EXO1 in order to better understand the role and the regulation of EXO1 in DNA-end resection. In a large-scale mass spectrometry analysis, we successfully identified novel EXO1 interacting proteins that could have a potential role in DNA repair and that we are currently evaluating.

Zusammenfassung

Zellen sind konstant endogenen und exogenen Formen von DNS Schäden ausgesetzt die die Integrität des Genomes gefährden. Das Erbgut komplett und ungeschädigt zu erhalten, ist essentiell für die Zelle. Eukaryonten haben dafür einen komplexen Signaltransduktionsweg entwickelt, welcher Schäden erkennt und anschliessend die Reparatur derselben erlaubt. Dieses Netzwerk der DNS Reparatur ist als DNS-damage response bekannt. DNS Doppelstrangbrüche (DSBs) sind die am zytotoxischsten Erbgutschäden und unvollständige oder falsche Reparatur kann Chromosomenschäden verursachen. Diese können durch Aktivierung von Onkogenen oder Deaktivierung von Onkosuppressoren schlussendlich eine Zelltransformation hervorrufen und Krebs verursachen. Die Hauptformen der DNS Doppelstrangbruchreparatur sind non homologous end-joining (NHEJ) und homologe Rekombination (HR). NHEJ ist während des ganzen Zellzyklus aktiv, HR nur in der S-und der G2 Phase. Homologe Rekombination beginnt mit einer 5'-3' DNS Resektion, ein konservierter Mechanismus der sowohl in Hefe- als auch in menschlichen Zellen stattfindet. Die Resektion findet in zwei Schritten statt. Anfangs arbeiten der MRN-Komplex und CtIP zusammen um einige wenige Nukleotide des Doppelstrangbruches zu prozessieren. Die Resektion wird durch EXO1 und/oder BLM und DNA2 in einem zweiten Schritt vervollständigt.

Im ersten Teil dieser Studie haben wir die molekularen Mechanismen der DNS Resektion untersucht. Wir zeigen, dass EXO1 zu laser-induzierten DSBs rekrutiert wird und die Rekrutierung von MRN und von CtIP abhängig ist. Weiters konnten wir zeigen, dass CtIP und EXO1 *in vitro* und *in vivo* interagieren und CtIP die Aktivität der Exonuklease EXO1 *in vitro* hemmt. Wir schlagen ein Modell vor, in dem CtIP die Aktivität von EXO1 *in vivo* einschränkt und somit die exessive Formation von einzelstraengiger DNS verhindert. Übermäβige DNS Resektion könnte den normalen HR Ablauf beeinträchtigen. Dementsprechend zeigen wir, dass CtIP und EXO1 zusammenarbeiten um NHEJ zu verhindern und die Reparatur der DSBs durch HR begünstigen. Somit wird die Stabilität des Genomes aufrechterhalten.

Der zweite Teil unserer Studie ist der Identifikation von Interaktionspartnern von EXO1 gewidmet. In einem auf Massenspektrometrie basierenden Screen konnten wir bisher unbekannte Interaktionspartner von EXO1 identifizieren die potentiell eine wichtige Rolle in der DNS Reparatur haben könnten.

1.INTRODUCTION

1.1. DNA damage, genomic instability and cancer

The human genome is subject to constant damage induced by environmental agents (exogenous) or generated spontaneously during normal cellular processes (endogenous). Exogenous sources of DNA damage can be of physical or chemical type. Examples of physical genotoxic agents are ultraviolet (UV) radiation from sunlight and ionizing radiation (IR) from medical imaging and treatments employing X-rays. Chemical agents used in cancer therapy, such as cisplatin or etoposide can also cause different types of DNA lesions. Furthermore, DNA damage can be the result of endogenous metabolic processes producing reactive oxygen species (ROS) or may arise from inaccurate DNA replication. DNA lesions generated from these sources represent a constant threat to genome stability.

DNA repair and maintenance of a stable genome are crucial to cellular and organismal function. This is illustrated by the fact that deficiencies or abnormalities in DNA repair pathways lead to several pathological conditions. Mutations in DNA repair genes have been implicated in the development of neurological diseases and aging, in increased risk of cancer development, in less favorable cancer therapy outcomes, in inflammation and in a number of genetic syndromes that often show a cancer-prone phenotype, such as Ataxia-telangiectasia (A-T), Nijmegen breakage syndrome (NBS) or Fanconi Anemia (FA) (Ciccia and Elledge, 2010).

To counteract DNA damage and to maintain genome integrity, cells need to adequately respond to various types of genotoxic stress. This is achieved by activation of evolutionary conserved DNA-damage response (DDR) pathways that results in a two-pronged effect: a block in cell cycle progression and the concomitant induction of DNA repair. Depending on the extent of damage suffered by DNA, cells may repair all lesions and re-enter the cell cycle, a condition known as checkpoint recovery or, in the case of excessive damage, be eliminated by programmed cell death (apoptosis). Alternatively, cells undergo an apparently permanent arrest after DNA damage. This state is known as "replicative senescence" and consists of an irreversible growth-

arrest program that prevents unlimited cell proliferation. Although senescent cells *in vitro* may remain indefinitely viable, this may not be the case *in vivo* (Collado et al. 2007). Genes coding for proteins that are involved in genome surveillance, such as DNA repair genes, are referred to as “caretakers”. Mutations or defects in such genes predispose an individual to cancer and may enhance tumorigenesis, a common condition in numerous hereditary cancer syndromes. Affected individuals inherit a defective allele of a caretaker gene and eventually acquire a mutation of the second allele in a somatic cell, an event that facilitates tumour survival and disease progression. Examples of inherited mutations in caretaker genes are those of the WRN DNA-helicase that are linked to the development of lymphomas, mutations in the BLM DNA-helicase that result in a leukemia-prone phenotype and mutations in the BRCA1 or BRCA2 genes that lead to increased incidences of breast and ovarian cancers, respectively (Machwe et al. 2011).

Current cancer chemotherapy is based on the use of chemical agents that cause a variety of DNA lesions: alkylating agents, such as methyl methanesulfonate (MMS), attach alkyl groups to DNA bases, while crosslinking agents such as mitomycin C (MMC), cisplatin and nitrogen mustard introduce covalent links between bases of the same DNA strand (intrastrand crosslinks) or of opposite DNA strands (interstrand crosslinks or ICLs). Other chemical agents, such as the topoisomerase I inhibitor camptothecin (CPT) and the topoisomerase II inhibitor etoposide, induce the formation of single-strand breaks (SSBs) or double-strand breaks (DSBs) by trapping topoisomerase-DNA covalent complexes (Helleday et al. 2008). Cancer cells are usually more susceptible to genotoxic agents than normal cells, likely due to the fact that they divide more rapidly than normal cells and, in addition, because cancer cells usually carry alterations in some components of DNA repair pathways that arise during tumour development. Another important consideration in this respect is that the high proliferation rate of cancer cells and the associated metabolic stress, like hypoxia and mitotic stress, renders them more reliant on anti-stress mechanisms, such as DDR pathways (Finn et al. 2011). Thus, combinatorial treatments with conventional DNA-damaging chemotherapeutic drugs and inhibitors of specific DNA repair pathways might prove to be the best choice in the

treatment of cancer. Proofs of this principle, called synthetic lethality, have been provided for the treatment of BRCA1-mutated breast cancers with PARP-inhibitors (Javle and Curtin, 2011).

A deeper understanding of the mechanisms that are involved in the recognition and repair of DNA lesions may therefore provide the ground for designing novel strategies and therapeutic protocols in cancer treatment. The fact mentioned above, that components of DDR pathways are commonly mutated in cancer cells but are perfectly proficient in normal cells, offers a therapeutic window for this type of intervention and an edge over conventional cancer therapies.

1.2. The DNA damage response

To properly protect the genome, all types of DNA structural damages must be detected and repaired. This includes nicks, gaps, single strand breaks (SSBs), double strand breaks (DSBs) and all alterations that block DNA replication. To achieve this, mammalian cells have evolved a complex signaling network that senses DNA damage and replication stress and activates signal transduction cascades These, in turn, slow down transition through the cell cycle and activate DNA repair. Collectively, this signaling network is known as DNA damage response (DDR).

Proteins that play a role in the DDR have been initially classified into four subtypes (Figure 1). Sensors are protein complexes or enzymes that recognize the DNA damage, bind to the altered DNA structures and initiate a signaling cascade by recruiting a second set of proteins referred to as transducers. Transducers are proteins of the phosphatidylinositol 3-kinase-like protein kinases (PIKK) family that includes ATM, ATR and DNA-PKcs or proteins of the poly(ADP-ribose) polymerase (PARP) family. PIKKs phosphorylate and activate the transducer kinases CHK1 and CHK2 that further amplify the signal and activate effector proteins via phosphorylation. In addition, effector proteins have been shown to undergo regulation by other post-translational modifications such as ubiquitylation. Effector proteins translate the signal into various cellular responses such as cell cycle arrest, senescence, DNA repair, transcriptional regulation or apoptosis. Recently, a

fourth subtype of proteins has been identified as an independent entity in the DDR pathway, the so-called mediators or adaptors. These are ATM and ATR substrates and essentially act as recruiters of additional substrates and as scaffolds to bring transducers in close proximity to their substrates and facilitate protein complex formation.

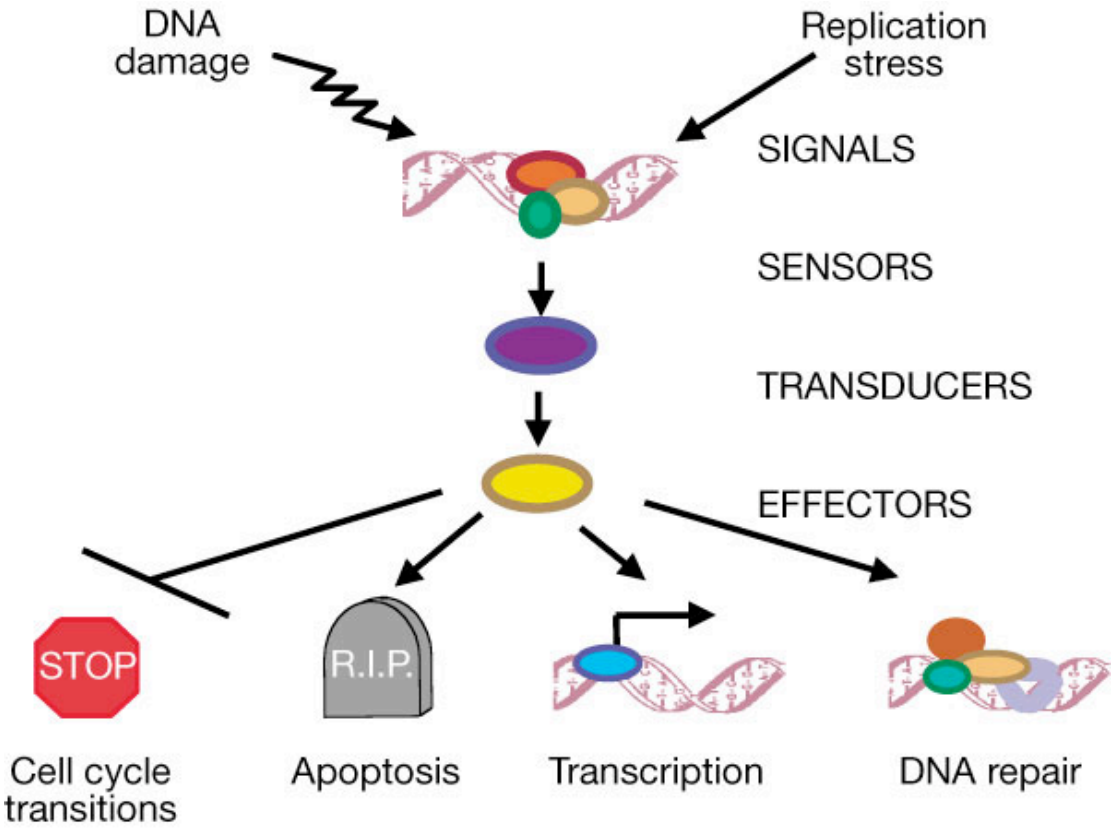

Fig.1

DNA damage response. The interactive signaling network of the DNA damage response, represented here as a linear pathway. DNA damage is recognized by sensor proteins that initiate a network of signal transduction cascades. This eventually results in the activation of effector proteins that mediate cell cycle arrest, the recruitment of DNA repair proteins, transcription or the induction of apoptosis. *Modified after (Zhou and Elledg, 2000)*

1.2. DNA double-strand breaks

DNA double-strand breaks (DSBs) are one of the most cytotoxic forms of DNA damage, and their faithful repair is critical for cell survival and the maintenance of genome integrity. DSBs can result from either endogenous or

exogenous sources. Naturally occurring DSBs can occur accidentally during DNA synthesis when replication forks encounter lesions that block their progression and eventually lead to fork collapse. Other important sources of endogenous DSBs are certain specialized cellular processes, including V(D)J recombination in developing lymphocytes, class-switch recombination at the immunoglobulin heavy chain (IgH) locus and meiosis (Longhese et al. 2009). DSBs are also produced when cells are exposed to DNA damaging agents including ionizing radiation (IR), which creates DSBs directly and indirectly via the generation of reactive oxygen species (ROS) (Ward J. 1998); chemical agents and UV light that create replication blocking lesions such as pyrimidine dimers and crosslinks (Bosco et al. 2004); and chemotherapeutic drugs that are used to treat cancer, such as camptothecin that poisons topoisomerase I producing replication-blocking lesions, or etoposide that inhibits topoisomerase II trapping the enzyme-DNA complex after DSB induction (Degrassi et al. 2004). Failure to repair DSBs, or their misrepair, can result in cell death or gross chromosomal rearrangements (GCRs) including deletions, translocations and chromosome fusions that enhance genome instability, promote carcinogenesis, accelerate aging and are hallmarks of cancer cells. It is well established that inherited defects in DSB repair genes cause embryonic lethality, sterility, developmental disorders, immune deficiencies and predisposition to neurodegenerative diseases and cancer.

1.3.1 Double-strand break signaling

The response to DSBs is coordinated in time and space and involves the assembly of a number of proteins at the DSB-flanking chromatin in a highly ordered and strictly hierarchical fashion. In mammalian cells, DSBs are directly sensed by the MRN (MRE11, RAD50, NBS1) complex. MRN is a highly conserved protein complex that plays a critical role in DNA damage sensing, signaling and repair. Its importance is illustrated by the fact that the genes (*MRE11*, *RAD50* and *NBS1*) encoding the proteins for the MRN complex are vital for cell survival, since null mutations in any of the 3 genes lead to embryonic lethality in mice (Luo et al. 1999). Mutations in these genes cause human genome instability syndromes, namely ataxia-telangiectasia-like disorder (ATLD) if the *MRE11* is mutated (Stewart et al. 1999), Nijmegen

breakage syndrome (NBS) if the mutation occurs in *NBS1*, and a variant form of Nijmegen breakage syndrome (NBS-variant) in *RAD50* mutants (Waltes et al. 2009). The MRN complex has been shown to independently tether and process broken DNA ends. Moreover, it is required to recruit and activate the ATM (ataxia-telangiectasia mutated) kinase (Lee and Paul 2004). ATM belongs to the family of phosphatidylinositol 3-kinase-like protein kinases (PIKK), which also includes ATR (ataxia-telangiectasia and Rad3-related) kinase, DNA-PKcs (DNA protein kinase catalytic subunit), mTOR (mammalian target of rapamycin) and SMG1 (suppressor with morphological effect on genitalia). Of this family, only the first three members are involved in DDR.

Activation of ATM in human cells is mediated by the autophosphorylation on S1981, resulting in the dissociation of latent ATM homodimer into active monomers (Bakkenist and Kastan, 2003). The exact mechanism by which ATM gets activated has been the subject of a long-standing debate and is likely to involve components that are yet to be discovered or that we do not currently appreciate in full (reviewed in Bekker-Jensen and Mailand, 2010). In addition to ATM, DNA-PKcs is also activated in response to DSBs under certain conditions and it facilitates their repair via non-homologous end joining (NHEJ). DNA-PKcs is believed to act redundantly with ATM as it can phosphorylate H2AX in ATM-deficient cells (Stiff et al. 2004). ATR signaling is more prominent in the presence of single stranded DNA stretches that are generated in response to UV photoproducts or bulky base adducts that cause replication fork stalling. Moreover, in response to DSBs, ATR activity is triggered in an ATM-dependent manner in the S and G2 phase of the cell cycle (Jazayeri et al. 2006). Jazayeri et al., as well as Shiotani and Zou demonstrated that this ATM-mediated ATR activation depends on the resection of DSBs. In this process, a DSB is sensed and bound by the MRN complex, which subsequently recruits ATM. Ongoing resection leads to the generation of single stranded DNA stretches that get coated by replication protein A (RPA). RPA provides a platform for the recruitment of ATR through its cofactor ATRIP (ATR-interacting protein) to the sites of DNA damage, resulting in ATR activation followed by ATM inactivation (Shiotani and Zou, 2009).

Among the different targets of PIKKs is H2AX, a histone H2A variant that comprises 10-15% of total cellular H2A in higher eukaryotes (Rogakou et al. 1998). While several of the PIKKs, including ATM, ATR and DNA-PKcs, are capable of phosphorylating H2AX, ATM has emerged as the main kinase responsible of performing this function (Stiff et al. 2004). Activated ATM phosphorylates H2AX at the conserved C-terminal S139 residue in response to DSBs (Burma et al. 2001). H2AX phosphorylation occurs on megabase regions flanking the DSBs within seconds of DNA damage, suggesting that H2AX phosphorylation may be a critical component in early DNA damage signaling (Rogakou et al. 1998). One key function of phosphorylated H2AX (γ-H2AX) is to provide a high-affinity binding site for MDC1 (mediator of DNA damage checkpoint 1), which binds γ-H2AX via its C-terminal tandem BRCT repeats. MDC1 functions as a molecular bridge between γ-H2AX and the NBS1 component of the MRN complex, and helps providing a platform for various dynamic interactions for these and additional checkpoint and DNA repair proteins within the vicinity of the damage sites. Moreover, this interaction protects γ-H2AX from de-phosphorylation (Stucki et al. 2005).

The key function of activating ATM/ATR signaling is the initiation of cell cycle arrest at G1/S, intra-S-phase and G2/M checkpoints. ATM phosphorylates the checkpoint kinase-2 (CHK2) at Thr-68, while ATR phosphorylates the checkpoint kinase-1 (CHK1) at Ser-317 and Ser-345 (Bartek and Lukas, 2003). Specifically, ATM/ATR-dependent phosphorylation of CHK2 and CHK1 facilitates intra-molecular auto-phosphorylation leading to full checkpoint kinase activation and further transmission of the signal to key cell-cycle regulators, including the CDC25 family of phosphatases, the kinase WEE1 and p53, which itself can undergo phosphorylation by ATM at Ser-15. Temporal cell-cycle arrest induced in response to DNA damage is established through activation of the kinase WEE1 and inhibition of CDC25 activity, which results in inactivation of cyclin-dependent kinases (CDKs) at different stages of the cell cycle. A more sustained arrest is instead provided by p53-induced transcription of the CDK inhibitor p21 (Lukas et al. 2004). Cell cycle arrest presumably provides time to allow DNA repair to occur before the lesions are encountered by a replicative polymerase during DNA replication as well as to prevent the mis-segregation of chromosomal fragments during anaphase.

1.3.2. Ionizing radiation-induced foci formation

In response to DSBs, a number of proteins are recruited to the chromatin regions flanking the DNA lesion where they form aggregates. These protein aggregates are a hallmark of DSB signaling/repair and are so-called Ionizing Radiation-Induced Foci (IRIF; Bekker-Jensen and Mailand. 2010). Foci can be visualized by immunofluorescence and light microscopy as distinct speckles, in which one individual focus reflects protein accumulation at a single DSB. It has been demonstrated that DSB factors accumulate in the chromatin compartment flanking the DNA lesion in a hierarchical manner (Lukas et al. 2004).

The formation of γ-H2AX and the subsequent recruitment of MDC1 are exceedingly rapid, reaching maximal accumulation within minutes. This is then followed by a second wave of protein accumulation at DSBs (Mailand et al. 2007). This second wave of proteins arriving with delayed kinetics includes the DNA repair factors BRCA1 (breast cancer type 1 susceptibility protein) and 53BP1 (p53-binding protein 1), both being recruited via the instrumental role of an important ubiquitin ligase, the RNF8. Through its phospho-binding FHA domain, RNF8 directly binds MDC1 and gets recruited to the DNA damage sites. RNF8 then initiates a complex ubiquitylation cascade of histones H2A and H2AX at the DSB-flanking chromatin, an event that causes chromatin remodeling (Mailand et al. 2007). This initial ubiquitylation step leads to the recruitment of another E3 ubiquitin ligase, RNF168 that, through its two Motifs Interacting with Ubiquitin (MIUs), recognizes ubiquitylated forms of H2A and H2AX produced by RNF8. Subsequently, RNF168 extends ubiquitylation of H2A-type histones (Doil et al. 2009). These ubiquitin chains generated by the action of both RNF8 and RNF168 at the sites of DNA damage serve as “beacons” that mark the spot for the important downstream factors 53BP1 and BRCA1 (Figure 2). The ubiquitin-dependent recruitment of BRCA1 has been shown to be mediated through the so-called BRCA1 A complex (Huen and Chen, 2010). An important component of this complex is the RAP80 protein, which directly binds to ubiquitylated histones via its two Ubiquitin Interaction Motifs (UIMs) (Yan et al. 2007). The function of the other components of the BRCA1 A complex (Abraxas, BRCC36, BRE and NBA1),

are not yet completely clarified (Huen and Chen, 2010). The core component, Abraxas, remains stably expressed throughout the cell cycle in contrast to BRCA1 that exhibit low protein levels during G1. Thus, it is likely that Abraxas might have additional functions besides recruiting BRCA1 to damaged chromatin (Wang et al. 2009; Choudhury et al. 2004). The retention of 53BP1 at sites of DNA damage is also dependent on the above mentioned ubiquitylation cascade, although neither bridging factors comparable to the BRCA1 A complex were identified for 53BP1 nor direct interaction between 53BP1 and ubiquitylated H2A-type histones was observed. On the other hand, 53BP1 seems to be recruited to DSBs in a slightly different manner that employs its tandem Tudor domain. This domain has been shown to be capable of binding methylated Lysine residues on core histones, preferentially binding di-methylated H4K20 (Huyen et al. 2004; Botuyan et al. 2006). Nevertheless, the precise role of the Tudor domain in targeting 53BP1 to DNA damage sites remains elusive. A recent study by Pei et al. demonstrated that the histone methyltransferase MMSET is recruited to DSBs via its interaction with the BRCT domain of MDC1. MMSET then mediates the local methylation of H4K20 at the DNA damage sites that, in turn, facilitates 53BP1 recruitment (Pei et al. 2011).

Due to the complex nature of the ubiquitylation cascades regulating IRIF formation, protein de-ubiquitylation via de-ubiquitylating enzymes (DUBs) likely plays an important role in the control of the duration and the magnitude of the response (Vissers et al. 2008). With the emerging roles of DUBs and the sumoylation machinery in regulating IRIF formation, this process could soon be exposed in its full complexity.

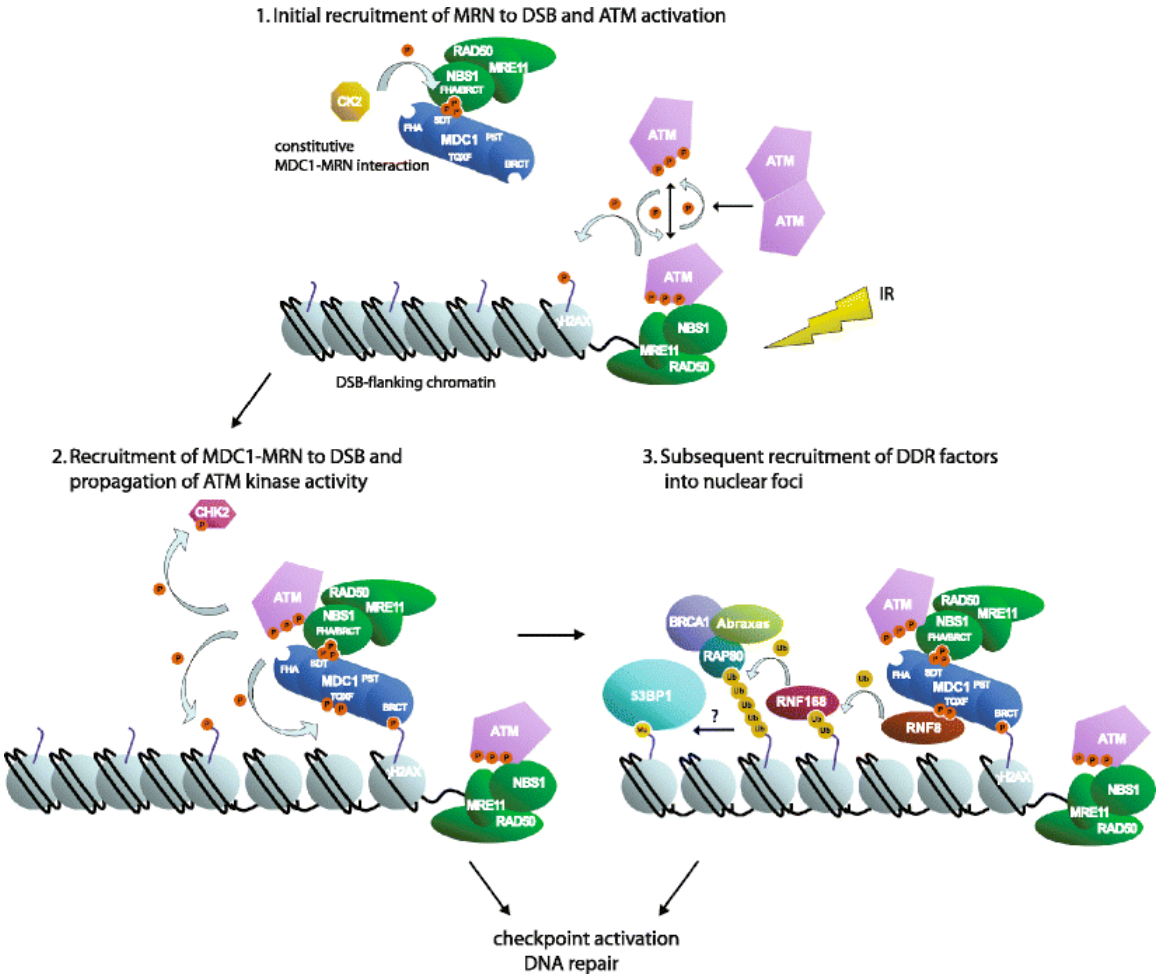

Fig. 2

Model of IRIF formation and checkpoint activation. (1) MRN recognizes and binds to a DSB, thus facilitating recruitment of ATM. ATM undergoes autophosphorylation, which leads to dissociation into active monomers. ATM phosphorylates H2AX in the DSB-flanking chromatin. (2) The γH2AX is recognized by MDC1, which in turn further recruits MRN via interacting with NBS1. (3) MDC1 is phosphorylated and itself recruits the E3 ubiquitin ligase RNF8 as well as additional DDR proteins. This triggers a signaling cascade that is dependent on the ubiquitylation of H2A-type histones and ultimately results in checkpoint activation and DNA repair. *Modified after (Jungmichel and Stucki, 2010)*

1.3. The DNA damage checkpoints

The term ‘cell-cycle checkpoint’ refers to mechanisms put in place to enforce dependency in the cell cycle by ensuring timely execution of process such as DNA replication or mitosis (Hartwell and Weinert, 1989). Thus, checkpoint pathways have the ability to control phase transitions. Given the critical significance of error-free DNA replication and chromosome segregation for the maintenance of genomic integrity and the prevention of cancer, cells have evolved the ability to trigger different cell cycle checkpoints upon DNA damage. These can transiently delay cell-cycle progression in G1, S or G2 phases or even impose prolonged cell-cycle arrests in either G1 or G2 before entry into the subsequent S phase or mitosis (Figure 3). At the molecular level, common denominator of all checkpoint pathways is the inhibition of cell cycle "controllers", namely the cyclin-dependent kinases. These are protein complexes responsible of ensuring the timely triggering and the execution of key events at phase transitions.

1.4.1. The G1/S checkpoint

To prevent the replication of damaged DNA, cells exposed to genotoxic stress in G1 phase activate ATM/ATR. The latter, in a cascade of phosphorylation events, activate the downstream kinases CHK2/CHK1 that, in turn, directly phosphorylate the protein kinase WEE1. WEE1 phosphorylates CDK2 at two residues (Thr14/Tyr15) located in Gly-rich P-loop of the kinase, which is the ATP binding site. Such phosphorylation does not affect nucleotide binding but hampers catalysis (reviewed in Ferrari 2006). In addition, checkpoint kinases phosphorylate members of the CDC25 family of double-specificity phosphatases on several serine or threonine residues. CDC25 phosphatases specifically remove phosphate from the two inhibitory sites in CDKs ATP-binding site, thus causing full activation of the CDK/Cyclin complexes (reviewed in Ferrari 2006). Whereas Cdc25B and -C are not required for mouse development or checkpoint function (Ferguson et al. 2005), and inhibition of these phosphatases by DNA damage essentially occurs by sequestration mechanisms (see below), CDC25A degradation via ubiquitin-proteasome pathways is a primary control mechanism both in dividing cells

and in response to DNA damage (Donzelli et al. 2003). Phosphorylation of CDC25A at Ser-124 by CHK2 was reported to be the primary event responsible for ubiquitylation-dependent degradation of the phosphatase (Falck et al. 2001). Later work showed, however, the inconsistency of these observations (Jin et al. 2008). Specifically, phosphorylation of CDC25A on Ser-76 by CHK1 was shown to serve as priming event that facilitates phosphorylation on Ser-79 and Ser-82 by protein kinase CK1 or glycogen synthase kinase-3β (GSK-3β) (Kang et al. 2008; Honaker and Piwnica-Worms, 2010). This, in turn, allows recruitment of the $SCF^{\beta\text{-}TRCP}$ E3 ligase that promotes CDC25A ubiquitylation (Busino et al. 2003).

The CHK1/CHK2-CDC25A checkpoint is rapid, since it is dependent on post-translational modifications, but it is also transient and can delay the G1/S transition only for a few hours. If cells need to impose a prolonged G1 arrest, a second pathway involving the tumour suppressor p53 is activated. Briefly, upon DNA damage p53 is directly phosphorylated by both ATM/ATR at Ser-15 and Ser-37 and the transducer kinases CHK2/CHK1 at Ser-20. In addition, the E3 ubiquitin ligase MDM2 that normally binds p53 and ensures rapid p53 turnover, is targeted by ATM/ATR, as well as by CHK2/CHK1 (Maya et al. 2001). These simultaneous modifications of p53 and MDM2 lead to disruption of the dimeric complex, $p19^{ARF}$-mediated sequestration of MDM2 in the nucleolus with consecutive stabilization and accumulation of the p53 protein (Meek 2009). Acetylation of p53 at the C-terminal Lysines that were target of MDM2 as well as at additional sites in the DNA binding domain facilitate p53 tetramerization, binding to its responsive elements in gene promoters and induction of transcription (Meek 2009). p53 most prominent target at the G1/S transition is $p21^{CIP1/WAF1}$ (inhibitor of cyclin-dependent kinases). Specifically, $p21^{CIP1/WAF1}$ inhibits kinase activity by physical engaging the complex with an inhibitory domain that stretches over both CDK2 and Cyclin E to obstruct substrate binding (Pei et al. 2005). Inhibition of CDK2/Cyclin E activity, in turn, results in incomplete phosphorylation of the tumor suppressor pRb, with consequent failure in releasing E2F1-3, the activating members of the E2F family of transcription factors, that are responsible for the transcription of Cyclin A and other S-phase genes (Attwooll et al. 2004)

1.4.2. The S-phase checkpoint

During the S phase of cell cycle, human cells replicate the entire genome, which is composed of some three billion base pairs, to obtain two identical copies. In order to preserve genetic information, duplication must be carried out with highly fidelity. Cells encountering altered DNA structures during replication activate the so-called intra-S-phase checkpoint, which slows down ongoing DNA synthesis and prevents firing of new origins (Bartek et al., 2004). This checkpoint operates via two parallel pathways, both of which are regulated by the ATM/ATR signaling cascade.

One branch of these effector mechanisms is through the CDC25A-degradation cascade described above. In addition to regulating CDK2/CyclinE, CDC25A is able to remove inhibitory phosphates from CDK2/CyclinA complexes to promote loading of the initiation factor CDC45 onto chromatin. CDC45 is a protein required for the recruitment of DNA polymerase α into assembled pre-replication complexes, hence the inhibition of CDK2 activity results in the inhibition of new origin firing (Bartek and Lukas, 2003).

The other branch of the intra-S-phase checkpoint operates through the ATM-mediated phosphorylation of NBS1 (Shiloh. 2003) and SMC1 (Structural maintenance of chromosomes 1) (So et al. 2011) on several sites. However, how phosphorylated SMC1 contributes in slowing down DNA replication is unknown.

Both branches of the intra-S-phase checkpoint lead to a transient slow down of DNA replication, allowing the repair of lesions before completion of replication. In case of failure to repair damage during this transient delay, cells complete replication and exit S phase. However, cells subsequently arrest in the G2 phase to tackle the persistent DNA damage.

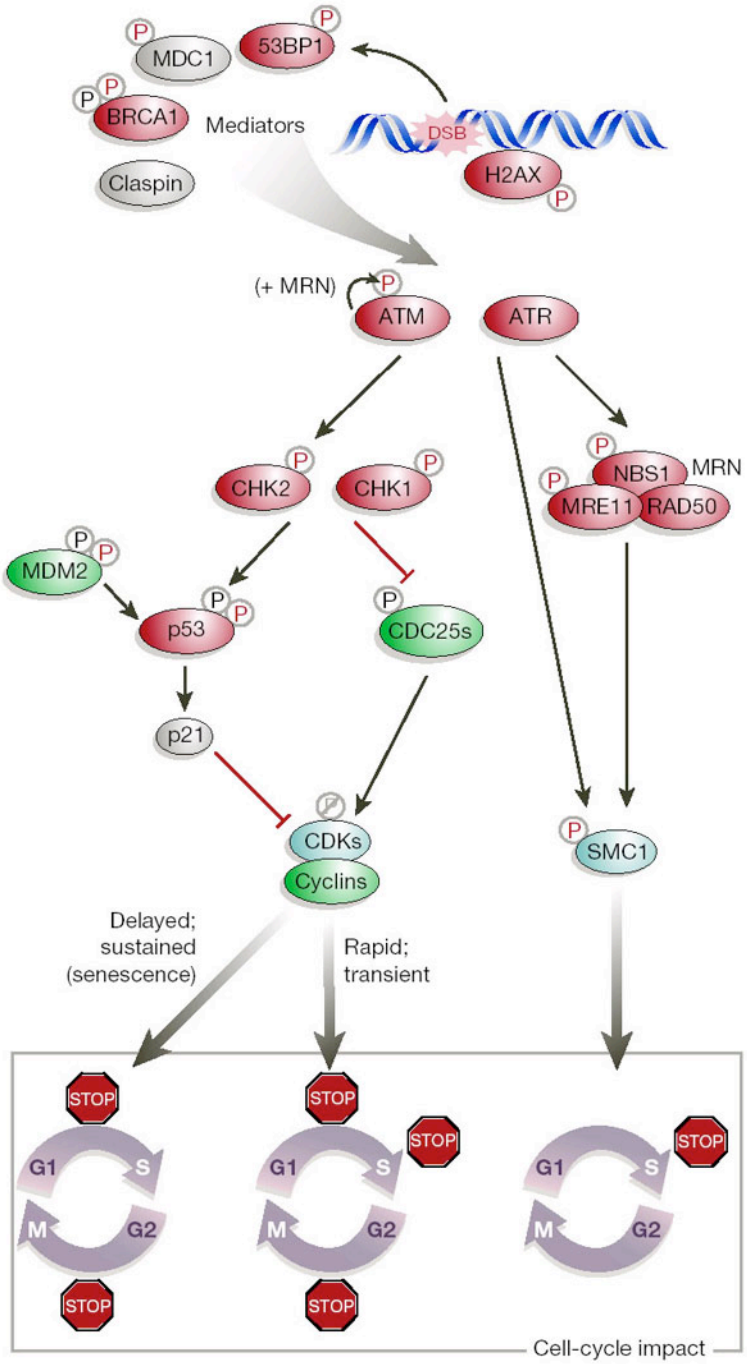

Fig.3

Cell-cycle checkpoints pathways. In response to DNA damage the checkpoint kinases ATM and ATR phosphorylate several targets including the transducing kinases CHK2 and CHK1. Phosphorylation of CHK2 and CHK1 leads to their activation and further transduction of the checkpoint signal to other important cell-cycle regulators, including the kinases WEE1/MYT1 (not shown), the CDC25 phosphatases and p53. Inhibition of CDKs leads to transient cell-cycle arrest, whereas p53 regulates the transcription of genes involved in DNA repair and apoptosis. *Modified after: (Kastan and Bartek, 2004)*.

1.4.3. The G2 checkpoint

The G2 checkpoint prevents cells from entering mitosis when they suffer DNA damage during transition through the G2 phase, or alternatively if they have progressed into G2 with unrepaired DNA lesions that occurred during the previous S or G1 phases. As sketched for the G1/S checkpoint, the final target of the G2 checkpoint is a CDK. Signals from unfinished DNA replication (through ATR/CHK1) or damaged DNA (through ATM/CHK2) activate the kinases WEE1/MYT1 that, in turn, phosphorylate active CDK1/CyclinB complexes causing inhibition of enzymatic activity. In parallel, checkpoint kinases phosphorylate CDC25 phosphatases (Donzelli and Draetta, 2003). Particularly, CHK1-dependent phosphorylation of CDC25A at Ser-124 and Thr-507 and of CDC25C at Ser-216 mediate recruitment of 14-3-3 proteins that displace the phosphatases from the nucleus, a mechanism that appears to be the primary way employed to inhibit CDC25A as well as CDC25C function during G_2 and mitosis (Uto et al. 2004). The mechanism of inhibition of CDC25B, which mediates the activation of CDK1/Cyclin B at the centrosome during prophase, has been extensively studied in relation to its mitotic role (Gabrielli 1996) but is less characterized in response to DNA damage.

Moreover, additional factors upstream of CDC25 or cyclin B/CDK1, such as the Polo-like kinases PLK3 and PLK1 (Nyberg et al. 2002), the PLK1 activator AurA (Krystyniak et al. 2006) and protein phosphatase PP2A (Yan et al. 2010) are also part of the G2/M checkpoint. Similar to G1 checkpoint, maintenance of the G2/M checkpoint partly relies on transcriptional regulation by p53 that, upon stabilization, induces transcription of the cell-cycle inhibitor $p21^{CIP1/WAF1}$. In addition, the expressions of 14-3-3σ (a scaffold and signaling protein), PUMA (BCL2 binding component 3), BAX (BCL2 partner and apoptotic activator), GADD45 (growth arrest and DNA-damage-inducible gene) are also regulated and are required for efficient arrest (Nyberg et al. 2002; Taylor and Stark, 2001).

1.4. DNA double-strand break repair

Classically, two conceptually different mechanisms can in principle repair DSBs occurring in the genome of higher eukaryotes: Non-homologous end joining (NHEJ) and homologous recombination repair (HR) (Heyer et al. 2010). As their names imply, NHEJ simply restores integrity in the DNA by joining the two ends without necessarily preserving the original sequence. As a result, it is error-prone. Because a second DNA molecule is not required for the function of this repair pathway, it is active throughout the cell cycle. HR, on the other hand is equipped to maintain fidelity in the sequence of the DNA molecule. To achieve this, HR requires an undamaged homologous sequence that serves as template for repair of the broken strands. There are two sources of homology in mammalian cells. The homologous chromosome that is present throughout the life cycle of the cell and the sister chromatid that is generated after DNA replication and which, therefore, exists only during the S and G2 phases of the cell cycle. Accumulating evidence supports the view that HR uses the sister chromatid as template rather than homologous chromosomes, a requirement that restricts the function of this pathway to the S and G2 phases of the cell cycle (Heyer et al. 2010). This requirement probably derives from the fact that in a eukaryotic cell nucleus the homologous chromosomes are accommodated in distinct and frequently distantly located domains that renders difficult the search for homology (a key step of HR) (Folle. 2008).

The fact that at least two genetically and conceptually distinct repair pathways are involved in the repair of DSBs raises questions regarding their coordination. If these pathways operate independently of each other it is possible that they compete against each other. On the other hand, if they collaborate, then the question is how their functions are coordinated. As stated above, the choice between the two pathways depends on the phase of the cell cycle. Studies of either NHEJ- or HR-deficient cells suggest that these two pathways compete for the repair of DSBs (Delacote et al. 2002). HR-deficient cells have a significant DSB repair defect only during the S/G2/M phases, whereas NHEJ-deficient cells showed reduced repair efficiency at all cell cycle stages (Hinz et al. 2005; Rothkamm et al. 2003). The mechanisms

by which cells decide between these two repair pathways have been studied for the past few years. According to the evidence obtained so far, DNA-end resection is a critical step that favors the choice of HR over NHEJ and it is regulated by cyclin-dependent kinases (CDKs) (Jazayeri et al. 2006), the master regulators of the cell cycle. Analysis carried out in yeast revealed that inhibition of CDK1/cdc28 in the G2-phase prevented end resection and checkpoint activation as well persistence of Mre11 at DSB sites, consistent with the idea that processing of the break had stalled (Ira et al. 2004). The authors also showed that CDK1 controls Mre11-associated nuclease function at the DSB, but does not influence its recruitment to DNA ends. In addition, Sae2, a DNA endonuclease that controls the initiation of DNA end resection in yeast (Lengsfeld et al. 2007; Clerici et al. 2005) is regulated by CDK-dependent phosphorylation (Huertas et al. 2008). Mutation of Sae2 Ser-267 to the non-phosphorylatable residue alanine (S267A) caused an end-processing phenotype comparable with deletion of Sae2. In contrast, mutating the same residue into a residue that mimics constitutive phosphorylation (S267E) complemented these phenotypes and bypassed the need for CDK activity in DSB end resection (Huertas et al. 2008). The Sae2-null and S267A mutants showed delayed HR and enhanced NHEJ, whereas the S267E mutant showed slightly enhanced recombination and a decrease in NHEJ. This indicates that CDK1/cdc28-mediated phosphorylation of Sae2 in yeast regulates the balance between HR and NHEJ during the cell cycle. The motif of Sae2 that contains the residue Ser-267 is highly conserved amongst orthologs in higher eukaryotes, and mutation of the analogous residue in human CtIP also resulted in hypersensitivity to camptothecin (Huertas et al. 2008). These results suggest that similar CDK control of DNA end resection exists in other organisms. Moreover, phosphorylation of a putative CDK site in human CtIP enables it to interact with the BRCA1 C-terminal tandem BRCT domain, an interaction that is required for efficient end resection (Yu and Hiom, 2009). This, in turn, suggests that the BRCA1-CtIP interaction influences the balance between HR and NHEJ. Collectively, these results support a model in which the commitment to DSB end resection and repair is regulated in order to ensure that the cell activates the most appropriate DSB repair pathway to optimize genome stability.

1.5.1. Non-homologous end-joining

NHEJ is the major pathway for DSBs repair in mammalian cells. It involves joining the two ends of a DSB through a process largely independent of homology. NHEJ provides a relatively simple mechanism for the repair of DSBs throughout the cell cycle, but of particular importance during G0-, G1-, and early S-phase (Delacote and Lopez, 2008). NHEJ only works efficiently and with high fidelity in the repair of DSBs displaying complimentary overhangs, 5' phosphates and 3' hydroxyl groups, so called 'clean' DSBs, such as those produced by nucleases. In yeast and mammalian cells, approximately 25-50% of nuclease DSBs is repaired by precise NHEJ (Clikeman et al. 2001). If the ends are not compatible, then processing is required and this can result in mutagenic deletions or insertions at the break site (Symington and Gautier, 2011). The molecular mechanism by which NHEJ operates could be simplified in three main steps: first both ends of the broken DNA are captured, second a molecular bridge is formed to bring the two DNA ends back together and, finally, the broken DNA ends are re-ligated.

Central to NHEJ in organisms from yeast to man is the Ku protein, a heterodimer of two subunits called Ku70 and Ku80 (Lieber 1999). Biochemical studies of mammalian Ku have showed that it can bind DNA in a non-sequence-dependent manner and that binding is dependent on DNA DSBs (Walker et al. 2001). The NHEJ process (Figure 4) is initiated by the binding of the Ku70/80 heterodimer to both ends of the broken DNA molecule, forming a ring-shaped structure, in which the opening of the ring accommodates a DNA helix. This feature allows the Ku heterodimer to slide over the ends of a broken DNA molecule (Walker et al. 2001). It is believed that the association of a DNA end with the Ku heterodimer creates a platform for the assembly of other NHEJ key enzymes and proteins. In vertebrates, Ku serves as the DNA targeting subunit for the DNA-dependent protein kinase catalytic subunit (DNA-PKcs), which together with the Ku forms the DNA-PK holoenzyme. The association of the DNA-PKcs with DNA activates its serine/threonine kinase activity. Among the different phosphorylation targets of DNA-PKcs are XRCC4, the nuclease Artemis and DNA-PKcs itself, which can undergo

autophosphorylation. This autophosphorylation is believed to influence its conformation and dynamics, serving to relieve blockage of the ends by DNA-PKcs, hence facilitating access of other repair factors (Weterings et al. 2003). Occasionally, the generated DSBs might require further processing to generate ligatable 5'-phosphorylated ends in order for repair to be completed. The nuclease Artemis, a single-stranded 5'-3' exonuclease, which upon phosphorylation by DNA-PKcs acquires an additional endonuclease activity specific for hairpins and ssDNA overhangs, as well as the polynucleotide kinase (PNK), together with DNA-PKcs have been shown to stimulate DNA-processing for efficient NHEJ (Ma et al. 2002). The processed DNA-ends might lead to the generation of DNA gaps that are filled in by DNA polymerases. Members of the DNA polymerase X family of polymerases, including polymerase μ, polymerase λ and terminal deoxyribonucleotidyltransferase (TdT), have been shown to fill the gaps generated during NHEJ (reviewed in McElhinny and Ramsden. 2004). Finally, NHEJ is completed by ligation of the DNA ends, a step carried out by the NHEJ ligase complex (also known as X4-L4), which is composed by XRCC4, DNA ligase IV and XLF (Grawunder et al.1997).

Alternative NHEJ acts in the absence of classical NHEJ factors such as Ku, XRCC4 or DNA ligase IV. There, repair events involve small deletions and require short stretches of homology between the ligatable DNA ends. Microhomology-mediated end-joining (MMEJ) is the dominant pathway during alternative end-joining. In this repair mechanism DNA is slightly resected (less than 100 nucleotides) to expose regions of homology, which lead to reattachment of the two DNA ends of the break. The DNA is further processed by nucleases that remove flaps and overhangs and eventually by DNA polymerases that fill in the gaps (Bennardo et al. 2008).

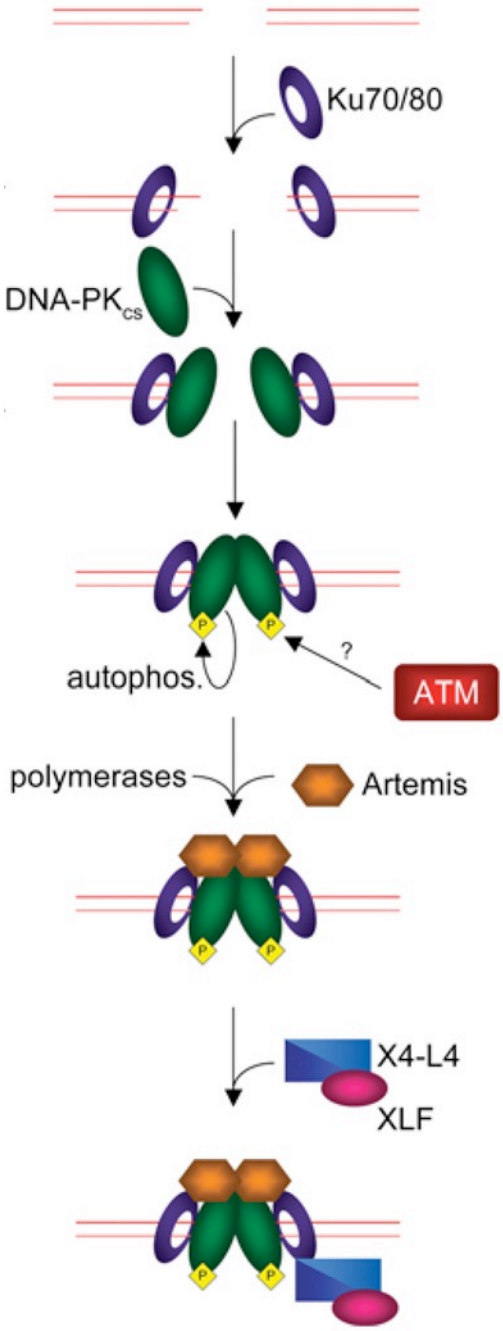

Fig. 4

NHEJ in mammalian cells. The Ku70/80 heterodimer binds broken DNA ends and recruits DNA-PKcs, which in turn tethers the DNA termini together. DNA-PKcs undergoes autophosphorylation-induced conformational alterations that allow the recruitment of Artemis and DNA polymerases of the X family of polymerases to generate ligatable DNA ends. Finally, the Ligase IV/XRCC4/XLF complex completes repair by ligating the two DNA ends. *Modified after (Hartlerode and Scully, 2009)*

1.5.2. Homologous recombination

The goal of HR is to facilitate recovery of information lost as result of damage to both strands by retrieving it from an undamaged homologous DNA sequence. To this end, damaged and undamaged DNA molecules need to directly interact. In particular, the damaged DNA molecule will need to first undergo processing in order to generate DNA structures that can “read-off” sequence information. Furthermore, the chromatin structure on both DNA molecules will need to be modified in order to facilitate the search for the homologous sequences in the sister DNA molecule. Once homology has been found, sequence information will need to be copied and finally the interacting DNA molecules will need to be separated.

HR starts with the resection of DNA ends around the DSB, forming 3’-single stranded DNA (ssDNA) stretches (Wyman and Kanaar, 2006). This form of DNA can invade and pair to homologous sequences present in an intact DNA molecule and is also suitable to be extended by DNA polymerases to copy the missing sequence information. In higher eukaryotes, initial resection of DNA ends is orchestrated by the MRN complex (D’Amours and Jackson, 2002), assisted by the function of the resection-promoting factor CtIP [CTBP (C-terminus-binding protein of adenovirus E1A)-interacting protein] (Sartori et al., 2007; Farah et al. 2009). These proteins collaborate to trim the DNA ends to an intermediate form in a process so-called “short-range” resection. The trimmed DSB is then resected more extensively in a step of “long-range” resection (Sartori et al. 2007; Jazayeri et al. 2006). Possible candidates are the exonuclease-1 (EXO1) and the Bloom’s syndrome protein (BLM) together with the nuclease DNA2 (Gravel et al. 2008; Nimonkar et al. 2011). The single-stranded 3’-overhangs generated in this process are coated by the replication protein A (RPA) heterotrimer, the major mammalian ssDNA binding protein (Figure 5). This rapid binding by RPA is believed to protect the ssDNA and to prevent the formation of secondary DNA structures (Fanning et al. 2006). In addition, RPA also mediates the recruitment of the ATR/ATRIP complex to the single stranded regions and initiates the DDR signaling cascades, which among others inhibit cell cycle progression through activation of the corresponding checkpoints (Cimprich and Cortez, 2008).

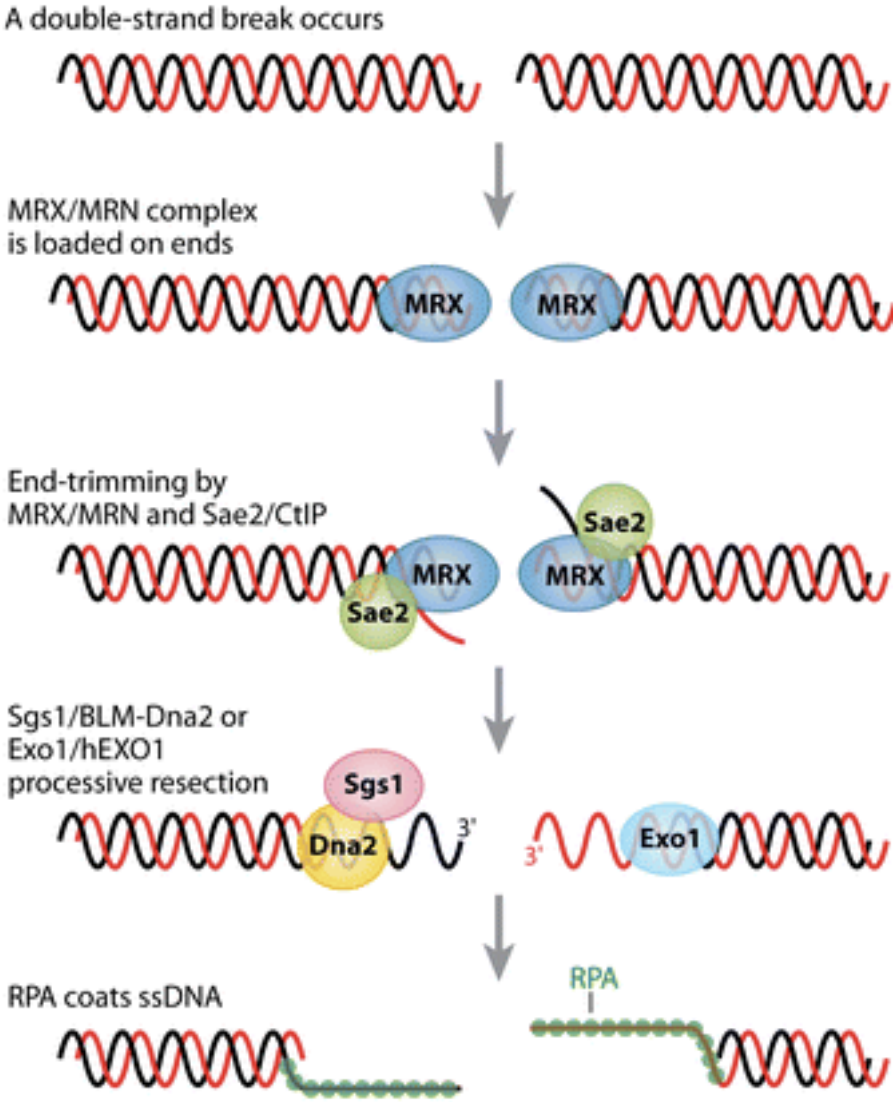

Fig. 5

Model for DNA double-strand break resection. The MRX complex in yeast or MRN in mammals recognizes DSBs. Mre11/MRE11 collaborates with the endonuclease Sae2/CtIP to trim the DNA ends, leaving short 3'-single stranded DNA overhangs. The DNA ends are further resected by either the Exo1/EXO1 exonuclease or by the Sgs1/BLM helicase and the Dna2/DNA2 nuclease, generating long stretches of ssDNA that are coated by RPA. *Modified after (Bernstein et al. 2010).*

The subsequent DNA strand invasion and homology search requires the formation of a nucleoprotein filament composed of Rad51 bound to ssDNA. Since RPA binds more avidly to ssDNA than Rad51, additional activities are required to load Rad51 onto RPA-coated ssDNA and to displace RPA. In mammalian cells, an important mediator complex is BRCA1/BARD1 and

BRCA2 (FANCD1)/DSS1, bridged by the PALB2 (partner and localizer of BRCA2) (FANCN) (Zhang et al. 2009). Loading of Rad51 is believed to occur through its direct interaction with BRCA2 (Pellegrini et al. 2002). This interaction is thought to be limited to S and G2 phases of the cell cycle, since CDK-dependent phosphorylation of BRCA2 during progression to mitosis leads to disruption of the complex (Esashi et al. 2005). The Rad51 nucleoprotein filament then invades a duplex DNA of the sister chromatid and searches for homology. Once found, the invading strand sets up a structure, which involves pairing with the complementary strand and displacement of the other, resulting in a so-called D-loop (displacement loop) structure. At this point, HR can be completed via several pathways and different outcomes. Synthesis-dependent strand annealing (SDSA) or double strand break repair (DSBR) have been described to occur in case of two-ended DSBs. In SDSA the elongated invading strand pairs with the second DSB end (Figure 6 pathway C). This process only produce non-crossovers, hence SDSA is the preferred recombination-mediated pathway for DSB repair in somatic cells to prevent loss of heterozygosity. Alternatively, during DSBR, the D-loop gets extended and captures the second DSB end, creating a double Holliday junction (HJ) between the four strands that can undergo branch migration, a process catalyzed by members of the RecQ helicase family (West 2003). HJ intermediates can be resolved in different ways resulting in either non-crossovers or crossovers, the later being predominant during meiotic recombination (Figure 6 pathway D and E). The BLM/Topo IIIα can dissolve HJ to form non-crossover products (Wu and Hickson, 2003). Alternatively, the MUS81-EME1 complex may cleave HJs to yeild crossovers (Chen et al. 2001). Two more HJ resolvases that has been recently identified in humans cells, GEN1 and SLX1/SLX4 promotes the resoultion of HJs by a mechanism that is believed to generate crossovers and non-crossovers (Ip et al. 2008; Svendsen et al. 2009; Fekairi et al. 2009).

In the abscence of a homology, single-strand annealing (SSA) can be the pathway of choice. SSA involves the exposing of repetitive sequences by resection of both 5'-strands until sequences are uncovered and annealed (Figure 6 pathway F). DNA flaps are then removed by nucleases followed by DNA synthesis and ligation of the nicks. Since SSA involves the deletion of

the intervening sequences, it is considered as a mutagenic repair pathway. One-ended DSBs generated through uncapping telomeres or collapsed replication forks after encountring a single strand break (SSB) or nick, are repaired by break-induced repair (BIR) (Figure pathway 6 G). In BIR, the invading 3'-strand forms a replication fork that copy long tracts from the donor DNA molecule. This process could potentially lead to loss of heterozygosity.

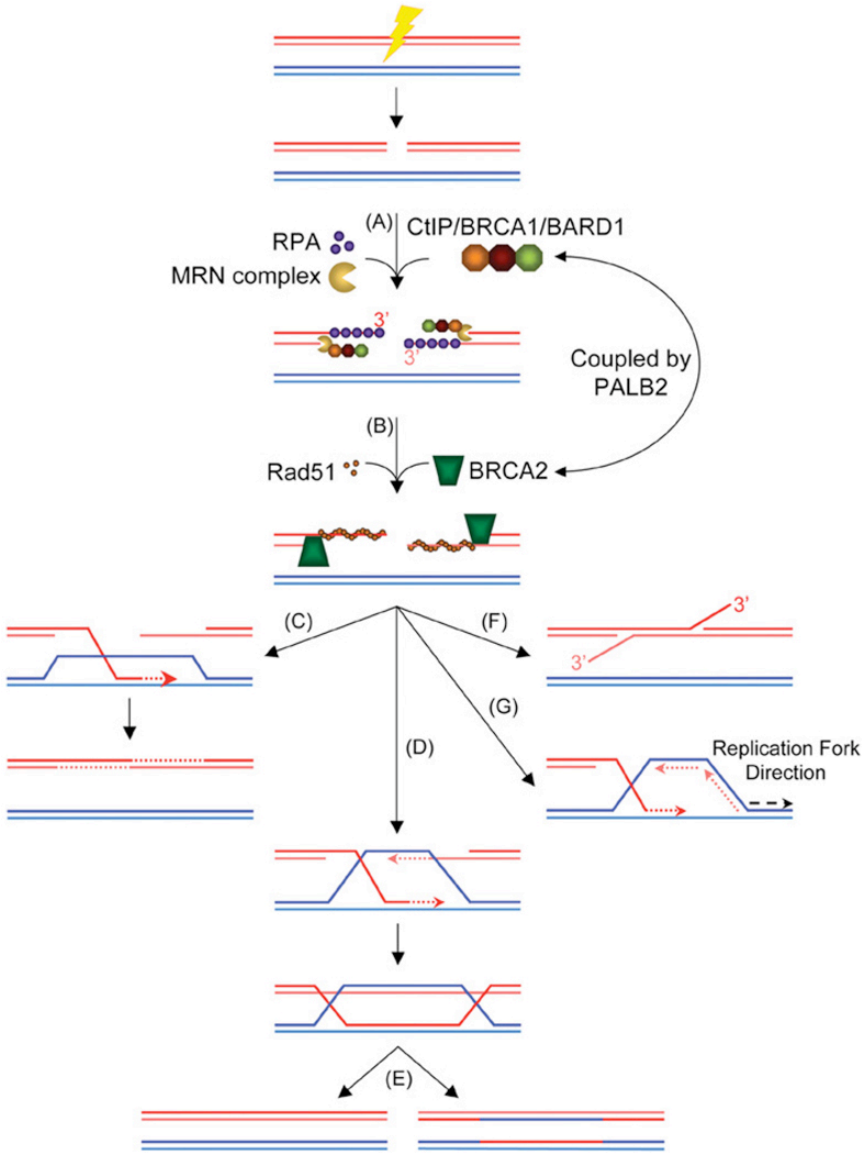

Fig. 6

Homology recombination in mammals. (A and B) The DSB is recognized by the MRN complex, which tethers the broken DNA ends and collaborates with the CtIP/BRCA1/BARD1 complex in DNA-end resection. The generated ssDNA is rapidly coated by the ssDNA binding protein RPA to prevent the formation of secondary structures. BRCA1/BARD1 promotes the accumulation of BRCA2 via PALB2. BRCA2 catalyze the loading of RAD51 to displace RPA molecules and form RAD51 nucleoprotein filaments. The RAD51 filament captures duplex DNA and searches for homology. Different repair

pathways can be initiated: (C) In SDSA the extended invading strand is displaced and anneals with the resected second DNA end. (D) In the DSB repair pathway both DNA ends are captured by annealing to the extended D-loop, forming a double HJ, which is resolved to generate either crossover or non-crossover products. (F) During SSA, direct repetitive sequences are revealed by resection of complementary strands that can be annealed while intervening sequences are deleted. (G) In BIR the 3'-end of the invading strand forms a replication fork that copy long tracts of the donor DNA strand. *Modified after (Hartlerode and Scully. 2009).*

1.6. DNA nucleases

1.6.1. General features of DNA nucleases

DNA, the carrier of genetic information of the majority of living organism, is composed of a sugar-phosphate backbone and four organic bases. DNA suffers from various environmental stresses, including damage caused by UV light, radiation and carcinogens that constantly modify its structure. Moreover, DNA accumulates errors that are intrinsic to the process of replication and displays unusual structures during recombination. In order to avoid alterations of the base sequence or entanglement of the DNA, these modifications must be corrected by the various repair protein machineries present in the cell. Such DNA repair proteins usually form complexes with other proteins, likely to facilitate targeting and gain efficiency. A core component of these complexes are nucleases, which play crucial roles in recognizing and processing replication or recombination intermediates. In addition, through their participation to various DNA repair processes such as mismatch repair (MMR), base excision repair (BER), nucleotide excision repair (NER) and double strand break repair, they also play a role in resolving DNA mismatches that occur during replication or eliminating damaged nucleotides.

Nucleases can be regarded as molecular scissors that catalyzes the cleavage of phosphodiester bonds between the phosphate and the sugar moieties in the backbone of the DNA. Nucleases can be generally divided into exonucleases and endonucleases. Exonucleases can be further classified as 5'-end processing or 3'-end processing enzymes, according to the polarity of consecutive cleavage. On the other hand, endonucleases hydrolyze internal

phosphodiester bonds within a polynucleotide chain, without the requirement of a free DNA end.

1.6.2. Exonuclease 1 (EXO1)

EXO1 is a member of the Rad2 family of nucleases. It was originally identified in the fission yeast *Schizosaccharomyces pombe* upon induction to undergo meiosis (Szankasi and Smith, 1992). *S. pombe* Exo1 was shown to catalyze the removal of mononucleotides from the 5' end of a DNA duplex or DNA nicks displaying 5'-3' polarity, acting preferentially on double-stranded DNA ends (dsDNA) to produce 3' single stranded overhangs (Szankasi and Smith, 1992). The human EXO1 gene encodes a protein that bears only 27% identity to its yeast ortholog (Tishkoff et al. 1998). However, it has been demonstrated that human EXO1 can complement the DNA damage sensitivity and the mutator phenotype that result from deletion of Exo1 in *Saccharomyces cerevisiae* (Qiu et al. 1999), indicating that at least certain aspects of EXO1 function appear to be conserved. *In vitro*, human EXO1 was show to be a structure specific nuclease, possessing 5'-3' exonuclease and 5'-flap endonuclease activities (Lee et al. 1999). EXO1 molecular mechanism of action was recently clarified and shown to be similar to that of other FEN nucleases (Orans et al. 2011)

EXO1 is involved in several DNA repair pathways including MMR, double strand break repair, post-replication repair as well as meiotic and mitotic recombination (Tran et al. 2004). The first established role for yeast EXO1 was deduced from its ability to physically interact with yeast and human MSH2 (Tishkoff et al. 1997), followed by the demonstration of its participation in MMR (Tishkoff et al. 1997; Tishkoff et al.1998). It was later demonstrated that EXO1 plays both catalytic and structural roles during MMR-mediated repair (Tran et al. 2002; Amin et al. 2001). Briefly, upon detection of a mismatched base, the MMR machinery is recruited (Figure 7), EXO1 carries out a controlled excision step that removes nucleotides in the newly made strand past the mismatch, creating a ssDNA gap that serves as a platform for DNA polymerase. The polymerase fills in the excised stretch and, finally, a DNA ligase seals the nick completing MMR (Jiricny 2006).

The involvement of EXO1 in DNA repair pathways suggests that it could play an important role in tumourigenesis. Consistent with this, a cancer-prone phenotype has been observed in Exo1-defiecient mice, where a clearly increased susceptibility to lymphoma development was observed (Wei et al. 2003).

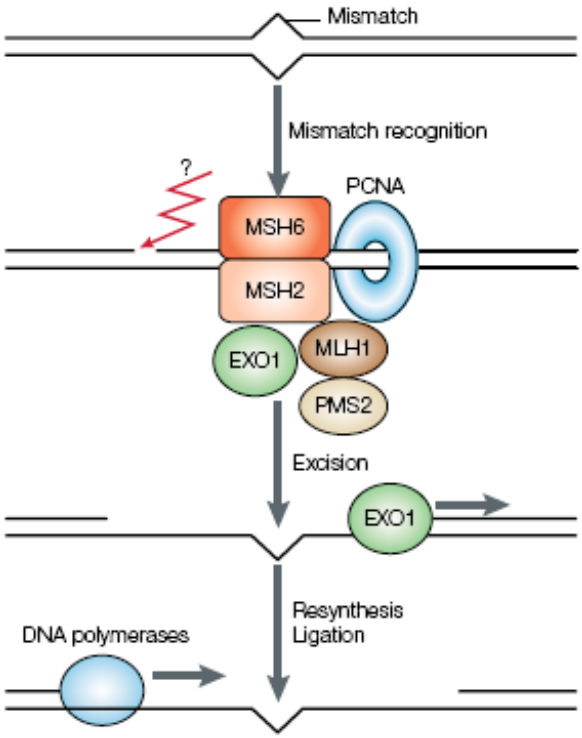

Fig. 7

The role of EXO1 in MMR. A single base-pair mismatch is detected and bound by MSH2-MSH6 heterodimers. This leads to the recruitment of the MMR machinery, including EXO1. The mismatched base is removed by an excision step executed by EXO1 and the generated gap is filled by DNA polymerases and DNA ligase. *Modified after (Martin and Scharff. 2002).*

Mounting evidence has shown that EXO1 plays an important role in DSB repair by executing a long-range resection step to generate extended stretches of ssDNA. This ssDNA serves to induce cell cycle checkpoints and is required for RAD51 mediated strand invasion of the sister chromatid for an efficient HR cascade. Cells depleted of EXO1 show chromosomal instability, hypersensitivity to IR and defects in HR-dependent DSB repair (Bolderson et al. 2010). Studies on the mechanism of DSB repair established that the MRN complex detects a DSB and, collaborating with CtIP, promotes DNA end

resection generating short ssDNA overhangs (Sartori et al. 2007). This initial resection step is followed by a more extensive step of resection carried out by redundant enzymes with EXO1 being an important exonuclease among them (Figure 8) (Mimitou and Symington, 2009).

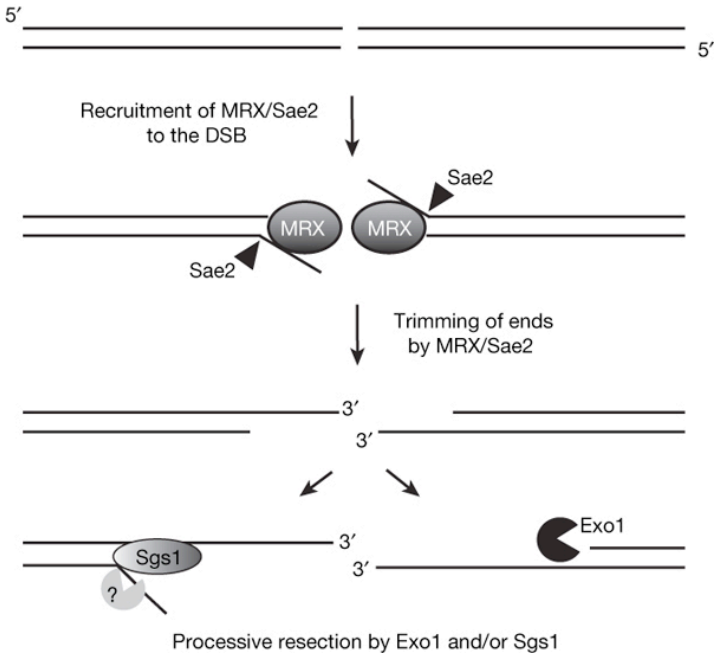

Fig. 8

DSB resection. The MRN complex (MRX in yeast) detects and binds a DSB. Together with CtIP (Sae2) they trim the free DNA ends creating short ssDNA overhangs that are suitable for a second resection step carried out by EXO1 (Exo1) or by the Sgs1 (BLM1) helicase and a single-stranded specific nuclease, believed to be DNA2 (Dna2). *Modified after (Mimitou and Symington, 2009).*

Accumulating evidence suggests that EXO1 plays also an important role at the replication fork. Data from *Saccharomyces cerevisiae* demonstrated that Exo1 acts in a redundant manner with Rad27 (FEN1 in human) in processing Okazaki fragments during the process of DNA replication (Tran et al. 2002). Moreover, Exo1 was shown to be recruited to stalled replication forks where it plays a role in preventing fork reversal by resecting newly synthesized strands and helping to resolve sister chromatid junctions (Cotta-Ramusino et al. 2005).

EXO1 nucleolytic activity is tightly regulated under DNA replication stress and other cellular responses to DNA damage. It was demonstrated in our and other laboratories that such control is exerted either by post-translational

modifications or by direct interaction with other proteins. Previous results from our laboratory showed that upon replication fork stalling in mammalian cells, EXO1 is phosphorylated in an ATR-dependent manner, a step that targets it to ubiquitin-mediated degradation through the proteosome pathway (El Shemerly et al. 2005; El Shemerly et al. 2008). In the study that is object of this thesis, we show that the interaction with CtIP restrains the exonucleolytic activity of EXO1 *in vitro* (Eid et al. 2010). Others have shown that, in response to ionizing radiation, ATM-mediated phosphorylation of EXO1 causes a decrease of its enzymatic activity, thus allowing to load RAD51 and complete HR (Bolderson et al. 2010). In line with this evidence, results from yeast demonstrated that Mec1-dependent phosphorylation of Exo1 modulate its activity at uncapped telomeres (Morin et al. 2008).

1.6.3. CtBP-interacting protein (CtIP)

CtIP, a protein conserved from yeast to humans, plays a critical role in multiple molecular pathways. Human CtIP was first identified by a yeast two-hybrid (Y2H) assay as one of the interacting proteins of the transcriptional suppressor CtBP (C terminus-binding protein) (Schaeper et al. 1998). CtBP binds to the c-terminal of adenovirus E1A, resulting in anti-tumourigenic activity (Boyd et al. 1993). Several other Y2H screenings with different “baits” identified CtIP. In another Y2H screen, in which the tumor suppressor retinoblastoma (Rb) protein was used as bait, CtIP was identified as RBBP8 (Retinoblastoma-binding protein 8) (Fusco et al.1998). Moreover, CtIP/RBBP8 was also found to associate with the Rb-related protein p130 in a different Y2H screen (Meloni et al. 1999). CtIP has also been isolated in another Y2H assay with LMO4 used as bait. LMO4 belongs to the LIM-only (LMO) group of transcriptional regulators (Sum et al. 2002). CtIP orthologs were also identified in yeast. Sae2/COM1 was identified in the budding yeast *Saccharomyces cerevisiae* (Prinz et al. 1997) and ctp1 was isolated from the fission yeast *Schizosaccharomyces pombe* (Limbo et al. 2007).

CtIP and its orthologs are involved in several biological processes. Among these is transcriptional regulation, where CtIP plays a central role by interacting with several proteins, primary among them being CtBP. CtBP acts

as a transcriptional co-repressor of a number of tumor suppressors such as PTEN and E-cadherin (Chinnadurai 2009). However, contrary to the proposed role of co-repressor, chromatin-immunoprecipitation (ChIP) experiments showed that CtIP can bind its own promoter and the promoter of another important E2F target such as cyclin D1 in late G1 and at the G1/S transition. In these experiments it was shown that concomitantly with the release of pRb, CtIP facilitated the G_1/S progression by activating transcription of a subset of E2F-responsive genes (Liu and Lee, 2006). In addition, it was also shown that CtIP can interact with the general transcription factors TATA binding protein (TBP) and transcription factor IIB (Koipally and Georgopoulos, 2002).

The role of CtIP in DSB repair (Figure 9) has been extensively studied. As mentioned above, CtIP plays an important role in HR by virtue of its function in the initial end-trimming of broken DNA ends of a DSB, a step that requires the combined action of both the MRN complex and CtIP (Sartori et al. 2007). Phosphorylation of Sae2 (Ser-267) by Cdc28 and of CtIP (Thr-847) by CDK2 is important for this initial resection step. Mutating this site into alanine was demonstrated to prevent phosphorylation and impair resection (Huertas and Jackson, 2009). Moreover, CtIP depletion using specific siRNA oligonucleotides sensitizes human cells to camptothecin and impairs HR (Sartori et al. 2007). CtIP is required not only for HR repair in S and G2 phases of the cell cycle but also for a specialized end-joining pathway known as microhomology-mediated end joining (MMEJ) or alternative-NHEJ (A-NHEJ), which is activated in G1 phase of the cell cycle upon generation of DSBs in human cells (Yun and Hiom, 2009; Quennet et al. 2010).

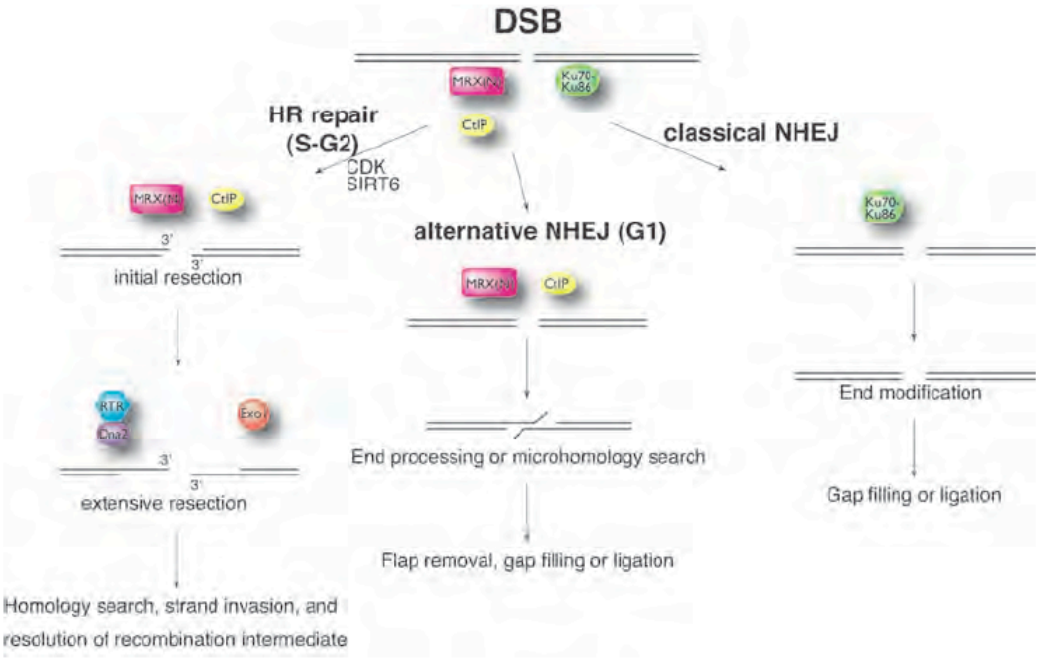

Fig. 9

Roles of CtIP in DSB repair. DSBs are detected and bound by the MRN complex that, together with CtIP, promotes an initial short-range resection step, generating short 3'- ssDNA overhangs. This is followed by a second more extensive resection step that is executed by EXO1 and/or other nucleases and helicases to promote homologous recombination in the S/G2 phases of the cell cycle. In addition, a DSB bound by MRN is processed by the combined action with CtIP to free DNA termini, leading to a microhomology search and subsequent gap ligation through a pathway called alternative NHEJ. Alternatively, a DSB can be bound by Ku70/86 heterodimer that activate the classical NHEJ pathway. Modified after (Tsutsui et al. 2011)

2. RESULTS

2.1. DNA end resection by CtIP and Exonuclease 1 prevents genomic instability

Wassim Eid[1,2], Martin Steger[1,2], Mahmoud El-Shemerly[2,3], Lorenza P. Ferretti[1], Javier Peña-Diaz[1], Christiane König[1], Emanuele Valtorta[1], Alessandro A. Sartori[1,4] and Stefano Ferrari[1,4]

[1]Institute of Molecular Cancer Research, University of Zurich, Winterthurerstrasse 190, CH-8057 Zurich, Switzerland

Running Title: DNA end resection by CtIP and EXO1

Keywords: DNA double-strand break repair, CtIP, Exonuclease 1, camptothecin

Character count (including spaces): 27'004

[2] These authors contributed equally to the study

[3] Present address: Biomedical Research Foundation, Lauchefeld 31, CH-9548 Matzingen, Switzerland

[4] Corresponding Authors:
sferrari@imr.uzh.ch
ph. (+41) 44 635 3471
fax (+41) 44 635 3484
sartori@imcr.uzh.ch
ph. (+41) 44 635 3473
fax (+41) 44 635 3484

ABSTRACT

DNA end resection, essential for the repair of DNA double-strand breaks (DSBs) by homologous recombination, relies initially on the partnership between MRE11-RAD50-NBS1 (MRN) and CtIP, followed by a processive step involving helicases and exonucleases such as EXO1. Here, we show that EXO1 localization to DSBs depends on both CtIP and MRN. Furthermore, we establish that CtIP interacts with EXO1 and restrains its exonucleolytic activity *in vitro*. Finally, we reveal that upon exposure to camptothecin, depletion of EXO1 in CtIP-deficient cells increases the frequency of DNA-PK-dependent radial chromosome formation. Thus, our study uncovers novel important functions of CtIP and EXO1 in DNA end resection and sheds new light on the regulation of DSB repair pathways, a key factor in the maintenance of genome integrity.

INTRODUCTION

DNA double-strand breaks (DSBs) are the most cytotoxic lesions that can be generated by ionizing radiation (IR), certain chemotherapeutic drugs, collapse of stalled DNA replication forks or during physiological processes such as meiotic recombination (Bassing et al, 2002; Whitby, 2005). Misrepaired DSBs may cause gross chromosomal aberrations that, in turn, trigger carcinogenesis through activation of oncogenes or inactivation of tumor suppressor genes. Cells utilize two main mechanisms to repair DSBs: non-homologous end-joining (NHEJ) and homologous recombination (HR) (Misteli & Soutoglou, 2009; Wyman & Kanaar, 2006). Rejoining of DSBs by NHEJ takes place throughout the cell cycle, whereas HR is restricted to S and G2 phases. HR is initiated by 5'-3' resection of DSBs to produce single-stranded DNA (ssDNA) tails that function as a signal for ATR-mediated DNA damage checkpoint activation prior to the recruitment of recombination proteins (Pardo et al, 2009).

A wealth of studies has addressed the molecular mechanisms of DNA end resection in different genetically amenable organisms. The evidence obtained has implicated the MRE11-RAD50-NBS1/Xrs2 (MRN/MRX) complex together with CtIP/Sae2 in the early stages of DSB processing, followed by the redundant action of BLM/Sgs1 helicase and exonuclease 1 (EXO1) in the generation of long stretches of ssDNA (Mimitou & Symington, 2009). Accordingly, only the simultaneous depletion of BLM and EXO1 resulted in accumulation of partially resected intermediates and hypersensitivity to DSB-inducing agents (Gravel et al, 2008; Mimitou & Symington, 2008; Zhu et al, 2008). These studies led to a two-step model according to which in human cells the initial "end-trimming" is carried out by MRN and CtIP, followed by a processive step of resection involving two alternative mechanisms depending either on EXO1 or BLM (Niu et al, 2009).

Here we show that EXO1 is recruited to laser-induced DSBs in a CtIP-dependent manner and that CtIP interacts with EXO1, thereby retarding processive degradation of DNA by EXO1 *in vitro*. Furthermore, we provide evidence that concomitant depletion of CtIP and EXO1 in camptothecin-

treated cells leads to chromosomal rearrangements, which is likely the result of illegitimate NHEJ-dependent repair of DSBs.

RESULTS AND DISCUSSION

EXO1 localization to sites of DNA damage

Based on the proposed two-step model of DNA end resection, we hypothesized that the recruitment of EXO1 to DSBs would depend on the initial processing by MRN and CtIP. Since endogenous levels of EXO1 are undetectable by direct immunostaining (El-Shemerly et al, 2005), we examined EXO1 localization to laser microirradiation-induced DSBs (Bekker-Jensen et al, 2006) using U2OS cells stably expressing GFP-tagged EXO1 (Gravel et al, 2008). Similar to what has been previously reported, we observed accumulation of EXO1 at sites of DSBs (Bolderson et al, 2010) (Fig 1A; supplementary Fig S1A, S1B). Consequently, we asked whether depletion of CtIP or the MRN complex (Fig 1B) would affect EXO1 recruitment to DSBs. Both fixed and live-cell imaging showed that depletion of either CtIP or MRE11 impaired the recruitment of EXO1 and RPA2 to DSBs (Fig 1C; supplementary Fig S1B). Furthermore, in CtIP-depleted cells we did not observe a delayed EXO1 recruitment at sites of damage (supplementary Fig S1A, S1B). In addition, downregulation of BLM did not impair EXO1 recruitment to DSBs (data not shown). Consistent with the S/G2-specific recruitment of CtIP to DSBs (Sartori et al, 2007), accumulation of GFP-EXO1 at DSBs was only observed in Cyclin A-positive cells and was strictly CtIP-dependent (Fig 1D). Finally, EXO1, but not CtIP, failed to localize to sites of laser-induced DSBs in ATLD1 cells, which are deficient in DSB resection due to a hypomorphic mutation of the MRE11 gene (Carson et al, 2003; Stewart et al, 1999) (supplementary Fig S1C-E). This defect was rescued upon re-expression of wild-type MRE11 (supplementary Fig S1F). From these observations, we concluded that the recruitment of EXO1 to DSBs depends on the initial DSB-end trimming carried out by MRN together with CtIP.

CtIP directly interacts with EXO1 and restrains its exonucleolytic activity

Although independently recruited to sites of DSB (supplementary Fig S1E) (Chen et al, 2008; Lisby et al, 2004), CtIP was shown to interact with MRN and to stimulate its endonuclease activity *in vitro* (Sartori et al, 2007), indicative of a functional relationship between these two key factors during DNA end resection. This prompted us to examine whether EXO1 physically associates with the MRN-CtIP complex. To test this hypothesis, CtIP or EXO1 were immunoprecipitated from HEK293T whole cell extracts (WCEs) and the recovered complexes analyzed by immunoblotting. Interestingly, CtIP, but not MRE11 was present in anti-EXO1-immunocomplexes both in non-stressed cells and in cells treated with camptothecin (Fig 2A), a chemotherapeutic agent known to induce DSBs exclusively during DNA replication by trapping DNA topoisomerase 1 cleavage complexes (Pommier, 2006). Even though we noticed that EXO1 preferentially interacts with the hyperphosphorylated form of CtIP in damaged cells (Fig 2A, lane 8), we did not observe any substantial differences in CtIP-EXO1 interaction upon phosphatase treatment of the CtIP-EXO1 immunocomplex (supplementary Fig S2A). While we confirmed the previously reported CtIP-MRE11 interaction, we were unable to detect EXO1 in anti-CtIP immunocomplexes, likely due to low cellular levels of EXO1 (El-Shemerly et al, 2005). Therefore, we immunoprecipitated CtIP from HEK293T cells transiently expressing OMNI-tagged EXO1. Under these conditions, we detected EXO1 in anti-CtIP immunocomplexes, both in presence and absence of hydroxyurea (supplementary Fig S2B).

To investigate whether the interaction between CtIP and EXO1 is direct or rather relies on additional bridging factors, we examined CtIP-EXO1 complex formation using purified, recombinant proteins in an anti-EXO1 immunoprecipitation experiment (Fig 2B). Although a minor fraction of CtIP was unspecifically bound to beads, CtIP was clearly enriched when equimolar amounts of EXO1 were present (Fig 2B, lane 4), thus demonstrating that the two proteins are able to directly bind to each other *in vitro*.

S. cerevisiae Sae2 displays endonuclease activity on defined substrates (Lengsfeld et al, 2007). Although a similar activity has not yet been reported for human CtIP, CtIP was shown to enhance the endonucleolytic activity of

MRE11-RAD50 complex (Sartori et al, 2007). Based on these observations, we addressed whether CtIP might also affect the 5'-3' exonuclease activity of EXO1 *in vitro*. For this purpose, we first examined the activity of purified recombinant EXO1 (supplementary Fig S2C) using a singly-nicked plasmid DNA substrate. Importantly, only wild-type EXO1, but not a catalytically-dead mutant, was able to completely degrade the nicked strand within 30 minutes of incubation, indicating that our preparation was devoid of contaminant exonuclease activities (supplementary Fig S2D). Remarkably, the addition of equimolar amounts of CtIP decreased exonucleolytic processing, while it did not inhibit the activity of *E. coli* exonuclease III (Fig 2C). Under similar assay conditions, MRE11-RAD50 did not substantially affect EXO1 activity (supplementary Fig S2E). In addition, we observed a similar inhibitory effect of CtIP on EXO1 activity using either a radiolabelled DNA oligonucleotide substrate (Fig 2D) or a linearized plasmid (Fig. 2E) both containing 3'-overhangs, the preferred substrate for EXO1 *in vitro* (supplementary Fig S2G) (Lee & Wilson, 1999). Electrophoretic mobility shift assays showed that, in contrast to EXO1, CtIP did not efficiently bind to the oligonucleotide substrate (supplementary Fig S2F), excluding the possibility of a non-specific inhibition of EXO1 by CtIP through steric hindrance. As observed with the nicked plasmid, CtIP did not inhibit the activity of *E. coli* exonuclease III on the linear substrate (data not shown). Moreover, neither MRE11-RAD50 nor BLM affected EXO1 activity on the plasmid with 3'-overhangs (supplementary Fig S2H). Interestingly, pre-incubation of CtIP with either blunt-ended or 5'-overhang substrates somehow facilitated processing by EXO1, compared to the situation in which the proteins were added in the reversed order (supplementary Fig S2I).

The evidence obtained from these biochemical data may suggest that CtIP is potentially able to restrain long-range resection by EXO1, thereby generating appropriate recombinogenic ssDNA structures (Mimitou & Symington, 2009; Niu et al, 2009). Inhibition of EXO1 activity was also reported during repair of DNA mismatches. However, while in mismatch repair RPA (Genschel & Modrich, 2009) or possibly MutLα (Zhang et al, 2005) are required for

terminating EXO1 activity upon removal of the mismatch, our data suggest that CtIP may act to fine-tune the nucleolytic activity of EXO1.

CtIP and EXO1 promote resistance to camptothecin and prevent genomic instability

Our observations indicate that the initial end-trimming activity of MRN-CtIP is required for the recruitment of EXO1 to sites of DNA damage and that CtIP may subsequently control EXO1 exonucleolytic activity to facilitate HR. This prompted us to examine whether some of the phenotypes reported for CtIP-deficient cells in response to camptothecin require EXO1 (Sartori et al, 2007). To this end, we employed siRNA-mediated downregulation of CtIP and EXO1 and monitored various DNA damage phenotypes in response to camptothecin. Importantly, single or combined depletion of CtIP and EXO1 did not significantly affect transition through S-phase, as judged by flow cytometry and incorporation of 5-ethynyl-2'-deoxyuridine in DNA (supplementary Fig S3A, S3B). As previously shown, CtIP knock down led to a decrease in CHK1 and RPA2 phosphorylation (supplementary Fig S3C), indicative of inefficient resection and impaired ATR activation (Sartori et al, 2007). On the other hand, EXO1 depletion had no major impact on ATR signaling, apart from a modest increase in RPA2 hyperphosphorylation (supplementary Fig S3C). Moreover, the pattern of camptothecin-triggered DNA damage signaling events in cells simultaneously depleted for CtIP and EXO1 did not vary from that of CtIP singly-depleted cells (supplementary Fig S3C). Taken together, these data strengthen the view that EXO1 acts downstream of CtIP and MRN in DNA end resection and are consistent with studies reporting an alternative, EXO1-independent mode of processive resection (Gravel et al, 2008; Mimitou & Symington, 2008).

Next, we analyzed the sensitivity of these cells to an acute treatment with camptothecin by colony formation assays. Consistent with previous reports, we found that CtIP downregulation caused hypersensitivity to camptothecin, while EXO1 depletion conferred only minor cytotoxicity (Fig 3A) (Gravel et al, 2008; Sartori et al, 2007). Interestingly, we observed a partial, but statistically significant rescue of sensitivity at low camptothecin concentrations by

simultaneous downregulation of CtIP and EXO1 (Fig 3A, 3B). Consistent with this, we monitored a similar increase in survival upon chronic treatment with camptothecin (Fig 3C). To extend our observations we treated cells with Olaparib, an inhibitor of poly(ADP-ribose) polymerase (PARP) (Helleday et al, 2008). Since PARP is involved in the repair of DNA single strand breaks (SSBs) (Hoeijmakers, 2001), it was proposed that PARP inhibition results in the accumulation of replication-associated DSBs (Bryant et al, 2005; Farmer et al, 2005), thus creating lesions similar to those caused by camptothecin (Pommier, 2006). Ultimately, treating singly- or doubly-depleted cells with Olaparib resulted in a pattern of hypersensitivity similar to that of camptothecin (supplementary Fig S3D).

Thus far, we conclude from our data that CtIP and EXO1 act in the same pathway, but they also point to a potentially novel genetic interdependency between these two factors during the repair of replication-associated DSBs. To gain further, structure-based insight into the repair of camptothecin-induced lesions, we analyzed metaphase spreads from cells lacking CtIP and EXO1. Compared to control cells, we observed that EXO1-deficient cells displayed a slight increase in broken chromatids, while depletion of CtIP led to a reduction of this type of chromosomal aberrations (supplementary Fig S3E). Interestingly, however, we noticed a significant increase of radial chromosomes specifically in doubly-depleted cells, indicative of repair by illegitimate end-joining of DSBs (Fig 3D; supplementary Fig S3F).

CtIP and EXO1 cooperate to prevent hazardous DNA-PK-dependent end-joining

It has been shown that DNA replication-associated DSBs, such as those induced by camptothecin, activates DNA-PKcs, judged by autophosphorylation on S2056 (Chen et al, 2005; Sakasai et al, 2010) (supplementary Fig S4A). Analyzing S2056 autophosphorylation, we observed increased DNA-PKcs activation particularly in doubly-depleted cells, and the signal was further amplified in response to camptothecin (Fig 4A). This prompted us to reexamine camptothecin-induced chromosomal aberrations upon inhibition of DNA-PKcs (supplementary Fig S4A). Under

these conditions we observed an almost 3-fold reduction of radial structures in EXO1/CtIP-deficient cells, while DNA-PKcs inhibition had no major effect in singly-depleted cells (Fig 4B; supplementary Fig S4B and data not shown). Consistently, and in agreement with an upregulation of NHEJ in absence of CtIP and EXO1, DNA-PKcs inhibition dramatically increased the number of camptothecin-induced breaks measured by PFGE (Fig 4C; supplementary Fig S4C).

CONCLUDING REMARKS

Taken together, our data imply that two factors involved in DNA end resection, CtIP and EXO1, most likely act as a unit to maintain genomic stability by protecting cells from the deleterious consequences of end-joining-mediated repair of camptothecin-induced DNA lesions. A similar scenario was reported for the repair defects in Fanconi anemia cells (Adamo et al, 2010; Pace et al, 2010). Therefore, we speculate that hypersensitivity to replication-associated DSBs in resection-compromised cells is most likely the result of inappropriate NHEJ rather than HR-deficiency *per se*.

METHODS

Live cell imaging and laser micro-irradiation - DSBs were generated in the nuclei of living cells on 18 mm glass cover slips by micro-irradiation of arbitrarily shaped regions of interest (ROI) at 355 nm with 15 mW output power of the laser (Genesis 355-80, Coherent Inc.) (Walter et al, 2003). ROIs were irradiated for 10 consecutive times and identical ROIs were used in all experiments. Subsequently, fluorescence time-lapse imaging was performed for GFP (488 nm excitation, 525-560 nm emission; SP5, Leica, Mannheim, Germany) using a HCX Plan-Apo 63X/NA 1.40 oil immersion objective. Pre-sensitization with 10 µM bromodeoxyuridine (BrdU) was used to avoid artifacts by high local density of DSBs. Non pre-sensitized, control cells showed lack of EXO1 and CtIP recruitment under the same settings. Cells were kept in complete growth medium under 5% CO_2 at 37°C during the experiments.

For fixed cell imaging, DSBs in defined nuclear volumes were generated by micro-irradiation (MMI CellCut) with a 355 nm UV-A laser adjusted at 50% of the power. Prior to irradiation, cells were grown for 24 h in the presence of 10 µM BrdU.

Cell culture and transfections - HEK293T cells were maintained as described (El-Shemerly et al, 2005). Human U2OS osteosarcoma cells and U2OS cells stably expressing GFP-HA-EXO1 (kindly provided by S. P. Jackson, University of Cambridge, UK) were cultured in DMEM supplemented with 10% fetal calf serum, standard antibiotics and G-418 (0.5 mg/ml). Immortalized ATLD1 cells transduced with retrovirus expressing the wild-type MRE11 cDNA (ATLD1/MRE11) or retrovirus harboring the empty vector (ATLD1/vector) (a kind gift of M. Weitzman, Salk Institute, S. Diego, CA) were grown in DMEM supplemented with 20% FCS, streptomycin/penicillin (100 U/ml) and 1 µg/ml puromycin (Sigma). GFP-EXO1 (kindly provided by F. Marini, University of Milano, Italy) was transiently transfected in ATLD1 cells using Fugene HD (Roche).

All siRNA duplexes were purchased from Microsynth (Switzerland) with the

exception of MRE11 siRNA, which was purchased from Dharmacon (USA). siRNA sequences are as follow: Luciferase (siCNTL) (CGUACGCGGAAUACUUCGATT) (Sartori et al, 2007), CtIP (GCUAAAACAGGAACGAAUCTT) (Sartori et al, 2007), EXO1 (CAAGCCUAUUCUCGUAUUUTT) (Gravel et al, 2008), and MRE11 (GAGCAUAACUCCAUAAGUATT) (Adams et al, 2006). siRNA duplexes were transfected into cells using Lipofectamine RNAiMAX (Invitrogen) in two consecutive rounds to a final concentration of 80 nM as follows: control (80 nM luciferase siRNA), EXO1 (40 nM EXO1 siRNA + 40 nM control siRNA), CtIP (40 nM CtIP siRNA + 40 nM control siRNA), or combined EXO1 and CtIP (40 nM EXO1 siRNA + 40 nM CtIP siRNA). Experiments were typically performed 72h.

Antibodies and chemicals - Antibodies were purchased from S. Cruz Biotech. (goat polyclonal anti-CtIP and anti-OMNI, mouse monoclonal anti-CHK1 and anti-GFP, rabbit polyclonal anti-Cyclin A); Sigma (mouse monoclonal anti-beta-tubulin and anti-FLAG); Cell Signaling Tech. (rabbit monoclonal anti-γH2AX and anti-CHK1-pS345); Upstate Biotech. Inc. (mouse monoclonal anti-γH2AX); Novus Biologicals (rabbit polyclonal anti-MRE11); GeneTex (mouse monoclonal anti-MRE11); Calbiochem (mouse monoclonal anti-RPA2); NeoMarkers (mouse monoclonal anti-EXO1); Abcam (rabbit polyclonal anti-pS2056-DNA-PKcs); or described previously (rabbit polyclonal anti-EXO1, F-15) (El-Shemerly et al, 2005)

Polyclonal and mouse monoclonal anti-CtIP antibodies (Sartori et al, 2007) were provided by R. Baer (Columbia University, New York, NY). Secondary HRP-conjugated anti-mouse and anti-rabbit antibodies were form GE-Healthcare and the HRP-conjugated anti-goat was from S. Cruz Biotech. Alexa Fluor-488, -594, and -647-conjugated secondary antibodies were from Invitrogen.

Camptothecin (Sigma) and AZD2281 (Olaparib, Selleck Chemicals) were dissolved in DMSO at 1 mM and 10 mM stock concentrations, respectively. Hydroxyurea (Sigma) was dissolved in water at 1 M stock concentration. EdU (5-ethynyl-2'-deoxyuridine) was from Invitrogen. The DNA-PKcs inhibitor

NU7441 (Tocris Bioscience) (Leahy et al, 2004) was dissolved in DMSO at 5 mM stock concentration. The *E. coli* exonuclease EXOIII was from New England Biolabs.

Immunofluorescence staining and analyses - Cells grown on cover slips were either fixed directly in ice-cold methanol for 15 min or pre-extracted for 5 min on ice using 25 mM HEPES pH 7.4, 50 mM NaCl, 1 mM EDTA, 3 mM $MgCl_2$, 300 mM sucrose and 0.5% Triton X-100 before fixation in 4% formaldehyde (w/v) in PBS for 15 min at room temperature (RT). Cover slips were incubated overnight at 4 °C with primary antibodies and Alexa–conjugated secondary antibodies for 1h at RT. The cover slips were mounted with Vectrashield® (Vector Laboratories) containing DAPI. Images were acquired either using a Leica confocal SP2 or an Olympus IX81 fluorescence microscope.

Western blotting and Immunoprecipitation – Cells lysis, immunoprecipitation and immunoblot analysis were performed as described previously (El-Shemerly et al, 2008). To ensure that the observed interactions were not DNA-mediated, ethidium bromide was included in all samples.

***In vitro* protein interaction -** 200 ng of purified, recombinant CtIP (Sartori et al, 2007) and EXO1 (El-Shemerly et al, 2005) were incubated either alone or together for 30 min at 4 ^{o}C in 1 ml TNE buffer containing 50 mM Tris-HCl, pH 7.5, 140 mM NaCl, 1 mM EDTA and 10 μg/ml BSA. Proteins were immunoprecipitated with the antibody F-15 for 2h at 4 ^{o}C. Protein-A sepharose (GE Healthcare) immunocomplexes were analyzed as described (El-Shemerly et al, 2005).

Exonuclease assays - The nicked substrate was generated by incubating the pGEM-13Zf(+) plasmid derivative with *N.Bst*NBI (Fischer et al, 2007) and purified by gel extraction (Qiagen). Exonuclease activities were assayed in a buffer containing 50 mM Tris-HCl pH 7.5, 50 mM NaCl, 2 mM $MgCl_2$, 1 mM DTT and 0.1 mg/ml BSA. Where indicated, final concentrations of purified

recombinant proteins were as follows: 15 nM EXO1, 15 nM CtIP and 300 nM RPA. Notably, the presence of purified RPA in the reaction resulted in a defined pattern of nucleolytic processing (Fig 2B) as compared to reactions without RPA (supplementary Fig 2E). Reactions were stopped by incubation in 10 mM EDTA, 0.25 % SDS and 100 μg/ml Proteinase K for 10 min at 37° C. DNA products separated on 0.8% agarose were stained with either ethidium bromide or SYBR Gold and analyzed with a Typhoon PhosphorImager (GE Healthcare).

Hairpin exonuclease assays were performed in 20 μl with 1 nM DNA substrate (annealed 3' labeled HL1: 5'-TCATTGCCTATCCTGACAGTCCGACACATCGGACTGTCAGGATAGGCAA TGATCTTTTTTTTT -3'), 50 mM Tris-HCl pH 7.5, 50 mM NaCl, 5 mM $MgCl_2$, 1 mM DTT and 50 ng/μl BSA at 37^{o}C with the indicated protein concentrations and time-points. Reactions were terminated by addition of an equal volume of 99% (v/v) formamide 0.1% (w/v) bromophenol blue and heating at 95°C for 5 min. Products were resolved by electrophoresis in 15% (w/v) polyacrylamide gel containing 8 M urea (acrylamide/bis-acrylamide 19:1) run in 1xTBE buffer at 25 mA. Gels were dried and analyzed with a Typhoon PhosphorImager (GE Healthcare).

Linearized plasmids were generated by incubating the pGEM-13Zf(+) plasmid derivative with either Ban*II* (5' overhangs), Hind*III* (3' overhangs) or Sca*I* (blunt ends) followed by column purification (Qiagen). Proteins used in the assay were mixed and incubated on ice prior to addition into reaction tubes containing 50 mM Tris-HCl pH 7.5, 50 mM NaCl, 2 mM $MgCl_2$, 1 mM DTT and 0.1 mg/ml BSA. DNA products were separated as described above.

DNA-Binding assays - Gel mobility shift assays were performed in a volume of 20 μl containing 5 nM of annealed 5' labeled HL1, 50 mM Tris-HCl pH 7.5, 50 mM NaCl, 1 mM EDTA, 1 mM DTT, 50 ng/μl BSA. The reactions were pre-incubated with the corresponding proteins, 10 nM EXO1, 50 nM CtIP for 15 min at RT before addition of the substrate and further incubated for 60 min. After addition of glycerol to a final 10% concentration, separation was

performed in a 6% (w/v) native polyacrylamide gel run in 1xTBE buffer at 25 mAmp. Gels were analyzed as described above.

Pulse-field gel electrophoresis - Subconfluent cultures of U2OS were mock-treated (DMSO) or camptothecin-treated for 4h. Cells were harvested by trypsinization, and agarose plugs of 10^6 cells were prepared in a disposable plug mold (BioRad). Plugs were then incubated in lysis buffer (100 mM EDTA, 1% (w/v) sodium lauryl sarcosyl, 0.2% (w/v) sodium deoxycholate, 1mg/ml proteinase K) at 37 ^{o}C for 72h. Plugs were then washed four times in 20 mM Tris-HCl pH 8.0, 50 mM EDTA before loading onto an agarose gel. Electrophoresis was performed for 23h at 14 ^{o}C in 0.9% (w/v) Pulse Field Certified Agarose (BioRad) containing Tris-borate/EDTA buffer according to the conditions described in (Hanada et al, 2007) and adapted to a BioRad CHEF DR III apparatus. The gel was then stained with ethidium bromide and analyzed using an Alpha Innotech Imaging system.

Colony formation assay - Cells were either mock-treated (DMSO) or treated with the indicated doses of camptothecin 72h after the first siRNA transfection. The drug was removed 1h upon treatment and cells were cultured for 10–14 days at 37°C. For the PARP-inhibitor AZD2281, continuous exposure to the compound was ensured by a first addition 72h after the siRNA transfection, and a second addition 72 h after the first. Colonies were stained with a crystal violet/ethanol (0.5%/20%) solution and counted.

Chromosome analysis - After treatment with camptothecin, cells were allowed to recover for 8h in complete medium before chromosome preparation. Caffeine (2 mM) was added for the last 5h to override the G2/M checkpoint, and colcemid (0.1 mg/ml) was added for the last 3h to arrest cells in metaphase. Metaphase chromosomes were stained with DAPI.

ACKNOWLEDGMENTS

We are grateful to S. Jackson for providing GFP-HA-EXO1 U2OS cells, R. Baer for CtIP antibodies and purified CtIP protein, M. Weitzman for ATLD1-Tert cells, F. Marini for the GFP-EXO1 construct and P. Janscak for purified RPA, BLM and MRE11-RAD50 complex. We would like to thank M. Stucki and P. Janscak for critical reading of the manuscript. We are also indebted to U. Ziegler (University of Zurich, Center for Microscopy and Image Analysis) for guidance in the optimization of live cell imaging.

This work was supported by grants of the Swiss National Science Foundation (SNF), the UBS-Foundation, the Novartis Foundation for Medical and Biological Research, the University of Zurich Priority Program and the Désirée and Niels Yde Foundation (to S.F.), by an Ambizione fellowship from the SNF (to A.A.S.), and by the Forschungskredit from the University of Zurich (to M.S.).

REFERENCES

Adamo A, Collis SJ, Adelman CA, Silva N, Horejsi Z, Ward JD, Martinez-Perez E, Boulton SJ, La Volpe A (2010) Preventing nonhomologous end joining suppresses DNA repair defects of Fanconi anemia. *Mol Cell* **39**(1)**:** 25-35

Adams KE, Medhurst AL, Dart DA, Lakin ND (2006) Recruitment of ATR to sites of ionising radiation-induced DNA damage requires ATM and components of the MRN protein complex. *Oncogene* **25**(28)**:** 3894-3904

Bassing CH, Swat W, Alt FW (2002) The mechanism and regulation of chromosomal V(D)J recombination. *Cell* **109 Suppl:** S45-55

Bekker-Jensen S, Lukas C, Kitagawa R, Melander F, Kastan MB, Bartek J, Lukas J (2006) Spatial organization of the mammalian genome surveillance machinery in response to DNA strand breaks. *J Cell Biol* **173**(2)**:** 195-206

Bolderson E, Tomimatsu N, Richard DJ, Boucher D, Kumar R, Pandita TK, Burma S, Khanna KK (2010) Phosphorylation of Exo1 modulates homologous recombination repair of DNA double-strand breaks. *Nucleic Acids Res* **38**(6)**:** 1821-1831

Bryant HE, Schultz N, Thomas HD, Parker KM, Flower D, Lopez E, Kyle S, Meuth M, Curtin NJ, Helleday T (2005) Specific killing of BRCA2-deficient tumours with inhibitors of poly(ADP-ribose) polymerase. *Nature* **434**(7035)**:** 913-917

Carson CT, Schwartz RA, Stracker TH, Lilley CE, Lee DV, Weitzman MD (2003) The Mre11 complex is required for ATM activation and the G2/M checkpoint. *EMBO J* **22**(24)**:** 6610-6620

Chen BP, Chan DW, Kobayashi J, Burma S, Asaithamby A, Morotomi-Yano K, Botvinick E, Qin J, Chen DJ (2005) Cell cycle dependence of DNA-dependent protein kinase phosphorylation in response to DNA double strand breaks. *J Biol Chem* **280**(15)**:** 14709-14715

Chen L, Nievera CJ, Lee AY, Wu X (2008) Cell cycle-dependent complex formation of BRCA1.CtIP.MRN is important for DNA double-strand break repair. *J Biol Chem* **283**(12)**:** 7713-7720

El-Shemerly M, Janscak P, Hess D, Jiricny J, Ferrari S (2005) Degradation of human exonuclease 1b upon DNA synthesis inhibition. *Cancer Res* **65**(9)**:** 3604-3609

El-Shemerly M, Hess D, Pyakurel AK, Moselhy S, Ferrari S (2008) ATR-dependent pathways control hEXO1 stability in response to stalled forks. *Nucleic Acids Res* **36**(2)**:** 511-519

Farmer H, McCabe N, Lord CJ, Tutt AN, Johnson DA, Richardson TB, Santarosa M, Dillon KJ, Hickson I, Knights C, Martin NM, Jackson SP, Smith GC, Ashworth A (2005) Targeting the DNA repair defect in BRCA mutant cells as a therapeutic strategy. *Nature* **434**(7035)**:** 917-921

Fischer F, Baerenfaller K, Jiricny J (2007) 5-Fluorouracil is efficiently removed from DNA by the base excision and mismatch repair systems. *Gastroenterology* **133**(6)**:** 1858-1868

Genschel J, Modrich P (2009) Functions of MutLalpha, replication protein A (RPA), and HMGB1 in 5'-directed mismatch repair. *J Biol Chem* **284**(32)**:** 21536-21544

Gravel S, Chapman JR, Magill C, Jackson SP (2008) DNA helicases Sgs1 and BLM promote DNA double-strand break resection. *Genes Dev* **22**(20)**:** 2767-2772

Hanada K, Budzowska M, Davies SL, van Drunen E, Onizawa H, Beverloo HB, Maas A, Essers J, Hickson ID, Kanaar R (2007) The structure-specific endonuclease Mus81 contributes to replication restart by generating double-strand DNA breaks. *Nat Struct Mol Biol* **14**(11)**:** 1096-1104

Helleday T, Petermann E, Lundin C, Hodgson B, Sharma RA (2008) DNA repair pathways as targets for cancer therapy. *Nat Rev Cancer* **8**(3)**:** 193-204

Hoeijmakers JH (2001) Genome maintenance mechanisms for preventing cancer. *Nature* **411**(6835)**:** 366-374

Leahy JJ, Golding BT, Griffin RJ, Hardcastle IR, Richardson C, Rigoreau L, Smith GC (2004) Identification of a highly potent and selective DNA-dependent protein kinase (DNA-PK) inhibitor (NU7441) by screening of chromenone libraries. *Bioorg Med Chem Lett* **14**(24)**:** 6083-6087

Lee BI, Wilson DM, 3rd (1999) The RAD2 domain of human exonuclease 1 exhibits 5' to 3' exonuclease and flap structure-specific endonuclease activities. *J Biol Chem* **274**(53)**:** 37763-37769

Lengsfeld BM, Rattray AJ, Bhaskara V, Ghirlando R, Paull TT (2007) Sae2 is an endonuclease that processes hairpin DNA cooperatively with the Mre11/Rad50/Xrs2 complex. *Mol Cell* **28**(4)**:** 638-651

Lisby M, Barlow JH, Burgess RC, Rothstein R (2004) Choreography of the DNA damage response: spatiotemporal relationships among checkpoint and repair proteins. *Cell* **118**(6)**:** 699-713

Mimitou EP, Symington LS (2008) Sae2, Exo1 and Sgs1 collaborate in DNA double-strand break processing. *Nature* **455**(7214)**:** 770-774

Mimitou EP, Symington LS (2009) DNA end resection: Many nucleases make light work. *DNA Repair (Amst)*

Misteli T, Soutoglou E (2009) The emerging role of nuclear architecture in DNA repair and genome maintenance. *Nat Rev Mol Cell Biol* **10**(4)**:** 243-254

Niu H, Raynard S, Sung P (2009) Multiplicity of DNA end resection machineries in chromosome break repair. *Genes Dev* **23**(13)**:** 1481-1486

Pace P, Mosedale G, Hodskinson MR, Rosado IV, Sivasubramaniam M, Patel KJ (2010) Ku70 corrupts DNA repair in the absence of the Fanconi anemia pathway. *Science* **329**(5988)**:** 219-223

Pardo B, Gomez-Gonzalez B, Aguilera A (2009) DNA repair in mammalian cells: DNA double-strand break repair: how to fix a broken relationship. *Cell Mol Life Sci* **66**(6)**:** 1039-1056

Pommier Y (2006) Topoisomerase I inhibitors: camptothecins and beyond. *Nat Rev Cancer* **6**(10)**:** 789-802

Sakasai R, Teraoka H, Tibbetts RS (2010) Proteasome inhibition suppresses DNA-dependent protein kinase activation caused by camptothecin. *DNA Repair (Amst)* **9**(1)**:** 76-82

Sartori AA, Lukas C, Coates J, Mistrik M, Fu S, Bartek J, Baer R, Lukas J, Jackson SP (2007) Human CtIP promotes DNA end resection. *Nature* **450**(7169)**:** 509-514

Stewart GS, Maser RS, Stankovic T, Bressan DA, Kaplan MI, Jaspers NG, Raams A, Byrd PJ, Petrini JH, Taylor AM (1999) The DNA double-strand break repair gene hMRE11 is mutated in individuals with an ataxia-telangiectasia-like disorder. *Cell* **99**(6)**:** 577-587

Walter J, Cremer T, Miyagawa K, Tashiro S (2003) A new system for laser-UVA-microirradiation of living cells. *J Microsc* **209**(Pt 2)**:** 71-75

Whitby MC (2005) Making crossovers during meiosis. *Biochem Soc Trans* **33**(Pt 6)**:** 1451-1455

Wyman C, Kanaar R (2006) DNA double-strand break repair: all's well that ends well. *Annu Rev Genet* **40:** 363-383

Zhang Y, Yuan F, Presnell SR, Tian K, Gao Y, Tomkinson AE, Gu L, Li GM (2005) Reconstitution of 5'-directed human mismatch repair in a purified system. *Cell* **122**(5)**:** 693-705

Zhu Z, Chung WH, Shim EY, Lee SE, Ira G (2008) Sgs1 helicase and two nucleases Dna2 and Exo1 resect DNA double-strand break ends. *Cell* **134**(6)**:** 981-994

FIGURE LEGENDS

Figure 1 - EXO1 localization to sites of DNA damage requires both CtIP and MRE11

(A) U2OS cells stably expressing GFP-EXO1 were microirradiated and 30 min later fixed, co-immunostained with γ-H2AX and RPA2 antibodies and analyzed by fluorescence microscopy. Nuclei were visualized with DAPI.

(B) GFP-EXO1 cells were transfected with Luciferase- (CNTL), CtIP-, or MRE11-specific siRNA oligonucleotides and grown for 72h. Protein expression was examined by immunoblot using the indicated antibodies.

(C) siRNA-transfected GFP-EXO1 cells from *(B)* were microirradiated, fixed and analyzed as in *(A)*.

(D) GFP-EXO1 cells treated as in *(A)* were co-immunostained with γ-H2AX, Cyclin A and CtIP antibodies. γ-H2AX positive cells were quantified for EXO1, Cyclin A and CtIP staining. 50 cells per sample were counted in two independent experiments.

Figure 2 - CtIP interacts with EXO1 and restrains its exonucleolytic activity

(A) WCEs (5 mg) from mock or camptothecin-treated (1 μM, 1h) HEK293T cells were immunoprecipitated with preimmune serum (PI), anti-CtIP or anti-EXO1 polyclonal antibodies. Proteins were detected by immunoblot with the indicated antibodies. For CtIP, short (S) and long (L) exposure times are shown. Arrows indicate the hyperphosphorylated form of CtIP. The membrane was stripped and re-probed using a monoclonal anti-EXO1 antibody. Input = 1% of the WCEs used for IP.

(B) Purified, recombinant EXO1 (200 ng) and FLAG-tagged CtIP (200 ng) were incubated either alone or together before immunoprecipitation with an anti-EXO1 antibody. Proteins were visualized with the indicated antibodies. Recombinant EXO1 (50 ng, lane 1) and FLAG-CtIP (20 ng, lane 5) were loaded as inputs.

(C) Nicked plasmid (3.75 nM) was incubated with EXO1 (15 nM) or EXOIII (10 U) in the presence or absence of CtIP (15 nM). RPA (300 nM) was present

were indicated. Products were resolved as described in Methods. The migration patterns of the double-stranded, nicked plasmid and of the single-stranded product are indicated.

(D) Radiolabelled oligonucleotide (1 nM, lane 1) was incubated with CtIP alone (1 nM, lane 2), EXO1 alone (1 nM, lanes 3-7) or both together at equimolar concentrations (lanes 8-12). Reactions were terminated at the indicated time-points and the products were analyzed as described in Methods.

(E) Linearized plasmid with 3'-overhangs (2.5 nM, 5 nM DNA ends) was incubated at 37°C with hEXO1 (15 nM), RPA (300 nM) and the indicated amounts of CtIP. Reactions were terminated at the indicated time-points and the products were analyzed as described in Methods.

Figure 3 - CtIP and EXO1 protect cells from chromosomal damage

(A) 72h after the transfection with the indicated siRNA oligonucleotides, U2OS cells were treated with either DMSO or camptothecin (1h, 1 μM; acute treatment) and survival was determined by colony formation. Data represent the mean ± standard error of the mean (SEM) of five independent experiments.

(B) Cell survival at low doses of camptothecin from the data shown in *(A)*. Data represent the mean ± standard error of the mean (SEM) of five independent experiments

(C) Cells transfected as in *(A)* were treated with either DMSO or camptothecin for 24h (chronic treatment) and survival was determined by colony formation. Data represent the mean ± SEM of three independent experiments.

(D) Metaphase spreads from cells transfected and treated as described in *(A)* were analyzed for chromosomal aberrations. 50 metaphase spreads were analyzed for each sample. The percentages of metaphase spreads displaying the indicated numbers of radial chromosomes are shown.

Figure 4 - Inhibition of DNA-PKcs rescues radial chromosomes formation

(A) U2OS cells transfected with siRNA oligonucleotides were treated with DMSO or camptothecin (1 μM, 1h) and DNA-PKcs autophosphorylation at S2056 was monitored.

(B) Metaphase spreads were generated from cells transfected as in *(A)* and treated with camptothecin (1 μM, 1h) in the presence or absence of NU7441 (10 mM). In total more than 100 spreads were analyzed for both conditions in two independent experiments. The average of radial chromsomes per spread was 1.65 (DMSO) and 0.59 (NU7441), equivalent to a 2.8-fold reduction in radial formation.

(C) Cells transfected as in *(A)* were treated with DMSO or camptothecin (2.5 μM, 4h) in the presence or the absence of NU-7441 (10 mM). The amount of broken DNA was assessed by PFGE.

Eid *et al.*, Figure 1

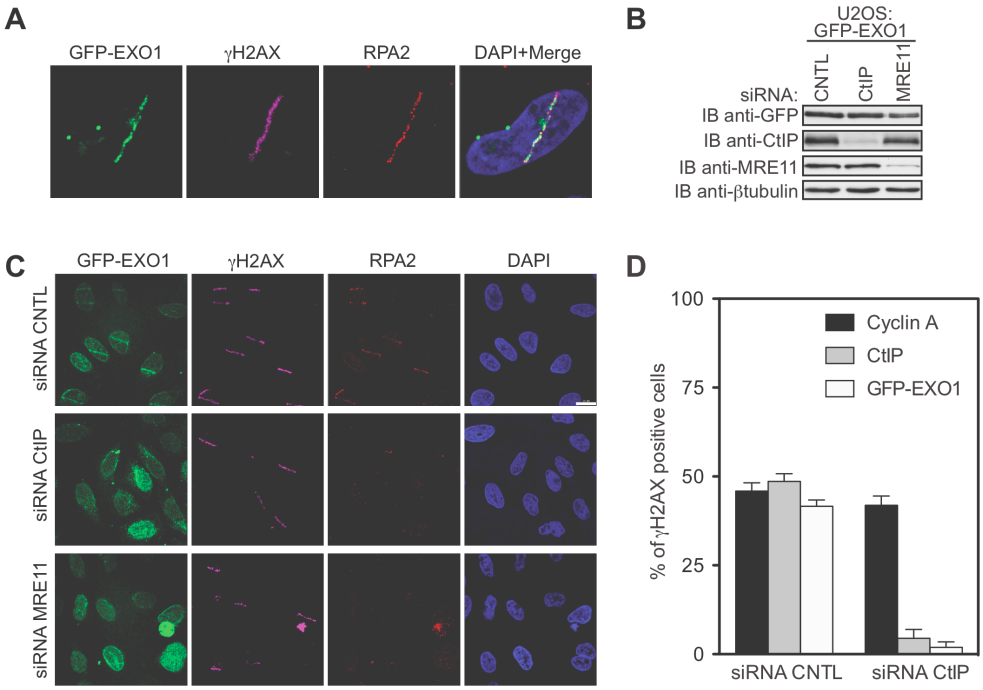

Eid *et al.*, Figure 2

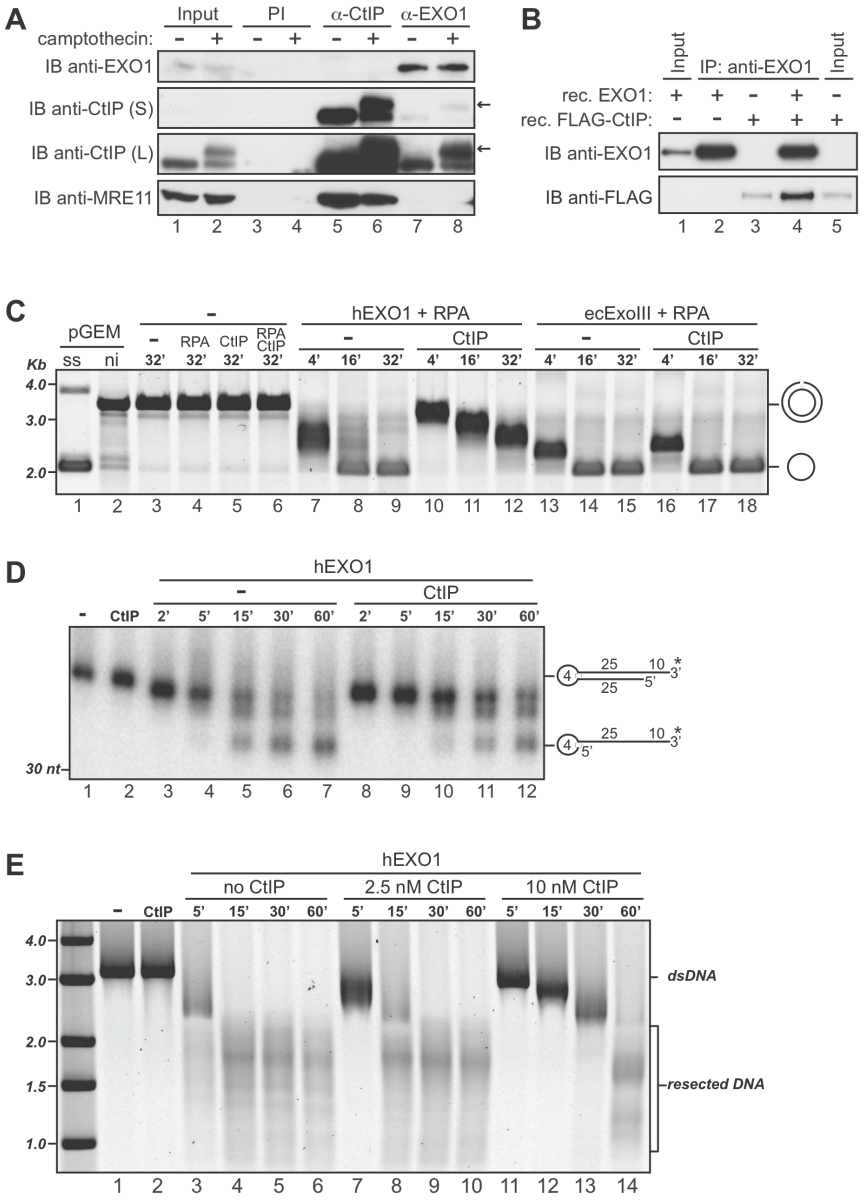

Eid *et al.*, Figure 3

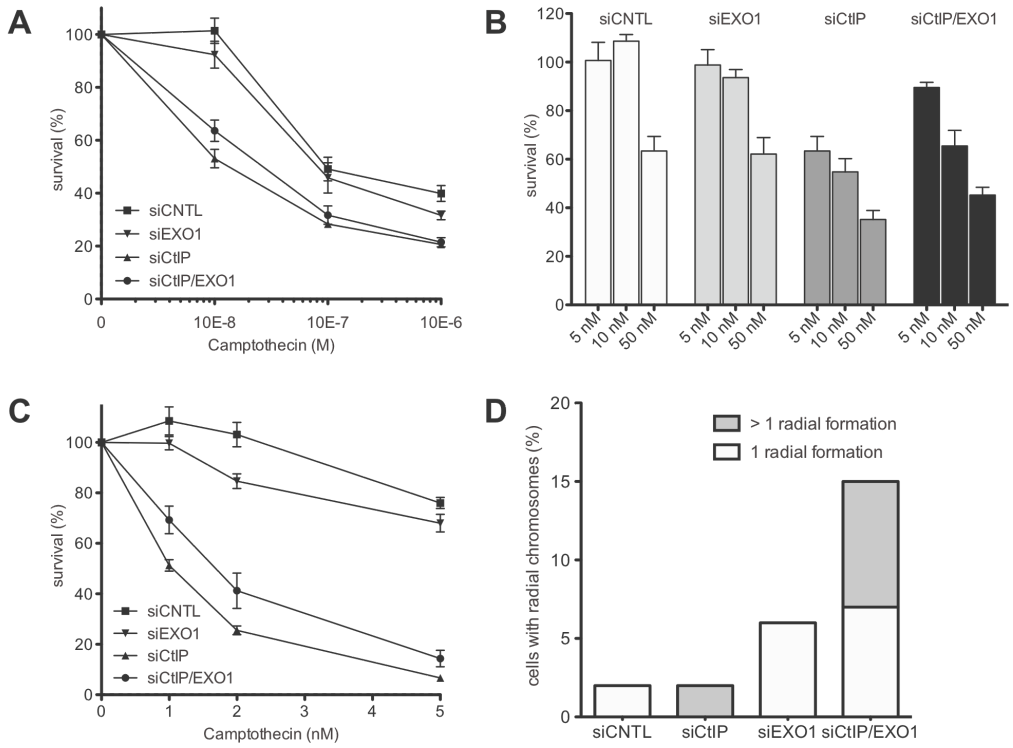

Eid *et al.*, Figure 4

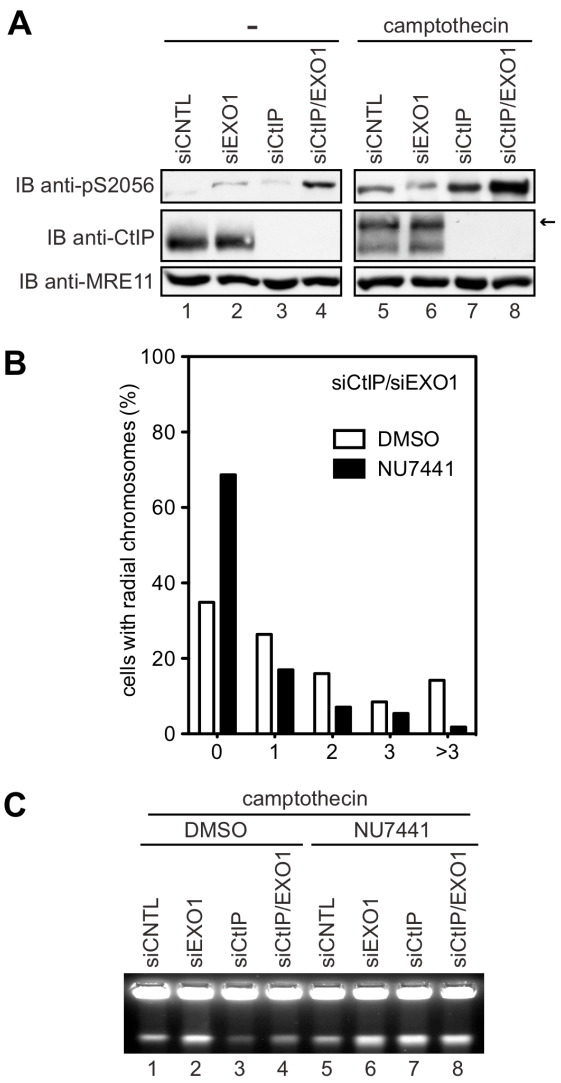

SUPPLEMENTAL FIGURE LEGENDS

Supplementary Figure S1 - CtIP- and MRN-dependent recruitment of EXO1 to DSBs

(A) Recruitment of GFP-EXO1 to laser lines visualized by fluorescence microscopy at early (5 min) and late (240 min) time points.

(B) Live cell imaging of microirradiated GFP-EXO1 cells transfected with control (CNTL), CtIP or MRE11 siRNA. Scale bar = 10 mm.

(C-E) CtIP recruitment to DSBs in ATLD1 cells is insufficient for DNA end resection. MRE11-deficient ATLD1 fibroblasts, stably transfected with an empty vector or with a vector directing the expression of full-length MRE11, were treated with camptothecin (1 μM, 1 h) and analyzed by immunoblotting with the indicated antibodies *(C)*. The same pair of cells was microirradiated, fixed after 30 min and co-stained with either γ-H2AX and RPA2 *(D)* or gH2AX and CtIP *(E)* antibodies. Nuclei were visualized with DAPI.

(F) Live cell imaging of vector- or wild-type MRE11-complemented ATLD1 fibroblasts, transiently transfected with GFP-EXO1 and microirradiated.

Supplementary Figure S2 - Biochemical characterization of the EXO1-CtIP interaction

(A) WCEs (5 mg) from DMSO or camptothecin-treated (2h, 2.5 μM) HEK293T cells were immunoprecipitated using an anti-EXO1 antibody. Immunocomplexes bound to sepharose beads were incubated with 10 units of calf intestinal phosphatase (CIP) for 10 min at 37 ^{o}C, washed with 3x 1ml TNET buffer (El-Shemerly et al, 2005), resolved by SDS-PAGE and analyzed by immunoblotting.

(B) WCEs (5 mg) from HEK293T cells overexpressing OMNI-tagged EXO1, treated or not with hydroxyurea (2 mM, 16h) were immunoprecipitated with PI serum or an anti-CtIP antibody. Proteins were detected by immunoblotting with the indicated antibodies.

(C) Human recombinant $EXO1_{wt}$ and the catalytically-dead mutant $EXO1_{D173A}$ were expressed and purified as described (El-Shemerly et al, 2005). Peak

fractions from the chitin affinity column were pooled, loaded on a Hi-Trap SP-FF (1 ml) cartridge and proteins eluted with a linear salt gradient (0.0 - 0.5 M NaCl). Aliquots of the load (L, 5 ml), flow-through (FT, 5 ml), wash (W, 5 ml) fractions and of the OD_{280} peak (20 ml) were resolved by 8% SDS-PAGE and stained with Coomassie brilliant blue.

(D) Purified wild-type EXO1 (15 nM; lanes 1-7) or catalytically-dead EXO1 (D173A, 15 nM; lanes 9-15) were incubated with 5 nM *N.BstNBI*-digested pGEM-13Zf(+) plasmid for the indicated time points and the products resolved on a 0.8% agarose gel before ethidium bromide staining.

(E) Gel-purified pGEM-13Zf(+)-nicked plasmid substrate (3.75 nM) was incubated at 37°C for the indicated time periods with purified EXO1 (15 nM) in the presence or absence of purified CtIP (15 nM) or MRE11-RAD50 (15 nM). The products were resolved as described in Supplementary Methods.

(F) Radiolabelled oligonucleotide (5 nM) was incubated for 60 min at room temperature with purified EXO1 (10 nM), CtIP (50 nM) or both together in a buffer containing 1 mM EDTA. The products were analyzed as described in Supplementary Methods. The migration patterns of free and EXO1-bound oligonucleotide are indicated.

(G) Purified linearized pGEM-13Zf(+) plasmid (2.5 nM, 5 nM DNA ends) containing either 3' overhangs, 5' overhangs or blunt ends was incubated for 30 min at 37°C with EXO1 (15 nM) in the presence or absence of RPA (300 nM) as indicated. The products were resolved as described in Supplementary Methods.

(H) Purified linearized pGEM-13Zf(+) plasmid containing 3' overhangs (2.5 nM, 5 nM DNA ends) was incubated at 37°C with EXO1 (15 nM) in the presence of RPA (300 nM) and either CtIP (15 nM), MRE11-RAD50 (15 nM) or BLM (15 nM). The products were resolved as described in Supplementary Methods.

(I) Purified linearized pGEM-13Zf(+) plasmid (2.5 nM, 5 nM DNA ends) containing either blunt ends or 5' overhangs was incubated at 37°C with EXO1 (15 nM) in the presence of RPA (300 nM) or pre-incubated with either EXO1 (15 nM) or CtIP (15 nM) for 5 min at RT, followed by addition of CtIP or

EXO1, respectively. The products were resolved as described in Supplementary Methods.

Supplementary Figure S3 - Effect of CtIP, EXO1 or CtIP/EXO1 downregulation on genome stability

(A) 72h after the transfection with the indicated siRNA oligonucleotides U2OS cells were subjected to propidium iodide (PI) staining for cell cycle analysis.

(B) U2OS cells grown on glass cover slips and transfected as described in *(A)* were incubated for 20 min with 10 μM EdU (5-ethynyl-2'-deoxyuridine). Immediately after fixation with 4% formaldehyde cover slips were processed following manufacturers instructions (Invitrogen). At least 150 cells were counted for each condition. Percentages indicate the number of EdU-positive cells.

(C) 72h after the transfection with the indicated siRNA oligonucleotides U2OS cells were treated with either DMSO or camptothecin (1h, 1 μM). WCEs were analyzed by immunoblot (*left panel*) or immunoprecipitation (*right panel*) with the indicated antibodies.

(D) Cells transfected as described in *(A)* were treated with the indicated doses of AZD2281 (Olaparib) and survival was determined by colony formation. Data represent the mean ± SEM of three independent experiments.

(E) Cells transfected as in (A) were treated with camptothecin (1 μM, 1h) and allowed to recover for 8h in complete medium before chromosome preparation. Caffeine (2 mM) was added for the last 5h to override the G2/M checkpoint, and colcemid (0.1 mg/ml) was added for the last 3h to arrest cells in metaphase. 50 metaphase spreads were analyzed for each sample. The percentages of metaphase spreads displaying the indicated numbers of broken chromosomes are shown.

(F) Representative images of chromosomal abnormalities detected in metaphase spreads of camptothecin treated cells: broken chromatids (arrowheads); radial chromosomes (ellipses). Scale bar, 10 μm.

Supplementary Figure S4 - Inhibition of DNA-PKcs rescues camptothecin-induced radials formation in CtIP/EXO1 depleted cells

(A) WCEs obtained from U2OS that were treated with camptothecin (1h, 1 mM) in the presence or the absence of NU7441 (10 mM), were analyzed by immunoblot with the indicated antibodies. Autophosphorylation at S2056 was use as read-out for inhibition of DNA-PKcs activity by NU7441.

(B) 72h after the transfection with the indicated siRNA oligonucleotides, U2OS cells were treated with DMSO or camptothecin (2.5 μM, 4h) in the presence or the absence of the DNA-PKcs inhibitor NU7441 (10 mM). Representative images of chromosomal abnormalities detected in metaphase spreads are shown. Radial chromosomes (ellipses) and broken chromatids (arrowheads) are indicated.

(C) Cells transfected as in *(B)* were treated with DMSO or camptothecin (1h, 1 mM). The amount of broken DNA was assessed by PFGE as described in supplementary Methods.

Eid *et al.*, Supplemental Figure 1

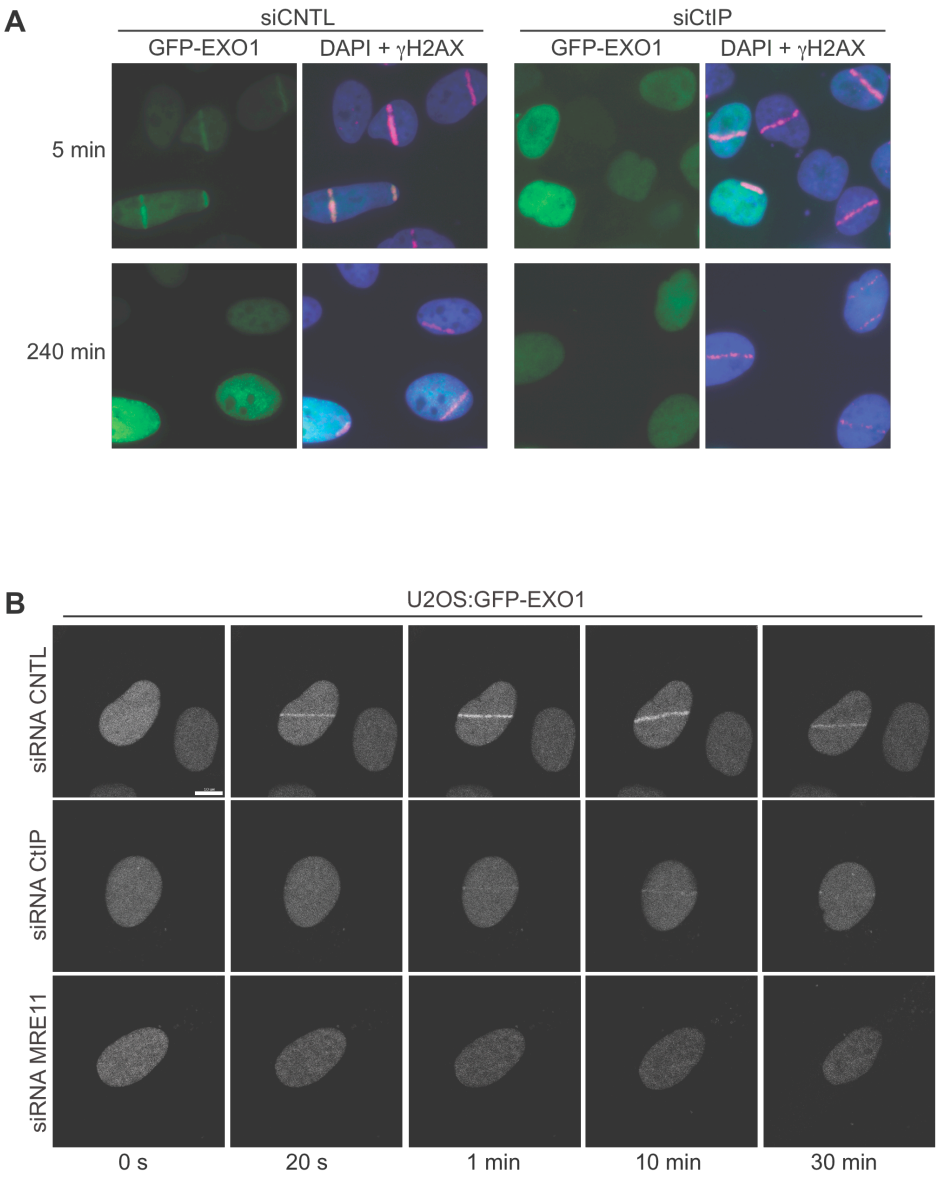

Eid *et al.*, Supplemental Figure 1

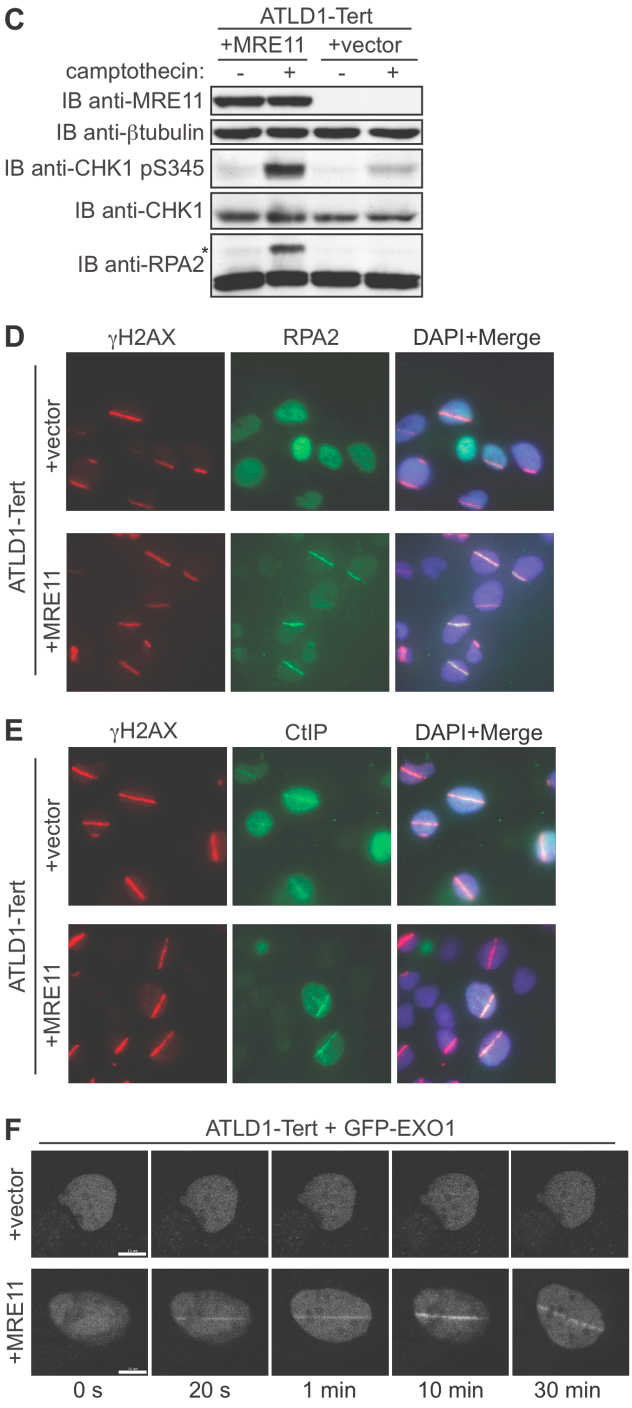

Eid *et al.*, Supplemental Figure 2

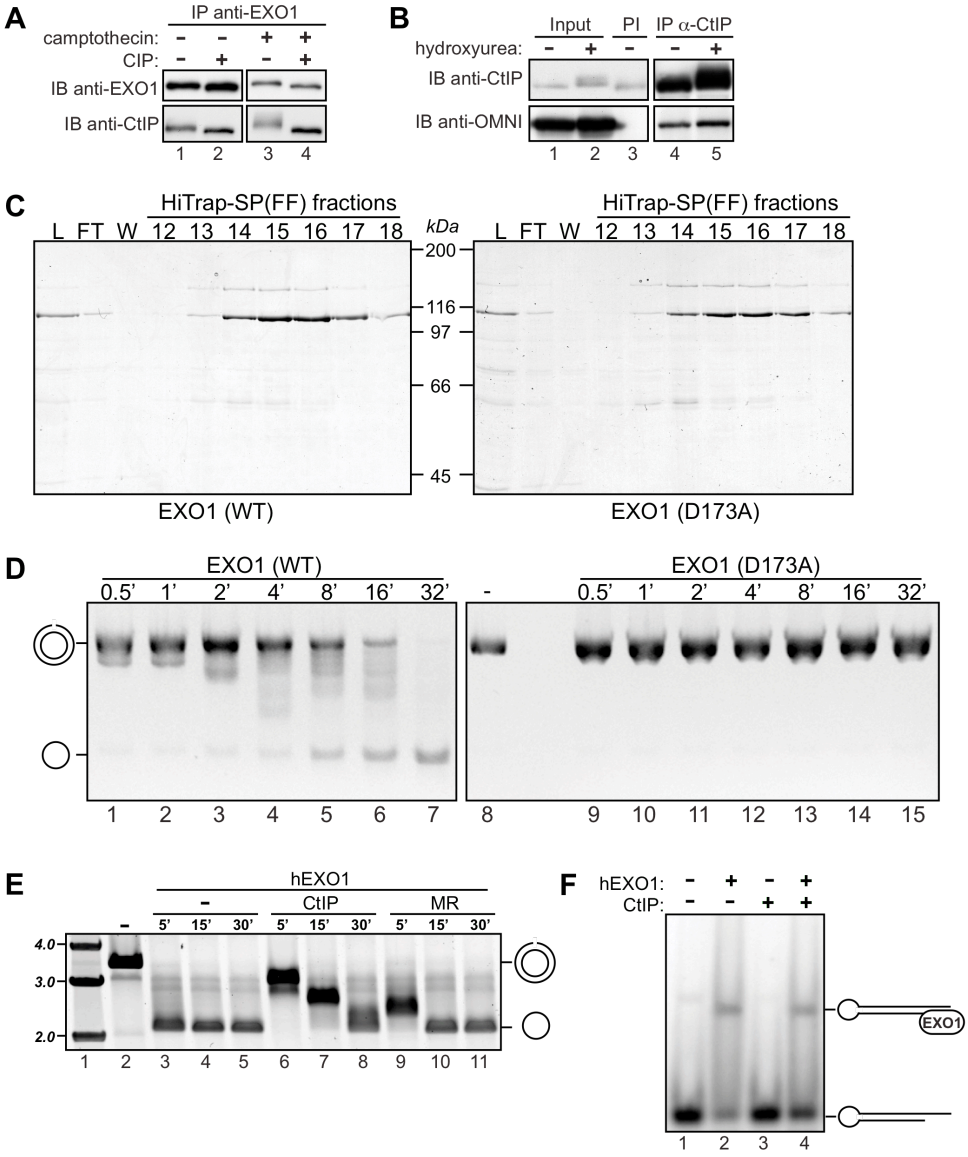

Eid *et al.*, Supplemental Figure 2

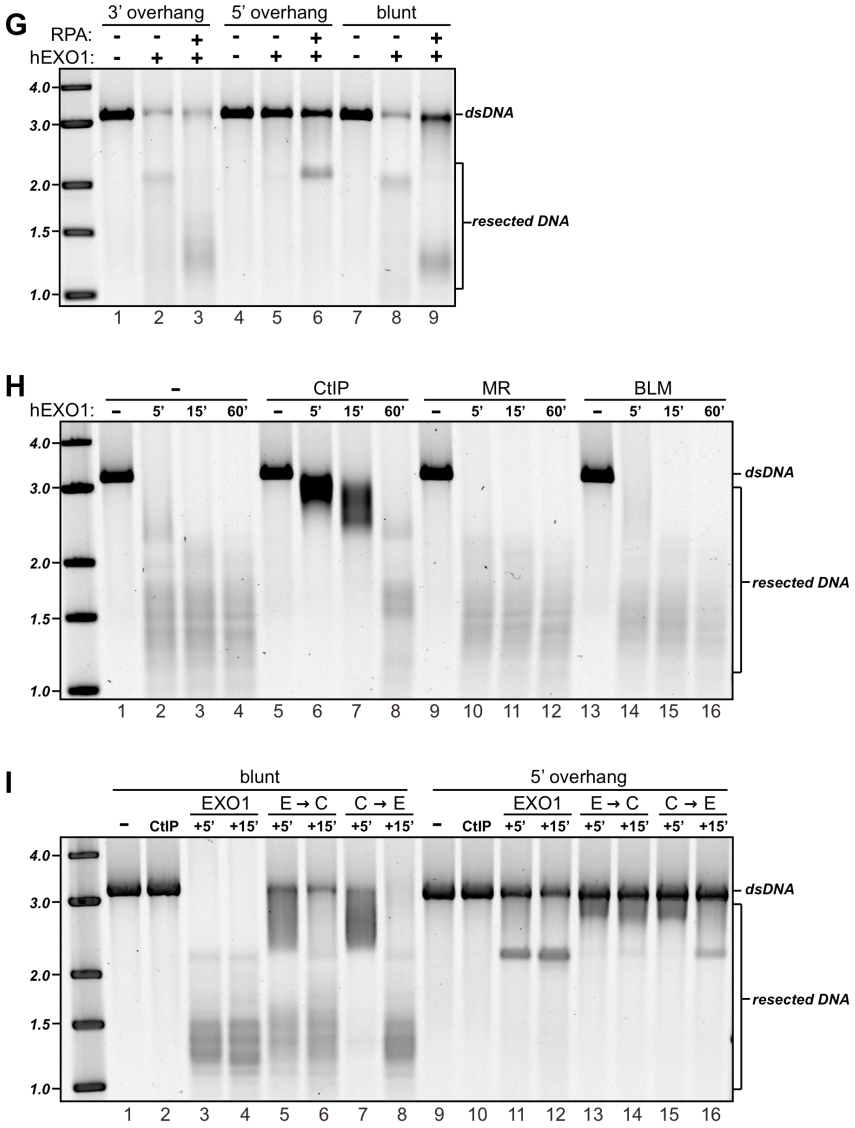

Eid *et al.*, Supplemental Figure 3

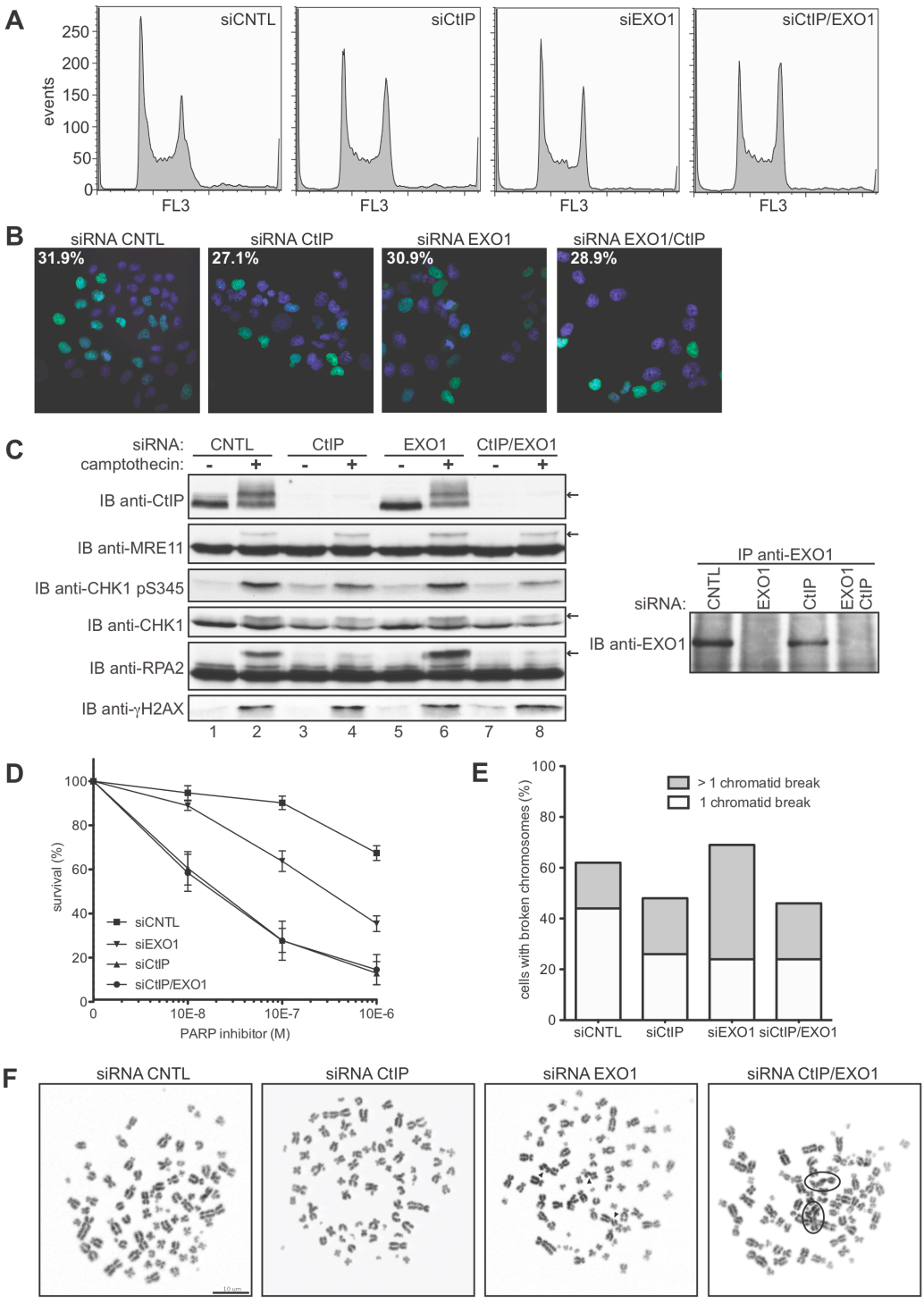

Eid *et al.*, Supplemental Figure 4

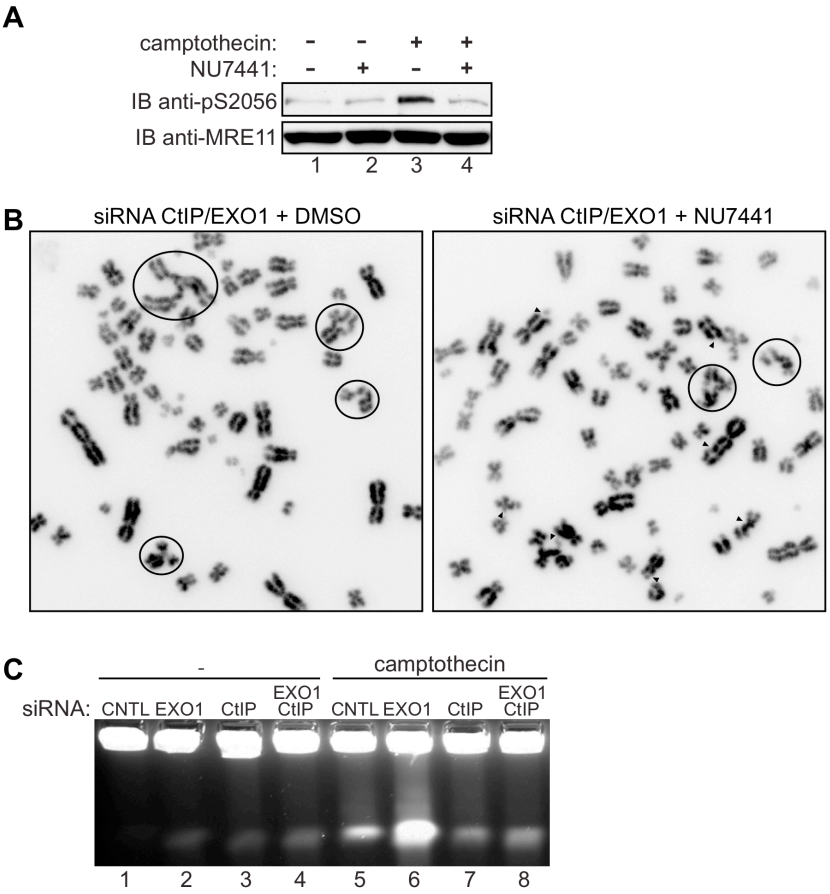

2.2. Refining the interaction domain between EXO1 and CtIP

Having found that EXO1 and CtIP interact, we set out to identify the interaction domain on EXO1. To this end, we generated OMNI-tagged EXO1 deletion mutants by introducing a stop codon at different positions in EXO1 using the QuickChange® mutagenesis kit (Stratagene). Briefly, we transiently transfected HEK 293T cells with an OMNI-tagged full-length EXO1 construct or with constructs encoding different OMNI-tagged EXO1 deletion mutants. We immunoprecipitated CtIP using a rabbit polyclonal antibody and detected the OMNI-tagged EXO1 proteins with a monoclonal antibody against EXO1 that recognizes a N-terminal epitope present in all deletion mutants. The data showed that OMNI-EXO1 and CtIP could be recovered as a complex in all cases examined (Figure 10), thus not allowing us to identify the exact domain in EXO1 that mediates interaction with CtIP. However, in the case of the smallest fragment examined ($EXO1_{1-348}$) we were not able to draw a definite conclusion since this mutant runs at the same molecular size as the heavy chain (IgG(H)) of the antibody used for the immunoprecipitation and it is therefore masked by the more abundant IgG(H). Thus, more work will be needed to nail down the domain in EXO1 mediating interaction with CtIP. One possible approach will be to pull-down OMNI-tagged EXO1 (which also contains a His-tag) using Nickel beads to avoid using an antibody for the immunoprecipitation.

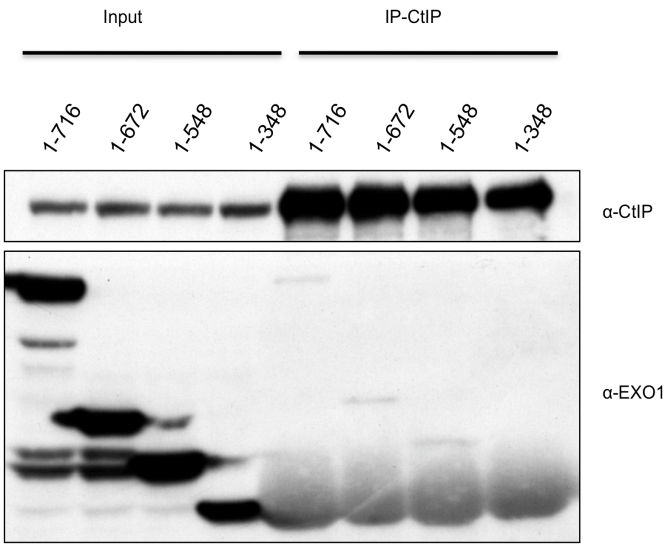

Fig. 10

Co-immunoprecipitation experiment to map the interaction domain between EXO1 and CtIP. HEK 293T cells were transfected with OMNI-tagged full-length or deletion mutant EXO1 constructs. CtIP was immunoprecipitated using a rabbit polyclonal antibody. The recovered protein complexes were resolved by SDS-PAGE and proteins were detected by immunoblotting using specific antibodies. 2% of the WCEs used for the immunoprecipitation were loaded as input. The membrane was first probed with a mouse monoclonal antibody against the N-terminus of EXO1, then stripped and re-probed with a mouse monoclonal antibody against CtIP.

2.3. Identification and functional evaluation of novel interacting partners of EXO1

2.3.1. Cloning Strep-tagged EXO1 and validating the system

DNA-damage signaling and repair is a complex process involving a myriad of different proteins and effectors. EXO1 plays a well established role in the context of DNA repair. In order to identify novel interaction partners of EXO1 that could be potentially involved in DNA-damage repair and signaling, we performed a large-scale mass spectrometry (MS) analysis. To this end, we

cloned full-length EXO1 into a plasmid containing a Strep-tag coding sequence 3' to the multiple cloning sites, such that the fusion protein generated upon transcription/translation features a Strep-tag at its C-terminus. Several clones were screened by colony-PCR, and only positive clones were further considered. Three positive clones were picked and their plasmids were sequenced to confirm both the presence and the integrity of the EXO1-Strep-tag sequence. Plasmid DNA from these clones were extracted, amplified and used to transfect HEK 293T cells. The extent of Strep-EXO1 expression was visualized by immunoblotting. The colony designated C10 showed the highest expression levels of Strep-EXO1 and was the one used for all subsequent experiments (Figure 11, lane 6).

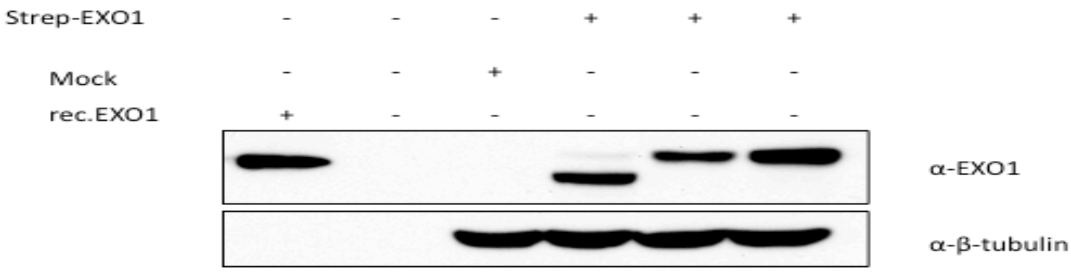

Fig. 11

Validation of Strep-EXO1 expression. HEK 293T cells transfected with a Mock plasmid (lane 3) or with DNA extracted from the three different positive clones C7, C9, and C10 (lanes 4,5 and 6), respectively. 50 µg of whole cell extract (WCE) were resolved on SDS-PAGE gel and proteins were detected by immunoblotting using specific antibodies. Human recombinant EXO1 expressed and purified from *E.coli* was loaded (100 ng, lane 1) as a control for the molecular size.

In order to validate our Strep-EXO1 expression system, we first ensured that overexpression of the fusion protein in cells did not result in artificial interactions, but would be a reliable tool to detect novel EXO1 interacting proteins. To this end, we examined both a known EXO1 interactor, namely

CtIP (Eid et al. 2010), and a protein that is known not to interact with EXO1, namely MRE11 (Eid et al. 2010). In addition, we enclosed TRIM27 in this analysis, a protein that functionally interacts with EXO1 according to evidence that was recently obtained in our laboratory.

To conduct these experiments, HEK 293T cells were transfected with either empty plasmid (Mock) or the plasmid coding for Strep-EXO1, Strep-pull down was performed and protein complexes resolved by SDS-PAGE were transferred to a PVDF membrane. Membranes were probed with specific antibodies to assess the presence of EXO1 interacting proteins. The data confirmed the presence of the established EXO1 interactor CtIP and absence of non-interacting protein MRE11. Interestingly, we could exclusively detect TRIM27 in the Strep-EXO1 pull-down but not in the Mock (Figure 12 lane 1 vs. lane 2), thus successfully identifying TRIM27 as novel EXO1 interactor.

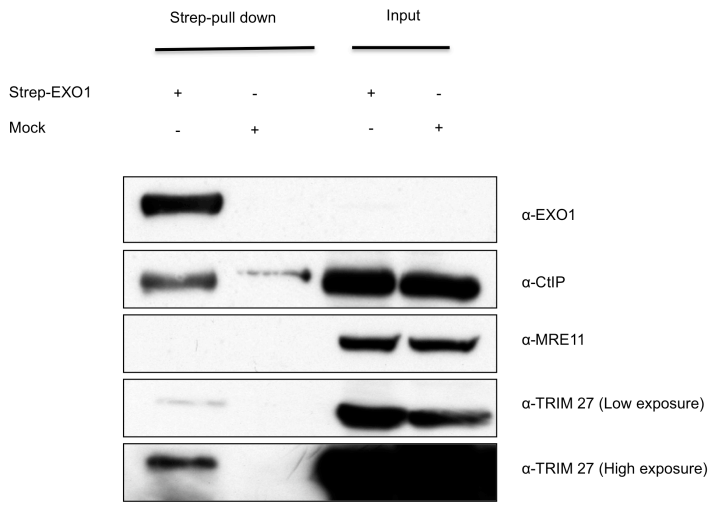

Fig.12

Reliability of the Strep-EXO1 system to the identification of novel interacting partners. HEK 293T cells were transfected with either empty vector (Mock) or the Strep-EXO1 construct. A Strep-pull down was performed as explained in Materials and Methods. Eluted proteins were resolved on 8% SDS polyacrylamide gel, proteins were transferred to PVDF and detected by immunoblotting using specific antibodies. 2% of WCE were loaded as input.

2.3.2. Large scale Strep-tagged EXO1 pull-down

Having validated the Strep-EXO1 expression system, HEK 293T cells were transfected with either Strep-EXO1 or empty vector. Pull-down studies were performed on whole cell extracts (WCE) using Strep-Tactin sepharose beads. Strep-EXO1 was eluted from the beads under mild conditions using D-desthiobiotin, an agonist that binds to Strep-Tactin with high affinity, hence eluting Strep-tagged EXO1 together with its bound proteins. In order to check for the Strep-EXO1 expression and pull-down, a fraction of the eluates were run on a 4-15% gradient SDS polyacrylamide gel and proteins were visualized by silver staining. The staining showed that Strep-EXO1 was successfully pulled-down from cells transfected with Strep-EXO1 but not from mock-transfected cells (Figure 13).

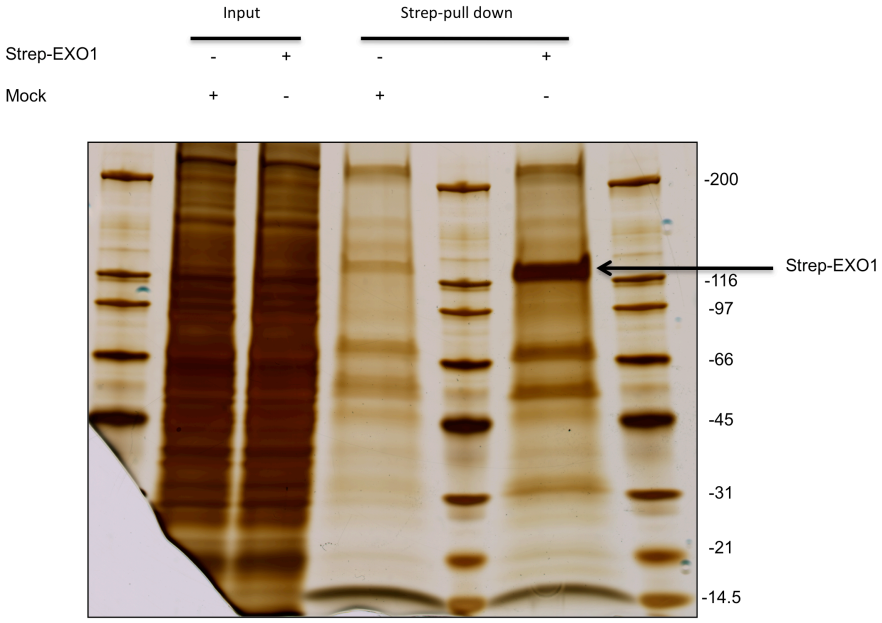

Fig. 13

Silver-stained gradient SDS polyacrylamide gel. Upon Strep-pull down from extracts of mock- or Strep-EXO1-transfected HEK 293T cells, proteins were eluted and 1% of each eluate was analyzed on a 4-15% gradient polyacrylamide gel that was silver stained. The arrow points to Strep-EXO1.

2.3.3. First mass spectrometry

Proteins eluted from Strep-Tactin beads were precipitated using TCA as described in Materials and Methods and analyzed by mass spectrometry (MS) using an LTQ Orbitrap Velos (Thermo Scientific). The data obtained were used for performing a BLAST search against the human subset of the protein sequence database Swiss-Prot. Table1 shows a selection of the proteins found to interact with EXO1.

2.3.4. Second mass spectrometry

Having found interesting interactors of EXO1 under basal conditions in our first MS analysis, we performed a second MS analysis in which we aimed at the following: (i) confirming the hits obtained in the previous experiment; (ii) checking for potential interactors in cells treated with DNA damaging agents, hence increasing our data output by looking at both untreated and treated conditions. The experiment was carried out in a similar way to the previous one, with the addition of two distinct DNA damage protocols. In one sample the cells were treated with 10 Gy of ionizing radiation (IR) and harvested after 1h. For the second sample, cells were treated for 16h with 2mM hydroxyurea (HU) before harvesting. Strep pull-down was performed, a fraction of each eluate was resolved by SDS-PAGE and proteins were visualized by silver staining (Figure 14 A). To ensure that agents and conditions used did result in adequate DNA damage, prior to MS analysis an aliquot of each sample was examined for markers of DNA-damage signaling, namely the phosphorylation of ATM at Ser-1981 and the phosphorylation of CHK2 at Thr-68 (Figure 14 B). Samples for MS analysis were prepared and processed as described in the previous chapter. Table 1 shows a selection of proteins identified in both experiments. The presence of known EXO1 binding proteins among the selected hits, namely MSH2 (Schmutte et al. 1998), and 14-3-3 (Engels et al. 2011), confirmed quality and reliability of the analysis.

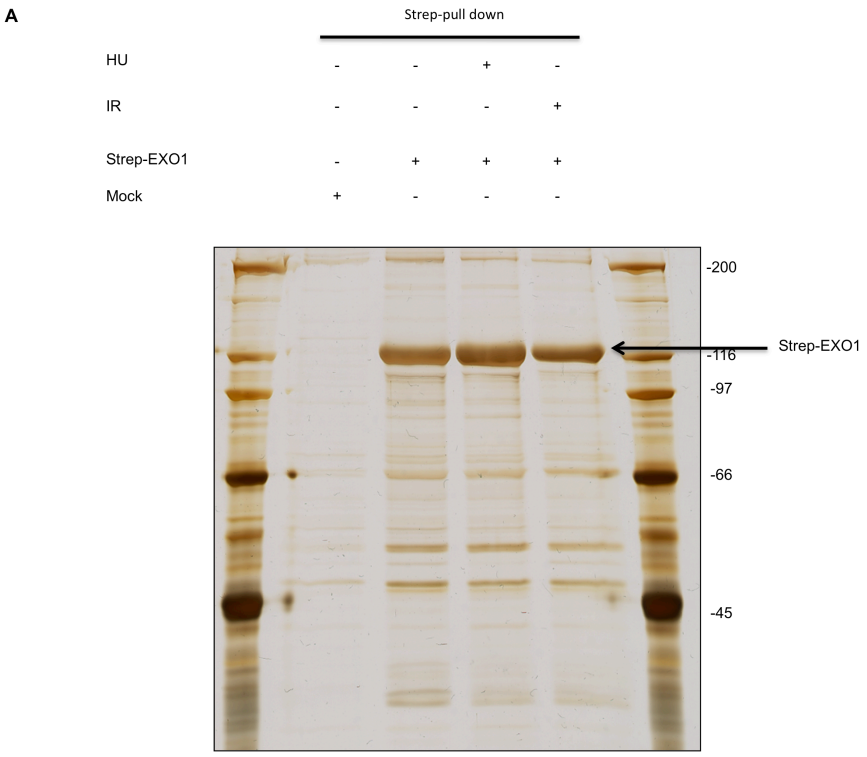

Fig. 14

Analysis of samples submitted to mass spectrometry. (**A**) Silver-stained SDS polyacrylamide gel of Strep pull-downs from HEK 293T cells. Cells were either mock-transfected (lane1) or Strep-EXO1-transfected and left untreated (lane2), treated with 2mM HU for 16h (lane3) or treated with 10 Gy IR (lane 4). 2% of the eluates were loaded on the gel. The arrow points to Strep-EXO1. (**B**) DNA damage signaling was detected upon treating cells with 2mM hydroxyurea for 16h (lane 3) or with 10 Gy ionizing radiation (lane 4). MRE11 served to confirm equal loading of the proteins.

Protein	Mw	Function	Mock	UT	HU	IR
MSH2	105 kDa	Mismatch repair	0	55	83	60
1433F	28 kDa	Adaptor protein	0	28	60	25
1433G	28 kDa	Adaptor protein	7	38	80	32
1433T	28 kDa	Adaptor protein	8	30	47	26
1433Z	28 kDa	Adaptor protein	11	47	86	37
1433E	29 kDa	Adaptor protein	18	42	115	64
1433B	28 kDa	Adaptor protein	7	32	64	28
PHF6	41 kDa	Transcriptional regulator?	1	16	16	14
THOC4	27 kDa	Transcriptional regulator?	1	21	14	21
CH033	25 kDa	?	1	7	9	9
ERH	12 kDa	Cell cycle?	1	6	9	8
PRP19	55 kDa	DDR and pre-mRNA splicing	0	6	4	8
RRP5	209 kDa	rRNA processing	0	6	2	5
RN138	28 kDa	E3 ubiquitin-protein ligase	0	3	2	2
FMR1	71 kDa	mRNA transport	0	4	1	4
KI67	359 kDa	Cell cycle?	0	9	15	11
ILF3	95 kDa	Transcriptional regulator?	5	21	9	17

Table 1.

Selection of EXO1 interacting proteins identified by mass spectrometry in both experiments. The table shows: hit (column 1), molecular weight (column 2), annotation (column 3) number of unique peptides (columns 4-7) obtained in the 2nd mass spectrometry analysis from untransfected cells (Mock), Strep-EXO1 transfected cells that were left untreated (UT), treated with hydroxyurea (HU) or ionizing radiation (IR).

3. Discussion

Double strand breaks and intra-strand crosslinks are the most toxic lesions that may occur to DNA. The error-free repair of DNA double strand breaks by homologous recombination is of vital importance for cells as it allows preventing oncogenesis by maintaining a stable genome. At the molecular level, one of the first steps of homologous recombination is the resection of the DNA termini present at double strand breaks to expose ssDNA. This, in turn, is an important intermediate for RAD51-mediated strand invasion, which promotes sequence homology search and facilitates successful completion of homologous recombination. Several studies have investigated the molecular mechanism of DNA end resection in yeast. Collectively, these studies led to a two-step model of DNA resection according to which DNA is resected by MRN and CtIP to generate short 3'-overhangs of ssDNA, followed by a more extensive resection step that is executed by EXO1 or BLM and DNA2 (Mimitou and Symington, 2008; Gavel et al. 2008; Nimonkar et al. 2011). Although these studies have significantly contributed to shed light on the overall process of homologous recombination, some specific aspects, such as the mechanism by which EXO1 is recruited to sites of DNA damage or the way the nuclease activity of EXO1 is regulated, remained elusive.

In the work that I carried out during my doctoral studies and that is presented here, we addressed these unresolved issues. Namely, we examined whether EXO1 recruitment to double strand breaks would depend on MRE11 and/or CtIP and, if this is the case, whether any of these earlier DNA double strand break-recognizing proteins would affect EXO1 activity at the site of damage. We also decided to investigate the functional role of components of the two-step resection model, such as MRE11, CtIP and EXO1, by examining the DNA damage sensitivity of cells depleted of these proteins. To carry out such studies, we took advantage of cell lines deficient in the expression of the proteins under investigation or of RNA-mediated interference of protein expression using specific oligonucleotides.

On the basis of the two-step model of resection, we initially set out to examine whether EXO1 recruitment to double strand breaks is dependent on the initial

resection step carried out by MRN and CtIP. Indeed, upon depletion of either CtIP or MRE11, we observed both in fixed and live cell imaging an impaired recruitment of EXO1 to laser microirradiation-induced double strand breaks. Consistent with published evidence on the S/G2-specific recruitment of CtIP to double strand breaks (Sartori et al. 2007), we observed accumulation of EXO1 at these sites exclusively in cyclin A-positive cells and such recruitment was strictly CtIP-dependent. Furthermore, transiently transfected GFP-EXO1 did not localize to double strand break sites in ATLD1 cells, which are deficient in DNA end resection due to a hypomorphic mutation of the *MRE11* gene. Accordingly, this phenotype was fully rescued upon re-expressing wild-type MRE11 in these cells. Taken together, these data indicate that the physical presence of the MRN/CtIP complex and/or its enzymatic activity is necessary for EXO1 loading and processing of DNA ends, thus confirming the findings that led to the proposal of the two step model of resection and extending them to include evidence on the molecular mechanism of EXO1 recruitment to sites of damage.

Another point that we address in this study was the mechanism of EXO1 regulation at the sites of double strand break. It is well established that DNA repair is carried out by a plethora of proteins displaying a variety of enzymatic activities that modify DNA prior to and during repair of damage. Since inappropriate recruitment or lack of regulation of the enzymatic activity of repair enzymes may result harmful to DNA and worsen the damage already present, a precise control of their timely localization and function must be put in place. To accomplish this, eukaryotic cells have developed sophisticated strategies that are based on the implementation of post-translational modifications (PTMs) as means to facilitate protein-protein interactions, allowing recruitment and activation of the right factors in the right place and at the right time. PTMs that play major roles in this context are phosphorylation, acetylation, ubiquitylation and sumoylation.

Previous members of the Ferrari laboratory showed that EXO1 activity in mammalian cells is controlled by post-translational modifications, with ATR-

dependent phosphorylation being a necessary and sufficient event for targeting EXO1 to ubiquitin-mediated degradation in cells experiencing stalled DNA replication (El-Shemerly et al. 2005; El-Shemerly et al. 2008). Moreover, Bolderson and colleagues recently showed that EXO1 undergoes phosphorylation in an ATM-dependent manner at sites of double strand break following its recruitment. As previously demonstrated in studies that were conducted in yeast (Morin et al. 2008), phosphorylation could be required to attenuate EXO1 activity and this would in turn be a means to prevent excessive resection of DNA ends (Bolderson et al. 2010).

In this work we also addressed the issue of regulation of EXO1 activity and provide results that suggest a novel mechanism by which EXO1 could be controlled at the site of the DNA damage. Our *in vitro* data showed a significant inhibition of the exonucleolytic activity of EXO1 in the presence of CtIP. Notably, we obtained evidence that the inhibitory effect exerted by CtIP was specific to EXO1, since the activity of an unrelated 5'-3' exonuclease was not affected by the presence of CtIP. We suggest that what we observed *in vitro* may reflect the sequence of events occurring *in vivo*, where a timely restraint of EXO1 activity could prevent the formation of excessively long recombination intermediates that may hamper the faithful execution of HR.

Thus, the evidence obtained in our study, along with data published in the literature, highlights the concept that EXO1 nucleolytic activity is tightly controlled in response to DNA damage.

Data obtained in cell survival assays, in which we analyzed the sensitivity of cells subjected to single or combined depletion of CtIP and EXO1 using siRNA and treated with different doses of camptothecin, further strengthen this concept. In agreement with other reports, we observed that CtIP depletion caused hypersensitivity to camptothecin (Sartori et al. 2007), whereas EXO1 downregulation conferred minor cytotoxicity (Gravel et al. 2008). Interestingly, we observed a partial but statistically significant rescue of sensitivity at low camptothecin doses upon co-depletion of EXO1 and CtIP. One possible explanation for this observation could be that, upon CtIP downregulation, EXO1 “over-resects” DNA giving rise to faulty recombination intermediates.

On the other hand, depletion of both proteins avoids the deleterious effects of uncontrolled EXO1 resection activity, allowing survival. The latter, however, may come at a price if it results from inappropriate NHEJ, the consequence of which are gross chromosomal aberrations and the onset of cancer.

In order to test this hypothesis, we analysed metaphase spreads from cells depleted for CtIP, EXO1 or both paying particular attention to the presence of radial chromosomes. We noticed a significant increase in the number of radial chromosomes in cells co-depleted for CtIP and EXO1, indicative of illegitimate repair by NHEJ. To further confirm our observation, we examined the activation of DNA-PKcs, a kinase that is instrumental in the process of DNA end ligation by NHEJ. It is known from the literature that camptothecin activates DNA-PKcs, as evidenced by its autophosphorylation (Sakasai et al. 2010). Interestingly, we observed increased DNA-PKcs activation in cells co-depleted for EXO1 and CtIP under "basal" conditions, and the signal was further amplified when cells were treated with camptothecin. This prompted us to re-examine the metaphase spreads for radial chromosome formation under conditions of DNA-PKcs inhibition. In this setting, we observed almost threefold reduction in the number of radial chromosomes in cells co-depleted for EXO1 and CtIP as well as an increase in broken chromatids, compared to cells where DNA-PKcs was not inhibited. Consistent with this, and in agreement with an upregulation of NHEJ in the absence of EXO1 and CtIP, DNA-PKcs inhibition significantly increased the number of DNA breaks measured by PFGE.

Upon conclusion of this interesting study that highlighted the precise control of EXO1 recruitment and enzymatic activity by the interacting protein CtIP, we undertook an explorative investigation aimed at identifying novel EXO1 interacting proteins that could be involved in DDR. This ongoing study is presented in the second part of the thesis as unpublished results.
The assembly and retention of different proteins at sites of damaged chromatin in so-called ionizing radiation-induced foci (IRIF) is a core feature of the DDR. IRIF formation is often used as read-out for the activation of DDR

that is triggered upon detection of damage as well as for the identification of novel proteins participating to the DDR. Over the last decade, insights into the architecture of IRIF and the identity of proteins residing in them as well as the molecular mechanisms of their retention at these structures have been vastly expanded. Despite such advances, however, many studies have been simply descriptive, thus lacking the necessary depth that would allow appreciating in which specific steps of the DDR the newly identified IRIF components are involved. The importance of studying IRIF is underlined by the fact that defects in IRIF formation or loss of DDR factors that accumulate at IRIF are often associated with genomic instability and cancer. For instance, an hypomorphic mutation in *NBS1* leads to Nijmegen breakage syndrome (NBS), which results in predisposition to cancer, immunodeficiency and growth retardation. Likewise, a mutation in the *RNF168* has been recently linked to the RIDDLE syndrome whose clinical features include increased radiosensitivity, immunodeficiency, dysmorphic features and learning difficulties (Stewart et al. 2007). Though, despite the effort of revealing the complexity of IRIF may seem to be a daunting undertaking, it will be the only way to expand our knowledge of them, thus facilitating the understanding of mechanisms that drive oncogenesis and other pathological syndromes.
Given these premises, we set out to identify proteins interacting with EXO1 in order to better understand the role and the regulation of EXO1 in DNA-end resection as well as to identify new factors that could have a role in IRIF formation. In a large-scale mass spectrometry analysis, using a tagged form of EXO1 we successfully identified a set of novel interacting proteins. Ongoing studies are clarifying whether these EXO1 partners might have a role in DNA repair, a finding that would enable us to shed more light on the complex process of DDR.

In conclusion, the first part of this study describes a novel functional role for the interaction of two important factors involved in DNA end resection, namely CtIP and EXO1. The findings reported here imply that both proteins likely act together to influence the selection between HR and NHEJ repair pathways, hence protecting cells from the deleterious consequences of end-joining-

mediated repair of double strand breaks. Based on our findings, we speculate that hypersensitivity to replication-associated double strand breaks in cells compromised for HR is probably due to inappropriate NHEJ, at least in part, rather than HR deficiency alone. In the second part of this study we present findings on novel proteins interacting with EXO1 that might have important roles in DDR and might, eventually, turn out to be new targets in cancer therapy.

4. MATERIALS AND METHODS

Cell lines and cell culture

293T human embryonic kidney cells were maintained in Dulbecco's modified Eagle's medium (DMEM; Invitrogen) supplemented with 10% fetal calf serum (Gibco), penicillin/streptomycin (100 U/ml; Gibco). Human U2OS osteosarcoma cells and U2OS cells stably expressing GFP-HA-EXO1 (kindly provided by S. P. Jackson, University of Cambridge, UK) were cultured in DMEM supplemented with 10% fetal calf serum, standard antibiotics and G-418 (0.5 mg/ml). Immortalized ATLD1 cells transduced with retrovirus expressing the wild-type MRE11 cDNA (ATLD1/MRE11) or retrovirus harboring the empty vector (ATLD1/vector) (a kind gift of M. Weitzman, Salk Institute, S. Diego, CA) were grown in DMEM supplemented with 20% FCS, streptomycin/penicillin (100 U/ml) and 1 µg/ml puromycin (Sigma). OMNI-EXO1 (El-Shemerly et al, 2005) was transiently transfected in 293T cells with Metafectene (Biontex) while GFP-EXO1 (kindly provided by F. Marini, University of Milano, Italy) was transiently transfected in ATLD1 cells using Fugene HD (Roche). For this, 1 µg of the DNA and 4 µl of the transfecting reagent were added to separate tubes, each containing 100 µl OptiMEM (Gibco). Both solutions were mixed by pipetting up and down and left for 15 minutes at room temperature; the transfection mix was added drop wise to cells (50-60% confluency). All siRNA duplexes were purchased from Microsynth with the exception of MRE11 siRNA, which was purchased from Dharmacon. siRNA sequences are as follow: Luciferase (siCNTL) (CGUACGCGGAAUACUUCGATT) (Sartori et al, 2007), CtIP (GCUAAAACAGGAACGAAUCTT) (Sartori et al, 2007), EXO1 (CAAGCCUAUUCUCGUAUUUTT) (Gravel et al, 2008), and MRE11 (GAGCAUAACUCCAUAAGUATT) (Adams et al, 2006). siRNA duplexes were transfected into cells using Lipofectamine RNAiMAX (Invitrogen) in two consecutive rounds to a final concentration of 80 nM as follows: control (80 nM luciferase siRNA), EXO1 (40 nM EXO1 siRNA + 40 nM control siRNA), CtIP (40 nM CtIP siRNA + 40 nM control siRNA), or combined EXO1 and CtIP (40 nM EXO1 siRNA + 40 nM CtIP siRNA). Cellular analysis was typically

performed 72h after transfection.

Antibodies and chemicals

Mouse monoclonal antibodies used in this study included CHK1, GFP, β-tubulin (Santa Cruz), FLAG (Sigma), γH2AX (Upstate), MRE11 (GeneTex), RPA2 (Calbiochem) and EXO1 (Neomarkers). Rabbit polyclonal antibodies included γH2AX and CHK1-pS345 (Cell Signaling), MRE11 (Novus), DNA-PKcs-pS2056 (Abcam). Goat polyclonal antibodies included CtIP and OMNI (Santa Cruz). Rabbit polyclonal EXO1 antibody, F-15 was generated in rabbit (Clonestar, Brno, Czech Republic) and purified using a protein A-Sepharose column (GE Healthcare) according to the manufacturer's instructions. The serum of a non-immunized rabbit (pre-immune) served as control. Rabbit polyclonal and mouse monoclonal CtIP antibodies (Sartori et al, 2007) were provided by R. Baer (Columbia University, New York, NY). Secondary antibodies included horseradish peroxidase (HRP)-conjugated anti-mouse and anti-rabbit antibodies (GE-Healthcare) and an HRP-conjugated anti-goat antibody (Santa Cruz). Alexa Fluor-488, -594, and -647-conjugated secondary antibodies for immunofluoresence were from Invitrogen.

Camptothecin (Sigma) and AZD2281 (Olaparib, Selleck Chemicals) were dissolved in dymethyl sulfoxide (DMSO) at 1 mM and 10 mM stock concentrations, respectively. Hydroxyurea (Sigma) was dissolved in water at 1 M stock concentration. EdU (5-ethynyl-2'-deoxyuridine) was from Invitrogen. The DNA-PKcs inhibitor NU7441 (Tocris Bioscience) (Leahy et al, 2004) was dissolved in DMSO at 5 mM stock concentration. The *E. coli* exonuclease EXOIII was from New England Biolabs.

Immunofluorescence

Cells were grown on coverslips and treated as planned. Coverslips with attached cells were then washed once in phosphate-buffered saline (PBS) and cells were either fixed in ice-cold methanol for 15 minutes on ice or in 4% formaldehyde (FA) (w/v) in PBS for 15 minutes at room temperature. Cells fixed in FA/PBS were then permeabilized using a 0.2% Triton X-100/PBS solution for 5 minutes at room temperature. When required, cells were pre-

extracted for 5 minutes on ice in pre-extraction buffer (25 mM HEPES pH 7.4, 50 mM NaCl, 1 mM EDTA, 3 mM $MgCl_2$, 300 mM sucrose and 0.5% Triton X-100) before fixation in 4% FA/PBS. Coverslips were then blocked in 3% non-fat milk/PBS solution for 30 minutes, stained with antibodies against proteins of interest for at least 2 hours up to overnight, washed three times in 3% non-fat milk/PBS, and incubated with secondary antibodies for 1 hour. Finally, coverslips were washed twice in PBS and once in ddH_2O before mounting on glass slides with Vectashield (Vector Laboratories) containing DAPI and sealed with nail polish. Images were acquired using either a Leica confocal SP2 or an Olympus IX81 fluorescence microscope.

Western blotting and Immunoprecipitation

Cellular proteins were extracted using ice-cold lysis buffer (50mM Tris–HCl pH 7.5, 120mM NaCl, 20mM NaF, 1mM EDTA, 6mM EGTA, 15mM Na-pyrophosphate, 0.5mM Na-orthovanadate, 1mM benzamidine, 0.1mM phenylmethylsulfonyl fluoride and 1% Nonidet P-40). Protein concentration was determined using the Bio-Rad Protein Assay Reagent (Bio-Rad). Proteins were separated by running whole cell extracts on SDS-polyacrylamide gels. Proteins were transferred to polyvinylidene difluoride (PVDF) (GE-Healthcare), probed with appropriate antibodies and immune complexes were revealed using the enhanced chemiluminescence (ECL) system (GE-Healthcare).

EXO1 and CtIP were immunoprecipitated from 5 mg total cell extracts for 2 hours at 4^{o}C using the polyclonal antibody F-15 and an anti-CtIP polyclonal antibody respectively. The antibodies were captured using protein A Sepharose beads (GE-Healthcare) for 1 hour at 4^{o}C. Beads were washed twice in 1 ml ice-cold TNET buffer (50 mM Tris-HCl pH 7.5, 140 mM NaCl, 1% Triton X-100) and twice in 1 ml ice-cold TNE buffer (50mM Tris-HCl pH 7.5, 140 mM NaCl). Beads were heated for 10 minutes at 95^{o}C in 2x Laemmli sample buffer, proteins were resolved by SDS-polyacrylamide gel electrophoresis and analyzed by Western blotting using appropriate antibodies. To exclude the possibility that the observed interactions are DNA-mediated, ethidium bromide (Sigma) was added to all samples.

In vitro protein interaction

200 ng of purified, recombinant CtIP (Sartori et al, 2007) and EXO1 (El Shemerly et al, 2005) were incubated either alone or together for 30 min at 4 ^{o}C in 1 ml TNE buffer containing (50 mM Tris-HCl pH 7.5, 140 mM NaCl, 1 mM EDTA and 10 μg/ml BSA). Proteins were immunoprecipitated with the antibody F-15 for 2h at 4^{o}C and processed as described in the immunoprecipitation section.

Exonuclease assay

The nicked substrate was generated by incubating the pGEM-13Zf(+) plasmid derivative with *N.Bst*NBI (Fischer et al, 2007) and purified by gel extraction (Qiagen). Exonuclease activities were assayed in a buffer containing (50 mM Tris-HCl pH 7.5, 50 mM NaCl, 2 mM $MgCl_2$, 1 mM DTT and 0.1 mg/ml BSA). Where indicated, final concentrations of purified recombinant proteins were as follows: 15 nM EXO1, 15 nM CtIP and 300 nM RPA. Reactions were stopped by incubation in 10 mM EDTA, 0.25 % SDS and 100 μg/ml Proteinase K for 10 min at 37° C. DNA products were separated on 0.8% agarose, stained with either ethidium bromide or SYBR Gold for 30 minutes and analyzed with a Typhoon PhosphorImager (GE Healthcare).

Hairpin exonuclease assays were performed in 20 µl with 1 nM DNA substrate (annealed 3' labeled HL1: 5'-TCATTGCCTATCCTGACAGTCCGACACATCGGACTGTCAGGATAGGCAA TGATCTTTTTTTTT -3'), 50 mM Tris-HCl pH 7.5, 50 mM NaCl, 5 mM $MgCl_2$, 1 mM DTT and 50 ng/µl BSA at 37^{o}C with the indicated protein concentrations and time-points. Reactions were terminated by addition of an equal volume of 99% (v/v) formamide 0.1% (w/v) bromophenol blue and heating at 95°C for 5 min. Products were resolved by electrophoresis in a 15% (w/v) polyacrylamide gel containing 8 M urea (acrylamide/bis-acrylamide 19:1) run in 1xTBE buffer (Tris/Borate/EDTA, pH 8.0) at 25 mA. Gels were dried and analyzed with a Typhoon PhosphorImager (GE Healthcare).

Linearized plasmids were generated by incubating the pGEM-13Zf(+) plasmid derivative with either Ban*II* (5' overhangs), Hind*III* (3' overhangs) or Sca*I*

(blunt ends) followed by column purification (Qiagen). Proteins used in the assay were mixed and incubated on ice prior to addition into reaction tubes containing 50 mM Tris-HCl pH 7.5, 50 mM NaCl, 2 mM $MgCl_2$, 1 mM DTT and 0.1 mg/ml BSA. DNA products were separated as described above.

DNA-binding assay

Gel mobility shift assays were performed in a volume of 20 µl containing 5 nM of annealed 5' labeled HL1, 50 mM Tris-HCl pH 7.5, 50 mM NaCl, 1 mM EDTA, 1 mM DTT, 50 ng/µl BSA. The reactions were pre-incubated with the corresponding proteins, 10 nM EXO1, 50 nM CtIP for 15 min at RT before addition of the substrate and further incubated for 60 min. After addition of glycerol to a final 10% concentration, separation was performed in a 6% (w/v) native polyacrylamide gel run in 1xTBE buffer at 25 mAmp. Gels were analyzed as described above.

Pulse-field gel electrophoresis

U2OS cells were mock-treated (DMSO) or camptothecin-treated for 4h. Cells were harvested by trypsinization and counted. Agarose plugs of 10^6 cells were prepared in a disposable plug mold (BioRad). Plugs were then incubated in lysis buffer (100 mM EDTA, 1% (w/v) sodium lauryl sarcosyl, 0.2% (w/v) sodium deoxycholate, 1mg/ml proteinase K) at 37^{o}C for 72h. Plugs were then washed four times in 20 mM Tris-HCl pH 8.0, 50 mM EDTA before loading onto an agarose gel. Electrophoresis was performed for 23h at 14^{o}C in 0.9% (w/v) Pulse Field Certified Agarose (BioRad) containing TBE buffer according to the conditions described in (Hanada et al, 2007) and adapted to a BioRad CHEF DR III apparatus.

The following parameters were used:

Block	I	II	III
Time (h)	9	6	6
Included angle	120	117	112
V/cm	5.5	4.5	4.0
Switch (s) (Initial-Final)	30-18	18-9	9-5

Under the electrophoresis conditions used, high molecular weight genomic DNA (more than several million base pairs (bp)) remains in the well, whereas low molecular weight DNA fragments (several Mbp to 500 kbp) migrate into the gel and are compacted into a single band. The gel was then stained with ethidium bromide for 30 minutes and analyzed using an Alpha Innotech Imaging system.

Colony formation assay

72 hours after siRNA transfection, cells were either mock-treated (DMSO) or treated with the indicated doses of camptothecin. The drug was removed 1h upon treatment, cells were washed twice in pre-warmed PBS and fresh medium was added. Cells were cultured for additional 10–14 days at 37°C, 5% CO_2. For the PARP-inhibitor AZD2281, continuous exposure to the compound was ensured by a first addition 72h after the siRNA transfection, and a second addition 72 h after the first. Colonies were washed once with PBS, stained with a crystal violet/ethanol (0.5%/20%) solution, dried and counted by eye. All measurements were performed in triplicates.

Chromosome analysis

72h upon siRNA transfection cells were treated with camptothecin for 1h. The drug-containing medium was removed, cells were washed twice in pre-warmed PBS and allowed to recover for 8h in complete medium before chromosome preparation. Caffeine (2 mM) was added for the last 5h to override the G2/M checkpoint, and colcemid (0.1 mg/ml) was added for the last 3h to arrest cells in metaphase. Cells were then trypsinized, centrifuged, re-suspended in 0.56% KCl solution and incubated for 6 minutes at room temperature. KCl was discarded after centrifugation and cells were re-

suspended in a pre-fixing solution (5% acetic acid in ddH_2O). Cells were then centrifuged and re-suspended in a fixing solution (Acetic acid: Methanol, 1:3) and incubated for 10 minutes at room temperature. The fixing solution was discarded after centrifugation and cells were re-suspended in 500 µl of the fixing solution. 25-30 µl of the cell suspension were spread on a glass microscope slide and air-dried. Coverslips were mounted using Vectashield with DAPI (Vector Laboratories). Images were acquired using a confocal Leica SP2 microscope using the 100X lens. 50 metaphase spreads were acquired per sample.

Live cell imaging and laser micro-irradiation

Prior to irradiation, cells were treated with 10 µM bromodeoxyuridine (BrdU) for 24h. DSBs were generated in the nuclei of living cells on 18 mm glass cover slips by micro-irradiation of arbitrarily shaped regions of interest (ROI) at 355 nm with 15 mW output power of the laser (Genesis 355-80, Coherent Inc.) (Walter et al, 2003). ROIs were irradiated for 10 consecutive times and identical ROIs were used in all experiments. Subsequently, fluorescence time-lapse imaging was performed for GFP (488 nm excitation, 525-560 nm emission; SP5, Leica, Mannheim, Germany) using a HCX Plan-Apo 63X/NA 1.40 oil immersion objective. During the experiments, cells were kept in complete growth medium under 5% CO_2 at 37°C in a climate chamber.

For fixed cell imaging, cells were grown on coverslips for 24h in the presence of 10 µM BrdU prior to irradiation. Coverslips were transferred to LabTek chamber slides (Nunc) and mounted on the microscope stage. In order to generate DSBs in a defined nuclear volume, laser micro-irradiation was performed using a MMI CELLCUT system equipped with a 355 nm UV-A laser (Molecular Machines & Industries) coupled to an Olympus IX71 microscope station. Experiments were performed using the 40X objective. The MMICELLTOOLS® software with MMIUVCUT® plug-in assisted the laser operation using an energy output of 50%. After irradiation, cells were returned to the incubator until the time of processing.

Cloning of Strep-EXO1 and Mass Spectrometric analysis

Strep-tagged EXO1 was generated by subcloning full-length human EXO1 cDNA in the mammalian expression vector pEXPR-IBA3 (IBA BioTAGnology), which allows adding a C-terminal Strep-tag to the protein of interest. EXO1 was cloned between the BamHI and SacII restriction sites, using the primers 5'- ATGGGAGACCGCGGGATACAGGGATTGCTACAATTTATC -3' (forward) and 5'- CTCGAGGGATCCCTGGAATATTGCTCTTTGAACACGG -3' (reverse). Constructs were verified by sequencing. HEK293T cells were transfected with either Strep-tagged EXO1 or with empty vector (mock), using Metafectene (Biontex). 72h after transfection cells were harvested in lysis buffer (50mM Tris–HCl pH 7.5, 120mM NaCl, 20mM NaF, 1mM EDTA, 6mM EGTA, 15mM Na-pyrophosphate, 0.5mM Na-orthovanadate, 1mM benzamidine, 0.1mM phenylmethylsulfonyl fluoride and 1% Nonidet P-40). 20mg of the whole cell lysate from each sample (mock and Strep-tagged EXO1) were incubated on a rotator for 1h in 4^{o}C with 70 µl of Strep-Tactin Sepharose beads (IBA BioTAGnology) equilibrated in lysis buffer. Beads were washed 3x with 1 ml of ice-cold lysis buffer, followed by 100 µl of 5mM D-Desthiobiotin (IBA BioTAGnology) and incubated at 4^{o}C for 2h with vigorous shaking. Beads were centrifuged, the supernatant (eluate) was transferred to a new tube and 100 µl of D-Desthiobiotin was added to each tube. Upon incubation at 4^{o}C for 1h with vigorous shaking supernatants were recovered as described above and pooled. Finally, supernatants were subjected to tri-chloracetic acid (TCA) precipitation by addition of the acid to a final concentration of 20% from a 50% stock (*m:v* in ddH_2O), vortexed and incubated on ice for 2h. Samples were centrifuged and protein pellets were washed in 1 ml of 10% ice-cold TCA, vortexed and centrifuged. Pellets were then washed with 1 ml of ice-cold HPLC-grade acetone, centrifuged and air dried. Protein pellets were stored at -80^{o}C until the time of analysis.

Precipitated proteins were digested with trypsin. Tryptic peptides were purified by HPLC chromatography and peptide masses were determined using an LTQ Orbitrap Velos (Thermo Scientific). Proteins were identified by comparing the obtained spectra against the human subset of the protein sequence database Swiss-Prot in order to identify the proteins.

5. REFERENCES

Aguilera, A. and Gomez-Gonzalez, B. (2008) Genome instability: a mechanistic view of its causes and consequences. *Nat Rev Genet*, **9**, 204-217.

Amin, N.S., Nguyen, M.N., Oh, S. and Kolodner, R.D. (2001) exo1-Dependent mutator mutations: model system for studying functional interactions in mismatch repair. *Mol Cell Biol*, **21**, 5142-5155.

Attwooll, C., Lazzerini Denchi, E. and Helin, K. (2004) The E2F family: specific functions and overlapping interests. *EMBO J*, **23**, 4709-4716.

Bakkenist, C.J. and Kastan, M.B. (2003) DNA damage activates ATM through intermolecular autophosphorylation and dimer dissociation. *Nature*, **421**, 499-506.

Bartek, J. and Lukas, J. (2003) Chk1 and Chk2 kinases in checkpoint control and cancer. *Cancer Cell*, **3**, 421-429.

Bartek, J. and Lukas, J. (2003) DNA repair: Damage alert. *Nature*, **421**, 486-488.

Bartek, J., Lukas, C. and Lukas, J. (2004) Checking on DNA damage in S phase. *Nat Rev Mol Cell Biol*, **5**, 792-804.

Bekker-Jensen, S. and Mailand, N. (2010) Assembly and function of DNA double-strand break repair foci in mammalian cells. *DNA Repair (Amst)*, **9**, 1219-1228.

Bennardo, N., Cheng, A., Huang, N. and Stark, J.M. (2008) Alternative-NHEJ is a mechanistically distinct pathway of mammalian chromosome break repair. *PLoS Genet*, **4**, e1000110.

Bernstein, K.A., Gangloff, S. and Rothstein, R. (2010) The RecQ DNA helicases in DNA repair. *Annu Rev Genet*, **44**, 393-417.

Bolderson, E., Tomimatsu, N., Richard, D.J., Boucher, D., Kumar, R., Pandita, T.K., Burma, S. and Khanna, K.K. (2010) Phosphorylation of Exo1 modulates homologous recombination repair of DNA double-strand breaks. *Nucleic Acids Res*, **38**, 1821-1831.

Bosco, E.E., Mayhew, C.N., Hennigan, R.F., Sage, J., Jacks, T. and Knudsen, E.S. (2004) RB signaling prevents replication-dependent DNA double-strand breaks following genotoxic insult. *Nucleic Acids Res*, **32**, 25-34.

Botuyan, M.V., Lee, J., Ward, I.M., Kim, J.E., Thompson, J.R., Chen, J. and Mer, G. (2006) Structural basis for the methylation state-specific recognition of histone H4-K20 by 53BP1 and Crb2 in DNA repair. *Cell*, **127**, 1361-1373.

Boyd, J.M., Subramanian, T., Schaeper, U., La Regina, M., Bayley, S. and Chinnadurai, G. (1993) A region in the C-terminus of adenovirus 2/5 E1a protein is required for association with a cellular phosphoprotein and important for the negative modulation of T24-ras mediated transformation, tumorigenesis and metastasis. *EMBO J*, **12**, 469-478.

Burma, S., Chen, B.P., Murphy, M., Kurimasa, A. and Chen, D.J. (2001) ATM phosphorylates histone H2AX in response to DNA double-strand breaks. *J Biol Chem*, **276**, 42462-42467.

Busino, L., Donzelli, M., Chiesa, M., Guardavaccaro, D., Ganoth, D., Dorrello, N.V., Hershko, A., Pagano, M. and Draetta, G.F. (2003) Degradation of Cdc25A by beta-TrCP during S phase and in response to DNA damage. *Nature*, **426**, 87-91.

Chen, Q., Samaranayake, L.P., Zhen, X., Luo, G., Nie, M. and Li, B. (1999) Up-regulation of Fas ligand and down-regulation of Fas expression in oral carcinogenesis. *Oral Oncol*, **35**, 548-553.

Chen, X.B., Melchionna, R., Denis, C.M., Gaillard, P.H., Blasina, A., Van de Weyer, I., Boddy, M.N., Russell, P., Vialard, J. and McGowan, C.H. (2001) Human Mus81-associated endonuclease cleaves Holliday junctions in vitro. *Mol Cell*, **8**, 1117-1127.

Chinnadurai, G. (2009) The transcriptional corepressor CtBP: a foe of multiple tumor suppressors. *Cancer Res*, **69**, 731-734.

Choudhury, A.D., Xu, H. and Baer, R. (2004) Ubiquitination and proteasomal degradation of the BRCA1 tumor suppressor is regulated during cell cycle progression. *J Biol Chem*, **279**, 33909-33918.

Ciccia, A. and Elledge, S.J. (2010) The DNA damage response: making it safe to play with knives. *Mol Cell*, **40**, 179-204.

Cimprich, K.A. and Cortez, D. (2008) ATR: an essential regulator of genome integrity. *Nat Rev Mol Cell Biol*, **9**, 616-627.

Cotta-Ramusino, C., Fachinetti, D., Lucca, C., Doksani, Y., Lopes, M., Sogo, J. and Foiani, M. (2005) Exo1 processes stalled replication forks and counteracts fork reversal in checkpoint-defective cells. *Mol Cell*, **17**, 153-159.

Czornak, K., Chughtai, S. and Chrzanowska, K.H. (2008) Mystery of DNA repair: the role of the MRN complex and ATM kinase in DNA damage repair. *J Appl Genet*, **49**, 383-396.

Daya-Makin, M., Szankasi, P., Tang, L., MacRae, D. and Pelech, S.L. (1992) Regulation of p105wee1 and p34cdc2 during meiosis in Schizosaccharomyces pombe. *Biochem Cell Biol*, **70**, 1088-1096.

Degrassi, F., Fiore, M. and Palitti, F. (2004) Chromosomal aberrations and genomic instability induced by topoisomerase-targeted antitumour drugs. *Curr Med Chem Anticancer Agents*, **4**, 317-325.

Delacote, F. and Lopez, B.S. (2008) Importance of the cell cycle phase for the choice of the appropriate DSB repair pathway, for genome stability maintenance: the trans-S double-strand break repair model. *Cell Cycle*, **7**, 33-38.

Delacote, F., Han, M., Stamato, T.D., Jasin, M. and Lopez, B.S. (2002) An xrcc4 defect or Wortmannin stimulates homologous recombination specifically induced by double-strand breaks in mammalian cells. *Nucleic Acids Res*, **30**, 3454-3463.

Doil, C., Mailand, N., Bekker-Jensen, S., Menard, P., Larsen, D.H., Pepperkok, R., Ellenberg, J., Panier, S., Durocher, D., Bartek, J. *et al.* (2009) RNF168 binds and amplifies ubiquitin conjugates on damaged chromosomes to allow accumulation of repair proteins. *Cell*, **136**, 435-446.

Donzelli, M. and Draetta, G.F. (2003) Regulating mammalian checkpoints through Cdc25 inactivation. *EMBO Rep*, **4**, 671-677.

Eid, W., Steger, M., El-Shemerly, M., Ferretti, L.P., Pena-Diaz, J., Konig, C., Valtorta, E., Sartori, A.A. and Ferrari, S. DNA end resection by CtIP and exonuclease 1 prevents genomic instability. *EMBO Rep*, **11**, 962-968.

El-Shemerly, M., Hess, D., Pyakurel, A.K., Moselhy, S. and Ferrari, S. (2008) ATR-dependent pathways control hEXO1 stability in response to stalled forks. *Nucleic Acids Res*, **36**, 511-519.

El-Shemerly, M., Janscak, P., Hess, D., Jiricny, J. and Ferrari, S. (2005) Degradation of human exonuclease 1b upon DNA synthesis inhibition. *Cancer Res*, **65**, 3604-3609.

Esashi, F., Christ, N., Gannon, J., Liu, Y., Hunt, T., Jasin, M. and West, S.C. (2005) CDK-dependent phosphorylation of BRCA2 as a regulatory mechanism for recombinational repair. *Nature*, **434**, 598-604.

Falck, J., Mailand, N., Syljuasen, R.G., Bartek, J. and Lukas, J. (2001) The ATM-Chk2-Cdc25A checkpoint pathway guards against radioresistant DNA synthesis. *Nature*, **410**, 842-847.

Fanning, E., Klimovich, V. and Nager, A.R. (2006) A dynamic model for replication protein A (RPA) function in DNA processing pathways. *Nucleic Acids Res*, **34**, 4126-4137.

Farah, J.A., Cromie, G.A. and Smith, G.R. (2009) Ctp1 and Exonuclease 1, alternative nucleases regulated by the MRN complex, are required for efficient meiotic recombination. *Proc Natl Acad Sci U S A*, **106**, 9356-9361.

Fekairi, S., Scaglione, S., Chahwan, C., Taylor, E.R., Tissier, A., Coulon, S., Dong, M.Q., Ruse, C., Yates, J.R., 3rd, Russell, P. *et al.* (2009) Human SLX4 is a Holliday junction resolvase subunit that binds multiple DNA repair/recombination endonucleases. *Cell*, **138**, 78-89.

Ferguson, A.M., White, L.S., Donovan, P.J. and Piwnica-Worms, H. (2005) Normal cell cycle and checkpoint responses in mice and cells lacking Cdc25B and Cdc25C protein phosphatases. *Mol Cell Biol*, **25**, 2853-2860.

Ferrari, S. (2006) Protein kinases controlling the onset of mitosis. *Cell Mol Life Sci*, **63**, 781-795.

Finn, K., Lowndes, N.F. and Grenon, M. (2011) Eukaryotic DNA damage checkpoint activation in response to double-strand breaks. *Cell Mol Life Sci*.
Folle, G.A. (2008) Nuclear architecture, chromosome domains and genetic damage. *Mutat Res*, **658**, 172-183.

Fusco, C., Reymond, A. and Zervos, A.S. (1998) Molecular cloning and characterization of a novel retinoblastoma-binding protein. *Genomics*, **51**, 351-358.

Gabrielli, B.G., De Souza, C.P., Tonks, I.D., Clark, J.M., Hayward, N.K. and Ellem, K.A. (1996) Cytoplasmic accumulation of cdc25B phosphatase in mitosis triggers centrosomal microtubule nucleation in HeLa cells. *J Cell Sci*, **109 (Pt 5)**, 1081-1093.

Gravel, S., Chapman, J.R., Magill, C. and Jackson, S.P. (2008) DNA helicases Sgs1 and BLM promote DNA double-strand break resection. *Genes Dev*, **22**, 2767-2772.

Grawunder, U., Wilm, M., Wu, X., Kulesza, P., Wilson, T.E., Mann, M. and Lieber, M.R. (1997) Activity of DNA ligase IV stimulated by complex formation with XRCC4 protein in mammalian cells. *Nature*, **388**, 492-495.

Hartlerode, A.J. and Scully, R. (2009) Mechanisms of double-strand break repair in somatic mammalian cells. *Biochem J*, **423**, 157-168.

Hartwell, L.H. and Weinert, T.A. (1989) Checkpoints: controls that ensure the order of cell cycle events. *Science*, **246**, 629-634.

Helleday, T., Petermann, E., Lundin, C., Hodgson, B. and Sharma, R.A. (2008) DNA repair pathways as targets for cancer therapy. *Nat Rev Cancer*, **8**, 193-204.

Heyer, W.D., Ehmsen, K.T. and Liu, J. (2010) Regulation of homologous recombination in eukaryotes. *Annu Rev Genet*, **44**, 113-139.

Hinz, J.M., Yamada, N.A., Salazar, E.P., Tebbs, R.S. and Thompson, L.H. (2005) Influence of double-strand-break repair pathways on radiosensitivity throughout the cell cycle in CHO cells. *DNA Repair (Amst)*, **4**, 782-792.

Honaker, Y. and Piwnica-Worms, H. (2010) Casein kinase 1 functions as both penultimate and ultimate kinase in regulating Cdc25A destruction. *Oncogene*, **29**, 3324-3334.

Huen, M.S. and Chen, J. (2010) Assembly of checkpoint and repair machineries at DNA damage sites. *Trends Biochem Sci*, **35**, 101-108.

Huertas, P. (2010) DNA resection in eukaryotes: deciding how to fix the break. *Nat Struct Mol Biol*, **17**, 11-16.

Huertas, P., Cortes-Ledesma, F., Sartori, A.A., Aguilera, A. and Jackson, S.P. (2008) CDK targets Sae2 to control DNA-end resection and homologous recombination. *Nature*, **455**, 689-692.

Human CtIP and its Homologs: Team players in DSB Resection Games. Yasuhiro Tsutsui, Akihito Kawasaki and Hiroshi Iwasaki. Chapter 9 of 'DNA Repair - On the Pathways to Fixing DNA Damage and Errors' book edited by Francesca Storici. Publisher: InTech. **2011** Sept (ISBN 978-953-307-649-2).

Huyen, Y., Zgheib, O., Ditullio, R.A., Jr., Gorgoulis, V.G., Zacharatos, P., Petty, T.J., Sheston, E.A., Mellert, H.S., Stavridi, E.S. and Halazonetis, T.D. (2004) Methylated lysine 79 of histone H3 targets 53BP1 to DNA double-strand breaks. *Nature*, **432**, 406-411.

Ip, S.C., Rass, U., Blanco, M.G., Flynn, H.R., Skehel, J.M. and West, S.C. (2008) Identification of Holliday junction resolvases from humans and yeast. *Nature*, **456**, 357-361.

Ira, G., Pellicioli, A., Balijja, A., Wang, X., Fiorani, S., Carotenuto, W., Liberi, G., Bressan, D., Wan, L., Hollingsworth, N.M. *et al.* (2004) DNA end resection, homologous recombination and DNA damage checkpoint activation require CDK1. *Nature*, **431**, 1011-1017.

Jackson, S.P. (2002) Sensing and repairing DNA double-strand breaks. *Carcinogenesis*, **23**, 687-696.

Jalal, S., Earley, J.N. and Turchi, J.J. (2011) DNA Repair: From Genome Maintenance to Biomarker and Therapeutic Target. *Clin Cancer Res*, **17**, 6973-6984.

Javle, M. and Curtin, N.J. (2011) The potential for poly (ADP-ribose) polymerase inhibitors in cancer therapy. *Ther Adv Med Oncol*, **3**, 257-267.

Jazayeri, A., Falck, J., Lukas, C., Bartek, J., Smith, G.C., Lukas, J. and Jackson, S.P. (2006) ATM- and cell cycle-dependent regulation of ATR in response to DNA double-strand breaks. *Nat Cell Biol*, **8**, 37-45.

Jin, J., Ang, X.L., Ye, X., Livingstone, M. and Harper, J.W. (2008) Differential roles for checkpoint kinases in DNA damage-dependent degradation of the Cdc25A protein phosphatase. *J Biol Chem*, **283**, 19322-19328.

Jiricny, J. (2006) The multifaceted mismatch-repair system. *Nat Rev Mol Cell Biol*, **7**, 335-346.

Jungmichel, S. and Stucki, M. (2010) MDC1: The art of keeping things in focus. *Chromosoma*, **119**, 337-349.

Kang, T., Wei, Y., Honaker, Y., Yamaguchi, H., Appella, E., Hung, M.C. and Piwnica-Worms, H. (2008) GSK-3 beta targets Cdc25A for ubiquitin-mediated proteolysis, and GSK-3 beta inactivation correlates with Cdc25A overproduction in human cancers. *Cancer Cell*, **13**, 36-47.

Kastan, M.B. and Bartek, J. (2004) Cell-cycle checkpoints and cancer. *Nature*, **432**, 316-323.

Kobayashi, J., Iwabuchi, K., Miyagawa, K., Sonoda, E., Suzuki, K., Takata, M. and Tauchi, H. (2008) Current topics in DNA double-strand break repair. *J Radiat Res (Tokyo)*, **49**, 93-103.

Koipally, J. and Georgopoulos, K. (2002) Ikaros-CtIP interactions do not require C-terminal binding protein and participate in a deacetylase-independent mode of repression. *J Biol Chem*, **277**, 23143-23149.

Krystyniak, A., Garcia-Echeverria, C., Prigent, C. and Ferrari, S. (2006) Inhibition of Aurora A in response to DNA damage. *Oncogene*, **25**, 338-348.

Lee, B.I. and Wilson, D.M., 3rd. (1999) The RAD2 domain of human exonuclease 1 exhibits 5' to 3' exonuclease and flap structure-specific endonuclease activities. *J Biol Chem*, **274**, 37763-37769.

Lee, J.H. and Paull, T.T. (2004) Direct activation of the ATM protein kinase by the Mre11/Rad50/Nbs1 complex. *Science*, **304**, 93-96.

Liao, S., Toczylowski, T. and Yan, H. (2011) Mechanistic analysis of Xenopus EXO1's function in 5'-strand resection at DNA double-strand breaks. *Nucleic Acids Res*, **39**, 5967-5977.

Limbo, O., Chahwan, C., Yamada, Y., de Bruin, R.A., Wittenberg, C. and Russell, P. (2007) Ctp1 is a cell-cycle-regulated protein that functions with Mre11 complex to control double-strand break repair by homologous recombination. *Mol Cell*, **28**, 134-146.

Liu, F. and Lee, W.H. (2006) CtIP activates its own and cyclin D1 promoters via the E2F/RB pathway during G1/S progression. *Mol Cell Biol*, **26**, 3124-3134.

Longhese, M.P., Bonetti, D., Guerini, I., Manfrini, N. and Clerici, M. (2009) DNA double-strand breaks in meiosis: checking their formation, processing and repair. *DNA Repair (Amst)*, **8**, 1127-1138.

Longhese, M.P., Mantiero, D. and Clerici, M. (2006) The cellular response to chromosome breakage. *Mol Microbiol*, **60**, 1099-1108.

Lukas, C., Melander, F., Stucki, M., Falck, J., Bekker-Jensen, S., Goldberg, M., Lerenthal, Y., Jackson, S.P., Bartek, J. and Lukas, J. (2004) Mdc1 couples DNA double-strand break recognition by Nbs1 with its H2AX-dependent chromatin retention. *EMBO J*, **23**, 2674-2683.

Luo, G., Yao, M.S., Bender, C.F., Mills, M., Bladl, A.R., Bradley, A. and Petrini, J.H. (1999) Disruption of mRad50 causes embryonic stem cell lethality, abnormal embryonic development, and sensitivity to ionizing radiation. *Proc Natl Acad Sci U S A*, **96**, 7376-7381.

Ma, Y., Pannicke, U., Schwarz, K. and Lieber, M.R. (2002) Hairpin opening and overhang processing by an Artemis/DNA-dependent protein kinase complex in nonhomologous end joining and V(D)J recombination. *Cell*, **108**, 781-794.

Machwe, A., Karale, R., Xu, X., Liu, Y. and Orren, D.K. (2011) The Werner and Bloom syndrome proteins help resolve replication blockage by converting (regressed) holliday junctions to functional replication forks. *Biochemistry*, **50**, 6774-6788.

Mailand, N., Bekker-Jensen, S., Faustrup, H., Melander, F., Bartek, J., Lukas, C. and Lukas, J. (2007) RNF8 ubiquitylates histones at DNA double-strand breaks and promotes assembly of repair proteins. *Cell*, **131**, 887-900.

Marti, T.M. and Fleck, O. (2004) DNA repair nucleases. *Cell Mol Life Sci*, **61**, 336-354.

Martin, A. and Scharff, M.D. (2002) AID and mismatch repair in antibody diversification. *Nat Rev Immunol*, **2**, 605-614.

Maya, R., Balass, M., Kim, S.T., Shkedy, D., Leal, J.F., Shifman, O., Moas, M., Buschmann, T., Ronai, Z., Shiloh, Y. *et al.* (2001) ATM-dependent phosphorylation of Mdm2 on serine 395: role in p53 activation by DNA damage. *Genes Dev*, **15**, 1067-1077.

Medema, R.H. and Macurek, L. (2011) Checkpoint control and cancer. *Oncogene*.

Meek, D.W. (2009) Tumour suppression by p53: a role for the DNA damage response? *Nat Rev Cancer*, **9**, 714-723.

Meloni, A.R., Smith, E.J. and Nevins, J.R. (1999) A mechanism for Rb/p130-mediated transcription repression involving recruitment of the CtBP corepressor. *Proc Natl Acad Sci U S A*, **96**, 9574-9579.

Mimitou, E.P. and Symington, L.S. (2011) DNA end resection--unraveling the tail. *DNA Repair (Amst)*, **10**, 344-348.

Morin, I., Ngo, H.P., Greenall, A., Zubko, M.K., Morrice, N. and Lydall, D. (2008) Checkpoint-dependent phosphorylation of Exo1 modulates the DNA damage response. *EMBO J*, **27**, 2400-2410.

Nimonkar, A.V., Genschel, J., Kinoshita, E., Polaczek, P., Campbell, J.L., Wyman, C., Modrich, P. and Kowalczykowski, S.C. (2011) BLM-DNA2-RPA-MRN and EXO1-BLM-RPA-MRN constitute two DNA end resection machineries for human DNA break repair. *Genes Dev*, **25**, 350-362.

Nishino, T. and Morikawa, K. (2002) Structure and function of nucleases in DNA repair: shape, grip and blade of the DNA scissors. *Oncogene*, **21**, 9022-9032.

Nishino, T., Ishino, Y. and Morikawa, K. (2006) Structure-specific DNA nucleases: structural basis for 3D-scissors. *Curr Opin Struct Biol*, **16**, 60-67.

Nyberg, K.A., Michelson, R.J., Putnam, C.W. and Weinert, T.A. (2002) Toward maintaining the genome: DNA damage and replication checkpoints. *Annu Rev Genet*, **36**, 617-656.

Orans, J., McSweeney, E.A., Iyer, R.R., Hast, M.A., Hellinga, H.W., Modrich, P. and Beese, L.S. (2011) Structures of human exonuclease 1 DNA complexes suggest a unified mechanism for nuclease family. *Cell*, **145**, 212-223.

Pei, H., Zhang, L., Luo, K., Qin, Y., Chesi, M., Fei, F., Bergsagel, P.L., Wang, L., You, Z. and Lou, Z. (2011) MMSET regulates histone H4K20 methylation and 53BP1 accumulation at DNA damage sites. *Nature*, **470**, 124-128.

Pei, X.H. and Xiong, Y. (2005) Biochemical and cellular mechanisms of mammalian CDK inhibitors: a few unresolved issues. *Oncogene*, **24**, 2787-2795.

Pellegrini, L., Yu, D.S., Lo, T., Anand, S., Lee, M., Blundell, T.L. and Venkitaraman, A.R. (2002) Insights into DNA recombination from the structure of a RAD51-BRCA2 complex. *Nature*, **420**, 287-293.

Prinz, S., Amon, A. and Klein, F. (1997) Isolation of COM1, a new gene required to complete meiotic double-strand break-induced recombination in Saccharomyces cerevisiae. *Genetics*, **146**, 781-795.

Qiu, J., Qian, Y., Chen, V., Guan, M.X. and Shen, B. (1999) Human exonuclease 1 functionally complements its yeast homologues in DNA recombination, RNA primer removal, and mutation avoidance. *J Biol Chem*, **274**, 17893-17900.

Quennet, V., Beucher, A., Barton, O., Takeda, S. and Lobrich, M. (2010) CtIP and MRN promote non-homologous end-joining of etoposide-induced DNA double-strand breaks in G1. *Nucleic Acids Res*, **39**, 2144-2152.

Rogakou, E.P., Pilch, D.R., Orr, A.H., Ivanova, V.S. and Bonner, W.M. (1998) DNA double-stranded breaks induce histone H2AX phosphorylation on serine 139. *J Biol Chem*, **273**, 5858-5868.

Rothkamm, K., Kruger, I., Thompson, L.H. and Lobrich, M. (2003) Pathways of DNA double-strand break repair during the mammalian cell cycle. *Mol Cell Biol*, **23**, 5706-5715.

Sakasai, R., Teraoka, H. and Tibbetts, R.S. (2010) Proteasome inhibition suppresses DNA-dependent protein kinase activation caused by camptothecin. *DNA Repair (Amst)*, **9**, 76-82.

Sartori, A.A., Lukas, C., Coates, J., Mistrik, M., Fu, S., Bartek, J., Baer, R., Lukas, J. and Jackson, S.P. (2007) Human CtIP promotes DNA end resection. *Nature*, **450**, 509-514.

Schaeper, U., Subramanian, T., Lim, L., Boyd, J.M. and Chinnadurai, G. (1998) Interaction between a cellular protein that binds to the C-terminal region of adenovirus E1A (CtBP) and a novel cellular protein is disrupted by E1A through a conserved PLDLS motif. *J Biol Chem*, **273**, 8549-8552.

Schmutte, C., Sadoff, M.M., Shim, K.S., Acharya, S. and Fishel, R. (2001) The interaction of DNA mismatch repair proteins with human exonuclease I. *J Biol Chem*, **276**, 33011-33018.

Shiloh, Y. (2003) ATM and related protein kinases: safeguarding genome integrity. *Nat Rev Cancer*, **3**, 155-168.

Shiotani, B. and Zou, L. (2009) Single-stranded DNA orchestrates an ATM-to-ATR switch at DNA breaks. *Mol Cell*, **33**, 547-558.

Shrivastav, M., De Haro, L.P. and Nickoloff, J.A. (2008) Regulation of DNA double-strand break repair pathway choice. *Cell Res*, **18**, 134-147.

So, E.Y., Ausman, M., Saeki, T. and Ouchi, T. (2011) Phosphorylation of SMC1 by ATR is required for desferrioxamine (DFO)-induced apoptosis. *Cell Death Dis*, **2**, e128.

Stewart, G.S., Maser, R.S., Stankovic, T., Bressan, D.A., Kaplan, M.I., Jaspers, N.G., Raams, A., Byrd, P.J., Petrini, J.H. and Taylor, A.M. (1999) The DNA double-strand break repair gene hMRE11 is mutated in individuals with an ataxia-telangiectasia-like disorder. *Cell*, **99**, 577-587.

Stiff, T., O'Driscoll, M., Rief, N., Iwabuchi, K., Lobrich, M. and Jeggo, P.A. (2004) ATM and DNA-PK function redundantly to phosphorylate H2AX after exposure to ionizing radiation. *Cancer Res*, **64**, 2390-2396.

Stucki, M., Clapperton, J.A., Mohammad, D., Yaffe, M.B., Smerdon, S.J. and Jackson, S.P. (2005) MDC1 directly binds phosphorylated histone H2AX to regulate cellular responses to DNA double-strand breaks. *Cell*, **123**, 1213-1226.

Sum, E.Y., Peng, B., Yu, X., Chen, J., Byrne, J., Lindeman, G.J. and Visvader, J.E. (2002) The LIM domain protein LMO4 interacts with the cofactor CtIP and the tumor suppressor BRCA1 and inhibits BRCA1 activity. *J Biol Chem*, **277**, 7849-7856.

Svendsen, J.M., Smogorzewska, A., Sowa, M.E., O'Connell, B.C., Gygi, S.P., Elledge, S.J. and Harper, J.W. (2009) Mammalian BTBD12/SLX4 assembles a Holliday junction resolvase and is required for DNA repair. *Cell*, **138**, 63-77.

Symington, L.S. and Gautier, J. (2011) Double-strand break end resection and repair pathway choice. *Annu Rev Genet*, **45**, 247-271.

Szankasi, P. and Smith, G.R. (1992) A DNA exonuclease induced during meiosis of Schizosaccharomyces pombe. *J Biol Chem*, **267**, 3014-3023.

Taylor, W.R. and Stark, G.R. (2001) Regulation of the G2/M transition by p53. *Oncogene*, **20**, 1803-1815.

Tishkoff, D.X., Amin, N.S., Viars, C.S., Arden, K.C. and Kolodner, R.D. (1998) Identification of a human gene encoding a homologue of Saccharomyces cerevisiae EXO1, an exonuclease implicated in mismatch repair and recombination. *Cancer Res*, **58**, 5027-5031.

Tishkoff, D.X., Boerger, A.L., Bertrand, P., Filosi, N., Gaida, G.M., Kane, M.F. and Kolodner, R.D. (1997) Identification and characterization of Saccharomyces cerevisiae EXO1, a gene encoding an exonuclease that interacts with MSH2. *Proc Natl Acad Sci U S A*, **94**, 7487-7492.

Tran, P.T., Erdeniz, N., Dudley, S. and Liskay, R.M. (2002) Characterization of nuclease-dependent functions of Exo1p in Saccharomyces cerevisiae. *DNA Repair (Amst)*, **1**, 895-912.

Tran, P.T., Erdeniz, N., Symington, L.S. and Liskay, R.M. (2004) EXO1-A multi-tasking eukaryotic nuclease. *DNA Repair (Amst)*, **3**, 1549-1559.

Uto, K., Inoue, D., Shimuta, K., Nakajo, N. and Sagata, N. (2004) Chk1, but not Chk2, inhibits Cdc25 phosphatases by a novel common mechanism. *EMBO J*, **23**, 3386-3396.

Vissers, J.H., Nicassio, F., van Lohuizen, M., Di Fiore, P.P. and Citterio, E. (2008) The many faces of ubiquitinated histone H2A: insights from the DUBs. *Cell Div*, **3**, 8.

Walker, J.R., Corpina, R.A. and Goldberg, J. (2001) Structure of the Ku heterodimer bound to DNA and its implications for double-strand break repair. *Nature*, **412**, 607-614.

Waltes, R., Kalb, R., Gatei, M., Kijas, A.W., Stumm, M., Sobeck, A., Wieland, B., Varon, R., Lerenthal, Y., Lavin, M.F. *et al.* (2009) Human RAD50 deficiency in a Nijmegen breakage syndrome-like disorder. *Am J Hum Genet*, **84**, 605-616.

Wang, B., Hurov, K., Hofmann, K. and Elledge, S.J. (2009) NBA1, a new player in the Brca1 A complex, is required for DNA damage resistance and checkpoint control. *Genes Dev*, **23**, 729-739.

Ward, P., Dean, F.B., O'Donnell, M.E. and Berns, K.I. (1998) Role of the adenovirus DNA-binding protein in in vitro adeno-associated virus DNA replication. *J Virol*, **72**, 420-427.

Wei, K., Clark, A.B., Wong, E., Kane, M.F., Mazur, D.J., Parris, T., Kolas, N.K., Russell, R., Hou, H., Jr., Kneitz, B. *et al.* (2003) Inactivation of Exonuclease 1 in mice results in DNA mismatch repair defects, increased cancer susceptibility, and male and female sterility. *Genes Dev*, **17**, 603-614.

West, S.C. (2003) Molecular views of recombination proteins and their control. *Nat Rev Mol Cell Biol*, **4**, 435-445.

Weterings, E. and Chen, D.J. (2008) The endless tale of non-homologous end-joining. *Cell Res*, **18**, 114-124.

Weterings, E., Verkaik, N.S., Bruggenwirth, H.T., Hoeijmakers, J.H. and van Gent, D.C. (2003) The role of DNA dependent protein kinase in synapsis of DNA ends. *Nucleic Acids Res*, **31**, 7238-7246.

Wu, L. and Hickson, I.D. (2003) The Bloom's syndrome helicase suppresses crossing over during homologous recombination. *Nature*, **426**, 870-874.

Wyman, C. and Kanaar, R. (2006) DNA double-strand break repair: all's well that ends well. *Annu Rev Genet*, **40**, 363-383.

Yan, J., Kim, Y.S., Yang, X.P., Li, L.P., Liao, G., Xia, F. and Jetten, A.M. (2007) The ubiquitin-interacting motif containing protein RAP80 interacts with BRCA1 and functions in DNA damage repair response. *Cancer Res*, **67**, 6647-6656.

Yan, Y., Cao, P.T., Greer, P.M., Nagengast, E.S., Kolb, R.H., Mumby, M.C. and Cowan, K.H. (2010) Protein phosphatase 2A has an essential role in the activation of gamma-irradiation-induced G2/M checkpoint response. *Oncogene*, **29**, 4317-4329.

Yang, J., Xu, Z.P., Huang, Y., Hamrick, H.E., Duerksen-Hughes, P.J. and Yu, Y.N. (2004) ATM and ATR: sensing DNA damage. *World J Gastroenterol*, **10**, 155-160.

Yun, M.H. and Hiom, K. (2009) CtIP-BRCA1 modulates the choice of DNA double-strand-break repair pathway throughout the cell cycle. *Nature*, **459**, 460-463.

Zhang, F., Ma, J., Wu, J., Ye, L., Cai, H., Xia, B. and Yu, X. (2009) PALB2 links BRCA1 and BRCA2 in the DNA-damage response. *Curr Biol*, **19**, 524-529.

Zhang, Y. and Jasin, M. (2011) An essential role for CtIP in chromosomal translocation formation through an alternative end-joining pathway. *Nat Struct Mol Biol*, **18**, 80-84.

Abbreviations

53BP1	53-binding protein 1
ATM	Ataxia telangiectasia mutated
ATR	Ataxia telangiectasia and Rad3 related
BRCA1/2	Breast cancer susceptibility gene 1/2
BRCT	BRCA1 C-terminal
CHK1/2	Checkpoint protein 1/2
CDK	Cyclin-dependent kinase
CPT	Camptothecin
CtBP	Carboxyl-terminal binding protein
CtIP	CtBP interacting protein
DNA-PKcs	DNA-dependent protein kinase catalytic subunit
DSB	Double strand break
DDR	DNA damage response
EXO1	Exonuclease1
FHA	Forkhead-associated
GFP	Green fluorescent protein
GCRs	Gross chromosomal rearrangements
HR	Homologous recombination
IR	Ionizing radiation
MDC1	Mediator of DNA damage checkpoint 1
IRIF	Ionizing radiation induced foci
MRN	MRE11-RAD50-NBS1
MMEJ	Microhomology-mediated end joining
MS	Mass spectrometry
NBS	Nijmegen breakage syndrome
NHEJ	Non homologous end joining
PARP	Poly(ADP-ribose) polymerase
PIKK	Phosphoinositide-3-kinase-related protein kinase
PNK	Polynucleotide kinase
RNF8	Ring finger protein 8
ROS	Reactive oxygen species
SSB	Single-strand break
UV	Ultraviolet light
γH2AX	H2AX phosphorylated on Ser139

8. ACKNOWLEDGMENTS

I would like to take this opportunity to thank all who have helped me directly or indirectly in successful completion of my dissertation.

First of all, I would like to thank PD Dr. Stefano Ferrari for giving me the opportunity to do my PhD in his lab, and especially for the stimulating discussions, the ideas and the supervision he gave me.

I am very grateful to the head of my committee, Prof. Alessandro Sartori for his constant help, for giving me the chance to learn from him and for all the important inputs he gave during my PhD.

I also extend my sincere gratitude to my PhD committee members: Prof. Claus Azzalin and Prof. Martin Scheffner for all the help and inputs they have given throughout my PhD.

Furthermore, I would like to thank Prof. Josef Jiricny for giving me the opportunity to join his great institute and for accepting me in the highly competitive Cancer Biology PhD program.

I would like to sincerely thank Dr. Mahmoud El Shemerly for his help and support especially during the beginning of my PhD.

I would like to thank all past and present members of the Ferrari Lab, Serena, Kim, Payal, Christiane, Murat, Raj and Vanessa for their support and for the great working atmosphere. My thanks go also to members of the Sartori Lab for sharing ideas and reagents.

I would like to express my gratitude for all those who helped on my EMBO Reports paper, especially Martin, Lorenza, Javier and Emanuele.

Furthermore, I am grateful to the angels of the institute: the technicians, the cleaning staff as well as the administrative staff. I am very thankful to Farah and Malika for keeping the institute running all the time.
Last but not least, I would like to thank my parents for their continuous support throughout my studies and my PhD.

Dear Mona, thanks for being there by my side and for all the support you gave me!

Curriculum Vitae

Surname: EID
Name: Wassim
Date of birth: 28.01.1982
Nationality: Egyptian

Education

2007 - Present: PhD student in Institute of Molecular Cancer Research, Zurich University, Switzerland in Dr. Stefano Ferrari's laboratory. I will be finishing my PhD in January 2012.

June 2007- Sept 2007: Student fellowship given by the Egyptian Ministry for Higher Education from 09.06.2007 to 09.09.2007 at Institute of Medical Sciences, College of Life Sciences and Medicine, University of Aberdeen, Scotland. My training was in the context of the project " Docosahexaenoic acid and enhancing the efficacy of docetaxel in prostate cancer cells by modulation of apoptosis: the role of genes associated with the NFkappaB pathway".

Feb 2007: Master degree in Applied Medical Chemistry, Medical Research Institute, Alexandria University, Egypt. Title of thesis: Effect of treatment with chemotherapy alone or in combination with an anti-inflammatory drug on some angiogenic factors in breast cancer patients.

2004-2007: Master work in Medical Biochemistry, Applied Medical Chemistry and Oncology departments, Medical Research Institute, Alexandria University, Egypt.

2003-2004: Advanced courses in a preparatory year for master studies, Medical Research Institute, Alexandria University, Egypt.

May 2003: Bachelor degree in Biochemistry, Alexandria University, Egypt.

1999-2003: Biochemistry Department, Faculty of Science, Alexandria University, Egypt.

1986-1999: Elementary, secondary and high school, Alexandria, Egypt.

Publications

Eid W, Steger M,El-Shemerly M, Ferretti LP, Pena-Diaz J, Konig C, Valtorta E, Sartori AA, Ferrari S. 2010. DNA end resection by CtIP and exonuclease 1 prevents genomic instability. EMBO Rep 11: 962-968.

Presentations and courses

April 2011: Poster presentation. DNA repair conference. Egmond aan Zee, Netherlands.

January 2011: Practical course in Advanced Microscopy at the Swiss Federal Institute of Technology (ETH) and Zurich University. Module: Advanced life cell microscopy.

October 2010: Poster presentation. Cancer Research Student Retreat-Cancer Network Zurich. Wilderswil, Switzerland.

April 2010: Oral presentaion. RRR (Replication, Repair and Recombination) club. Cancer Biology, Zurich, Switzerland. hEXO1 and CtIP in the resection of DNA double strand breaks.

October 2009: Poster presentation. Cancer Research Retreat-Cancer Network Zurich. Ascona, Switzerland.

April 2009: Poster presentation. Cancer Research Student Retreat-Cancer Network Zurich. Bogis-Bossey, Switzerland.